CELLULAR AND MOLECULAR MECHANISMS CONTROLLING PYRAMIDAL NEURON AND INTERNEURON MIGRATION IN THE DEVELOPING NEOCORTEX.

Dante Stephen Bortone

A dissertation submitted to the faculty of the University of North Carolina at Chapel Hill in partial fulfillment of the requirements for the degree of Doctor of Philosophy in the Curriculum of Neurobiology.

Chapel Hill
2008

Approved by:

Franck Polleux, Ph.D.

Paul Manis, Ph.D.

Eva Anton, Ph.D.

Ben Philpot, Ph.D.

Mark Zylka, Ph.D.

ABSTRACT

DANTE STEPHEN BORTONE: Cellular and Molecular Mechanisms Controlling Pyramidal Neuron and Interneuron Migration in the Developing Neocortex.
(Under the direction of Franck Polleux, Ph.D.)

The development of the mammalian neocortex is contingent upon the successful migration of excitatory pyramidal neurons and inhibitory interneurons to the cortical plate. Pyramidal neurons migrate from the ventricular zones of the dorsal telencephalon along a radial glial scaffold, while interneurons migrate tangentially from the ventral telencephalon with no required substrate. The aim of my dissertation was to find the mechanisms by which these two distinct neuronal populations achieve the same task of migrating to the appropriate cortical position in spite of their differences. In pyramidal neurons, I characterized the role of Neurogenin2 (Ngn2) in specifying the migration properties and the dendritic morphology of pyramidal neurons by implementing confocal time-lapse microscopy and developing quantitative image analysis tools. In interneurons, I identified a novel molecular mechanism underlying the termination of their migration. I demonstrated that of $GABA_A$ receptor activation by ambient GABA is necessary and sufficient to stop interneurons migration an effect requiring theupregulation of the potassium chloride co-transporter, KCC2.

Taken together, my work has improved our understanding of some of the molecular mechanisms controlling the proper migration of pyramidal and non-pyramidal neurons during cortical development.

To love You with all my heart
and with all my soul
and with all my strength
and with all my mind.

ACKNOWLEDGEMENTS

Franck Polleux

Paul Manis, Eva Anton, Ben Philpot, Mark Zylka

Bob Rosenberg, Robert Peterson

Mary-Beth Hatten, Karl Kandler, Catherine Krull, Tom Maynard, David Mount

William O'Connell, Oeyvind Toft

Sabrice Guerrier

Paul Barnes, Randal Hand, Ashton Powell, Jacquie Powell, Takayuki Sassa

Lisa Plummer, Marie Rougie, Beth Boutte

Eldon Peters, Rocky Cheung

Scott Magness, Tomas Navratil

Lori Blalock, Megan Murphy, Patricia Owen, Denise Vandervort

Kara Bortone, Midge Bortone, Stephen Bortone

Benjamin Vincent, Mary Robbins, Caleb Hodson

Angela Bronwyn Cates Bortone

TABLE OF CONTENTS

List of Figures

List of Abbreviations

BrdU – Bromodeoxyuridine

CP – Cortical plate

DiI – 1,1'-dioctadecyl-3,3,3',3'-tetramethylindocarbocyanine perchlorate

E – Embryonic day (days past conception)

EGFP – Enhanced green fluorescent protein

LGE – Lateral ganglionic eminence

LGN – Lateral geniculate nucleus

MGE – Medial ganglionic eminence

MT – Middle temporal

MZ – Marginal zone

shRNA – short hairpin ribonucleic acid

SVZ – Subventricular zone

VZ – Ventricular zone

PMI – Pyramidal morphology index

GABA – Gamma-aminobutyric acid

P – Postnatal days (days past birth)

EPSC – Excitatory postsynaptic current

LTP – Long term potentiation

LTD – Long term depression

KCC2 – Potassium/chloride co-transporter 2

CHAPTER ONE

Introduction

The cerebral cortex has undergone an amazing transition in the evolution of mammals. This development is evident when one looks at a lower species such as reptiles. The reptilian cerebral cortex is composed of three loosely defined-layers in which the outer layers of neurons are formed first. Inner layers line up underneath their predecessors forming sequential waves of migrating neurons from the outside-in (Aboitiz and Montiel, 2007). In mammals however, these cortical layers are inverted. Each successive wave of neurons bypasses the previous layers to build the cortex from the inside-out (Angevine and Sidman, 1961; Marin and Rubenstein, 2003; Rakic, 1972). This three-layer inverted structure is unique to the mammalian class and is present in the archicortex and paleocortex, composing the hippocampus and olfactory cortex, respectively (Brown et al., 2001). This inside-out cortical organization expanded during evolution of the six-layered cerebral cortex, termed the neocortex. Neocortical evolution culminates in humans where it is the dominating structure of the brain, comprising 85% of its volume (Douglas and Martin, 2007).

I complete this dissertation thesis I utilized advanced techniques in imaging and image analysis to shed light on the developmental rules governing the assembly of the neocortex. In doing so this work provides a better understanding, not only of this novel trait of mammals, but also of that which makes us uniquely human.

Functions of the neocortex

Anyone who has dedicated a significant portion of his or her life to the study of the neocortex can be humbled with a simple question: What does it do? Horace B. Barlow echoed this sentiment:

> *I feel it is as if, in studying the heart, we had become involved in a detailed examination of the ionic currents and membrane channels of the Purkinje fibers* before *making the all-important discovery that the heart pumps blood around the body (Aertsen and Braitenberg, 1992).*

This humility reflects neither lack of effort nor progress. Diligent research has shown the involvement of the neocortex in the process of perception, decision-making, attention, learning, memory, consciousness, attention, speech, adaptability, voluntary movements, action planning (Aertsen and Braitenberg, 1992). The principal role of the cortex in these processes is to parse attributes of a sensory modality for parallel processing (Shephard, 1994).

The parsing of modalities is clearly evident in the processing of vision. Visual inputs are received from the optic nerve by the lateral geniculate nucleus (LGN) of the thalamus before proceeding to the neocortex. There visual processing is broken into over twenty distinct neocortical areas in the macaque monkey brain. Each area can be involved in different aspects of vision. Color information goes from the LGN to cortical area V1 to V2 to V4. Orientation information, however, goes from the LGN to V1 to V2 to V5, also known as the visual area MT (middle temporal), or can go directly from the V1 to the MT. Thus different aspects of vision are passed through distinct areas of visual cortex in our processing of vision (Shephard, 1994).

Although the parsing of sensory modalities is being understood to finer and finer degrees, this often leaves more questions than answers. Why is information broken apart in this way? How does the neocortex alter and preserve the information as it is being passed? Is this information reassembled to form a cohesive picture of the world or is our perception accomplished in the parsing itself? There are no clear answers to these questions. The

study of neocortical function often leads to higher and higher levels of complexity. Francis Crick has stated his strategy in the face of difficult problems:

> *If you do not make headway studying a complex system, study its structure and knowledge will follow automatically (Martin, 2002).*

Much has been learned in the study of neocortical structure in the hopes of doing just that.

Structure of the neocortex

The cortex is composed of two main cell types: pyramidal and non-pyramidal neurons (Peters and Edward, 1984). Pyramidal neurons provide the principal excitatory drive of the neocortex (Nieuwenhuys, 1994). These neurons derive their name from the pyramidal shape of their soma, which extends one large dendrite apically and two smaller dendritic tufts off the corner base of the 'pyramid.' Pyramidal neurons use glutamate to depolarize their postsynaptic targets and project over long distances to the thalamus, subcortical regions, ipsilateral cortex or contralateral cortex (Molyneaux et al., 2007; Nieuwenhuys, 1994). Non-pyramidal neurons (or interneurons) provide the inhibitory drive of the neocortex. The dendritic arbors of these neurons lack the large apical extension typically seen in pyramidal neurons. To the contrary, interneurons display a significant diversity of dendritic morphologies including among others bipolar, bi-tufted, multipolar morphologies. Interneurons use GABA to hyperpolarize their post-synaptic targets (mostly pyramidal neurons and other interneurons) and with few exceptions, project locally within the cerebral cortex (Nieuwenhuys, 1994; Peters and Edward, 1984).

The ratio of excitatory to inhibitory synaptic drive establishes a crucial balance in the functioning of the adult brain (Ben-Ari, 2002; Hensch, 2005). Pop-culture often cites that we only use 10% of our brains, suggesting if we could somehow unleash the remaining 90%, we would all be geniuses. To the contrary, in the face of such unbridled excitation, we would all be epileptic. Indeed, one of the most remarkable refinements of the neocortex lies in its focal activation of precise subsets of cells only when needed. The restriction of activity

is largely due to the inhibition provided by interneurons. The ratio of inhibitory interneurons to excitatory pyramidal cells is highly conserved, approximately 20%:80% respectively. This ratio is largely conserved between species, among individuals and across neocortical regions (Braak and Braak, 1986; DeFelipe et al., 2002; Sloper, 1973; Sloper et al., 1979; Tombol, 1974; Winfield et al., 1980). Even minor perturbations in this balance can result in epileptic activity (Cobos et al., 2005).

Another conserved component of the neocortex is its arrangement into columns. This network of neurons connects vertically, extending across layers II-VI to form functionally and anatomically distinct domains (Mountcastle, 1997). Again, the visual system provides an excellent example of this columnar organization. Ipsilateral and contralateral projections to the visual cortices form distinct alternating bands of interlacing columns called ocular dominance columns. Wiesel, Hubel and colleagues visualized these bands by injecting tritiated proline or fructose into one eye of the mouse. Autoradiography revealed ipsilateral and contralateral bands corresponding to the inputs of the injected eye (Wiesel et al., 1974). The division of the neocortex into minicolumns fuels the speculation that it is composed of a repetitive iteration of the same canonical microcircuit (Douglas and Martin, 2007), although the structure and function of that microcircuit remain unknown (Purves et al., 2004).

While significant in expanding our understanding, the study of structure has not been sufficient in uncovering the mysteries of the neocortex thus far. Much of the difficulty lies in the extreme complexity of the neocortical circuitry. Ideally we would like a map of every cell position, projection and synapse in the neocortex. Although sounding simple, such a map would be of astronomical proportions. The human neocortex contains up to 2.8×10^{10} neurons and 10^{12} synapses (Mountcastle, 1997). The means of obtaining this information far surpasses our current technology. Even storing the thousands of terabytes of

information within this 'projectome,' would exceed our present means (Kasthuri and Lichtman, 2007; Lichtman, 2007; Sporns et al., 2005).

Further complicating this massive undertaking is the flexibility of mammalian nervous systems. Mammals lack the rigid positioning of neuronal soma and projections found in other organisms (Lichtman, 2007). The nervous systems of *Caenorhabditis elegans* and *Drosophila melanogaster* are deterministic and often referred to as 'hard-wired' because it is thought that genetic information is sufficient to instruct every synaptic connections in these rather simple nervous systems. Furthermore, these organisms are *eutelic*, meaning all individuals have the same number and placement of neurons and neural projections (Sulston et al., 1983). Building a complete connectivity map of the nervous system of these organisms has been achieved (at least for *C. elegans*; White et al., 1976), because analysis of all individuals provides the same structural information. Although the same general layout of the neocortex is similar within a mammalian species, inter-individual variability disables this holistic approach to neural connectivity. The study of a non-eutelic mammalian neocortex thus requires one to make conclusions about a complex and inconsistent structure.

If the structure of mammalian neural networks is variable, then understanding the developmental laws governing the self-assembly of the neocortex may provide the necessary information critical to the understanding of its function. The study of neocortical development may not only uncover key constraints necessary towards understanding its function, but also provide insights into how it may be emulated and repaired.

Development of the neocortex

In this section, neocortical development of the mouse will be the primary animal model discussed. The genetic tools available for the mouse far exceed those available in other mammalian species. Mouse genetics has provided a tremendous amount of

information on the function of encoded proteins *in vivo*. Similarly, genetically engineered mice with enhanced green fluorescent protein (EGFP), ß-galactosidase (LacZ) or other genetic reporters expressed under the control of specific promoters allows the visualization of individual cells and the tracking of their migration. For example, the Gene Expression Nervous System Atlas (GENSAT) project has created many of these reporter mice (Gong et al., 2003; Heintz, 2004). GENSAT has produced a gene expression atlas of the mouse nervous system. To make this atlas, the promoter for a given gene is put in front of an EGFP reporter. Every cell that would express this gene now also expresses this fluorescent reporter. Our lab has made great use of the Lhx6-EGFP mice made by GENSAT. This mouse expresses EGFP primarily in parvalbumin positive interneurons and allows us to readily identify these cells even in live tissue. This NIH-based consortium produces approximately 250 different reporter strains per year (Heintz, 2004) and makes them freely available to labs across the world. As a result of these reporter mice and other genetically modified mice, a wealth of information has been gleaned from developmental studies of mouse neocortex.

Neurogenesis

The first phases in neocortical development are neurogenesis and differentiation. The time-course of neurogenesis has been revealed by labeling cells during S-phase, the period of DNA replication in mitosis. Tritiated thymidine or its non-radioactive analogue, bromodeoxyuridine (BrdU), incorporates into the replicating DNA, which is carried with the daughter cell as it migrates into the cortex and revealed via autoradiography or immunolabeling, respectively. Labeling studies of this type indicate that neurogenesis starts on embryonic day 11.5 (E11.5) and concludes by E18 (Angevine and Sidman, 1961; Molyneaux et al., 2007; Polleux et al., 1997).

Although the neurogenesis of pyramidal neurons and interneurons occurs along a similar time-course (McConnell, 1988; McConnell and Kaznowski, 1991; Valcanis and Tan, 2003), many differences lie in the details of their neural differentiation. Pyramidal cells originate in the ventricular zone (VZ) of the dorsal telencephalon (**Fig. 1.1**; Marin and Rubenstein, 2003) and are specified by the expression of specific transcription factors such as Emx1, Ngn1/2, Pax6, Tlx1/2 and FoxG1 (Molyneaux et al., 2007; Schuurmans and Guillemot, 2002). On the other hand, interneurons originate in the ventricular zone of the ganglionic eminences, located in the ventral telencephalon (**Fig. 1.1;** Wonders and Anderson, 2006). They are specified by the transcription factors Mash1, Nkx2.1, Lhx6 and Dlx1/2 (Rubenstein and Merzenich, 2003; Wonders and Anderson, 2006).

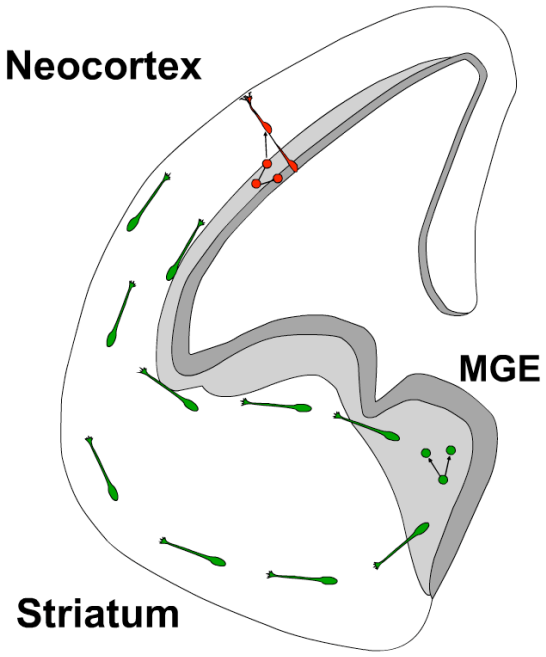

Figure 1.1 - Origins of radial and tangential migration in the developing neocortex
Tangentially migrating interneurons (green) migrate large distances from their germinal zone in the medial ganglionic eminence (MGE) up to the dorsal telencephalon (cortex). On the other hand, radially migrating pyramidal cells (red) migrate a relatively short distance from their germinal zone in the dorsal telencephalon.

Neuronal differentiation

The relationship between neurogenesis and neural differentiation is not always a straightforward one. Loss of the transcription factor Lhx2 prohibits the formation of neocortical pyramidal neurons. Instead, the entire dorsal telencephalon differentiates into cortical hem and choroid plexus (reviewed by Molyneaux et al., 2007). Similarly the loss of Nkx2.1 prevents the formation of the medial ganglionic eminence (MGE; Sussel et al.,

1999), the principle source of interneurons. Instead, the neurons in this region differentiate into cells resembling the olfactory neurons of the lateral ganglionic eminence (LGE).

Other aspects of neural differentiation are specified during neurogenesis. The laminar fates of both pyramidal neurons and interneurons are determined by the age of the surrounding tissue during G1/S-phase transition of their final division (McConnell, 1988; McConnell and Kaznowski, 1991; Valcanis and Tan, 2003). Some aspects of neuronal differentiation are specified after neurogenesis. In *Xenopus* spinal cord neurotransmitter specification can be modified by the enhancement or suppression of calcium transients (Borodinsky et al., 2004; Spitzer et al., 2004). The sequential order of differentiation and neurogenesis are not competing hypothesis, rather multiple routes by which different aspects of neural attributes may be specified.

Neuronal migration

Following neurogenesis (and perhaps differentiation), neurons of the developing neocortex must migrate from their germinal zones to the cortical plate. As mentioned previously, the generation of pyramidal neurons and interneurons occurs in the dorsal and ventral telecephalon, respectively. In traversing from these distinct proliferative zones, they have evolved remarkably different ways of migrating.

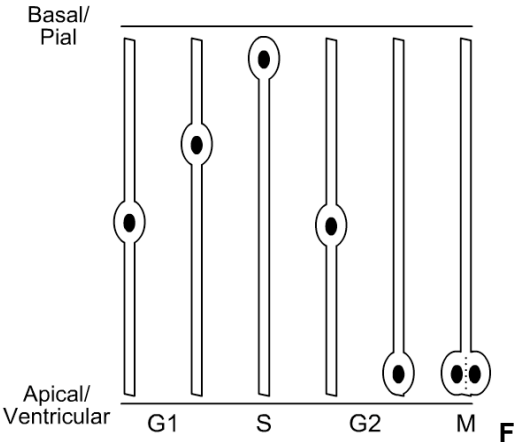

Figure 1.2 - Nuclear migration during the cell cycle
Cell body position corresponds to cell cycle phase in the developing neural epithelium (Reproduced from Brown et al., 2001).

The migration of pyramidal cells starts with a mono-layered neural epithelium located in the dorsal telencephalon. Each radial progenitor in this monolayer spans the width of the developing neocortex, maintaining both apical and basal attachments. As these progenitors

progress through the cell cycle, their soma undergoes interkinetic nuclear movement **Fig. 1.2**; Brown, et al., 2001; Sauer, 1935). Each cell soma progresses dorsally toward the pia as it undergoes G1, S-phase at its most dorsal position, G2 as it descends ventrally and finally M-phase upon reaching the ventricle (Brown et al., 2001). If this division is symmetrical, it will produce two identical radial progenitors. If the division is asymmetric, one of the cells will remain a radial glia; the other will detach from the ventricular side and pull its nucleus dorsally via nucleokinesis to form the preplate (Nadarajah and Parnavelas, 2002; Super et al., 1998).

The next wave of pyramidal cells will split this preplate into two layers. Again, radial progenitors undergo cell-cycle dependant interkinetic nuclear movements within the VZ. And again, symmetric divisions along the ventricular surface will produce two progenitor cells, while asymmetric divisions result in one radial progenitor and one radially migrating neuron (**Fig. 1.3**; Noctor et al., 2004). This neuron will then attach to its clonally-related radial glia and use this fiber as a substrate for migration to the future cortical plate (Noctor et al., 2004; Rakic, 1972). After exiting the VZ, the radially migrating neuron may detach from its radial glial substrate and enter a multipolar phase, forming the subventricular zone (SVZ) where it will divide symmetrically. These abventricular divisions produce either two multipolar progenitors or two radially migrating postmitotic pyramidal neurons (Noctor et al., 2001). The newly generated postmitotic neurons reattach to their scaffold and migrate to

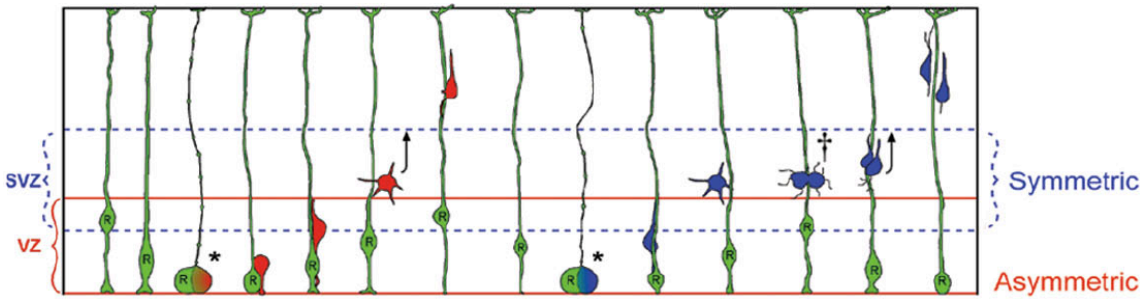

Figure 1.3 - Radial migration from the ventricular zones
Asymmetric divisions (red) in the ventricular zone (VZ) can produce a post-mitotic radially migrating pyramidal neuron. Symmetric divisions (blue) in the subventricular zone (SVZ) can produce two post-mitotic radially migrating pyramidal neurons (Copied from Noctor et al., 2004).

the preplate. Upon reaching the preplate, pyramidal neurons terminate their migration by detaching from radial glia, forming the cortical plate and layer VI of the neocortex. The formation of the cortical plate splits the preplate into two transient layers. The dorsal portion of the split preplate is called the marginal zone (MZ), while the ventral portion is called the subplate (Super et al., 1998).

The next generation of radially migrating pyramidal neurons will migrate in the same manner, bypassing layer VI to the ventral border of the MZ before they will also detach from their radial glia (Goffinet, 1984). Detachment from the radial glia is an important step as it allows subsequent generations of pyramidal neurons to pass them. This process results in the formation of the inner layers of cortex prior to the outer layers (**Fig. 1.4**; Angevine and Sidman, 1961).

Figure 1.4 - Pyramidal neuron radial migration is dependant upon radial glial substrate
Pyramidal cells migrate radially using radial glial processes as a scaffold (black) and accumulate in an inside-first outside-last pattern (red neuron is older than orange, which is older than yellow neuron). Termination of radial migration occurs at top of CP after detachment from radial glial substrate (CP – Cortical Plate; IZ – Intermediate zone; MZ – marginal zone).

Interfering with neuron-glial junction domain proteins causes a premature detachment of the pyramidal neuron and termination of radial migration illustrating the critical role of the scaffold in the continuation of radial migration (Anton et al., 1996). Should they fail to detach from the radial glial scaffold, future generations of neurons would not be able to pass forming an inside out cortex. Mice with a spontaneous mutation called *reeler* show this phenotype indicating the role of reelin in detachment from the radial glia (Dulabon et al., 2000; Goffinet, 1984; Pinto-Lord et al., 1982).

Following the last wave of pyramidal neurons forming layer II, the developmental scaffold is transformed. Radial glial cells lose their ventricular attachments and, drawing up dorsally towards their pial connection via nucleokinesis, become the astrocytes of the neocortex (Noctor et al., 2004; Schmechel and Rakic, 1979). The majority of reelin-secreting cells of the MZ, the Cajal-Retzius cells, die (Super et al., 1998); transforming the MZ into a cell sparse - and axon rich - layer I. A significant proportion of cells of the subplate die as well (Super et al., 1998). Since the VZ is also lost in the generation of astrocytes, the only remnant of the developing neocortex is the SVZ, which will continue to produce new neurons and glia into adulthood (Alvarez-Buylla et al., 2000).

The migration of interneurons to the neocortex is totally distinct from radial migration. Unlike the generation of pyramidal cells, which occurs in the dorsal telencephalon, interneurons are generated in the ventral telencephalon. Although early studies concluded interneurons originated from the lateral ganglionic eminence (LGE), subsequent studies revealed that the majority of cortical interneurons are generated in the medial ganglionic eminence (MGE) with the caudal ganglionic eminence (CGE) as a secondary source (Anderson et al., 1997; DeDiego et al., 1994; Nery et al., 2002; Polleux et al., 2002; Tamamaki et al., 1997; Wichterle et al., 2001). The LGE does produce a sparse population of cortical interneurons (Anderson et al., 2001), but primarily generates the olfactory interneurons that form the rostral migratory stream as well as striatal neurons (Wonders and Anderson, 2006).

There are more differences between interneuron and pyramidal cell migration than simply their physical origin. Where radially migrating pyramidal neurons only form one leading process along a radial glia (Rakic, 1972), interneurons are multipolar and tend to branch during migration. Even the manner in which these processes turn is different between the two cell types. Interneurons turn by growing a new process and following it in a

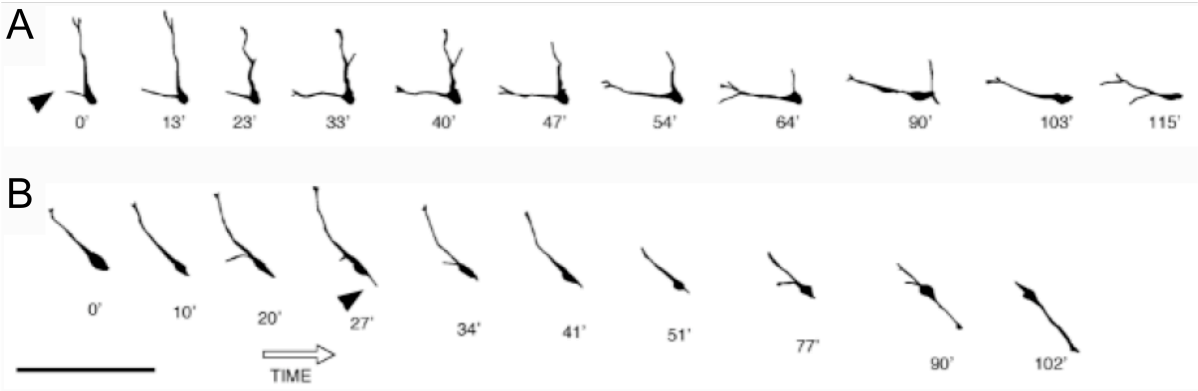

Figure 1.5 - Morphological dynamics of the leading process during a change in the direction of migration
These cells, migrating within the intermediate zone, make 90° **(A)** or 180° **(B)** changes in their trajectory in less than 2 hours (time interval is indicated below each drawing). Note that in each case, the turn is not initiated by the growth cone of the leading process, but instead by a second leading process that emerges from the cell body (Scale bar: 100 μm; copied from Polleux et al., 2002).

different direction (**Fig. 1.5**; Polleux et al., 2002), rather than simply turn the tip of the leading process itself as with radial migration.

The generation of new leading processes during interneuron migration may be due to the lack of a linear substrate providing a strong cell adhesion constraint as observed for radially migrating neurons. Where pyramidal neurons have radial glia to guide them to the cortical plate, interneurons have no such guide (**Fig. 1.6**). These tangentially migrating neurons do turn and migrate along radial glia when invading the cortical plate, but even within the cortical plate they are often oriented tangentially (O'Rourke et al., 1995; Polleux et al., 2002; Yokota et al., 2007). Some evidence suggests that interneurons

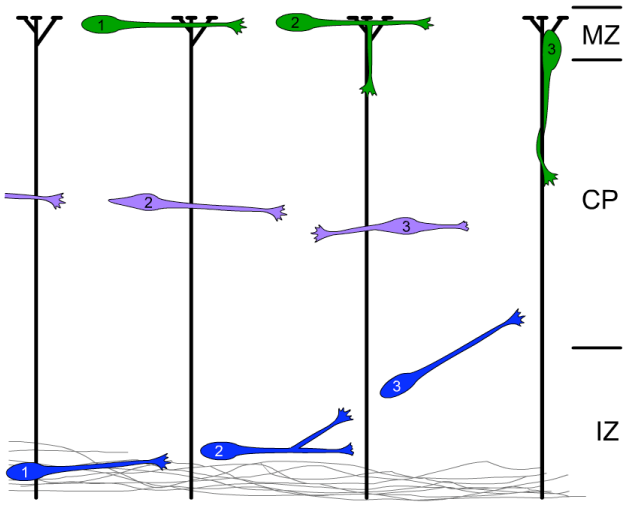

Figure 1.6 - Pyramidal neuron radial migration is dependant upon radial glial substrate
Interneurons migrate along a wide variety of paths and appear to require neither radial glia nor axons (grey) exclusively as a substrate. Cell numbers represent sequential order (CP – Cortical Plate; IZ – Intermediate zone; MZ – marginal zone).

use axons as a guide to the neocortex (Denaxa et al., 2001; McManus et al., 2004), although interneurons have been identified migrating independent of axons via immunostaining (Polleux and Ghosh, 2002; Wichterle et al., 2001). Furthermore, if axons were a required substrate for interneuron migration one would expect a pronounced interneuron migration deficit in the neocortex of mice lacking corticofugal axons. The conditional LKB1 Emx1-Cre knockout mouse has no corticofugal axons (Barnes et al., 2007) yet we have identified calbindin-positive interneurons in the neocortex of these animals (**Fig 1.7**). Although the distribution of these interneurons is slightly disorganized in the LKB1 cKO, they are nonetheless present in the cortex in appropriate numbers. If interneurons do have a required substrate, it has not yet been identified.

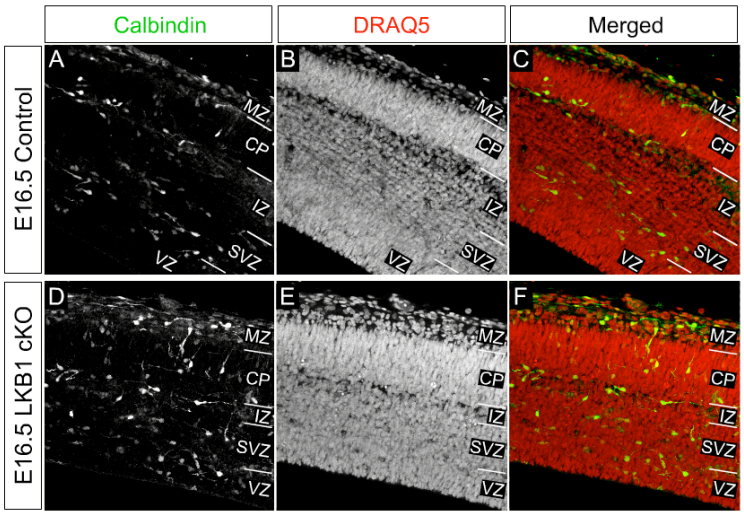

Figure 1.7 - Tangentially migrating interneurons migrate to cortex in genetically axotomixed mice
Immunostaining for calbindin positive interneurons in dorsal telencephalon of E16.5. **(A-C)** Wild-type mice show distinct bands of tangentially oriented interneurons in IZ and SVZ. **(D-E)** Although disorganized, interneurons migrate successfully to the IZ, SVZ and VZ of genetically axotomized LKB1 cKO (Emx1-Cre; CP - Cortical plate; IZ - Intermediate zone; MZ - Marginal zone; SVZ - Subventricular zone; VZ - ventricular zone).

The lack of a directing substrate suggests tangential migration is guided by moving towards or away from short or long-range diffusible, factors secreted in the extracellular matrix, a process called chemotaxis. Neuregulin-1 and GDNF both act as chemoattractants for interneurons (Flames and Marin, 2005; Pozas and Ibanez, 2005). As will be discussed in more detail later, GABA has long been proposed to affect interneuron migration to the neocortex, although conflicting results emerged from experiments assessing the role of $GABA_A$ receptor activation in neuronal migration (Behar et al., 1996; Behar et al., 1998;

Cuzon et al., 2006). $GABA_A$ receptor activation facilitates interneuron entry into the dorsal telencephalon (Cuzon et al., 2006), although activation appears to have no effect in attracting interneurons or in stimulating their movement (Behar et al., 1996; Behar et al., 1998; Cuzon et al., 2006).

Chemorepulsive cues have also been found for cortical interneurons. There is evidence that interneurons undergo chemorepulsion from the ventral telencephalon by Slit1/2 interactions (Marin et al., 2003; Zhu et al., 1999), although Slit1/2 knockouts show no significant deficit in interneuron migration (Marin et al., 2001). Interactions between Sema3A/3F expressed in the striatal mantle region and their corresponding receptors Neuropilin1/2 on interneurons is thought to force cortical interneurons to migrate dorsally into the cortex (Marin et al., 2001; Tamamaki et al., 2003). Interneurons are also repulsed from entering the cortical plate prematurely through Cxcr4 and its receptor Cxcl12 (Li et al., 2008; Lopez-Bendito et al., 2008).

Upon their entry into the cortical plate, another difference between interneurons and pyramidal cells arises. Rather than terminating migration immediately like their radially migrating counterparts, interneurons migrate inside the cortical plate for several days at least (Polleux et al., 2002; Tanaka et al., 2006). It is unknown how long this period lasts or what causes them to terminate their migration. It is surprising that so little attention has been given to this biological phenomenon, given how critical interneurons are for proper cortical function.

GABAergic interneurons form some of the first synaptic connections in the neocortex. Although the very first synapses in the developing neocortex occur in the subplate (Del Rio et al., 2000) these are transient, as a significant proportion of subplate neurons die before adulthood (Super et al., 1998). The first neocortical synapses to form in the laminar structures of the cortex are inhibitory and occur from P7 to P20 in the rat (Sutor and Luhmann, 1995). The development of GABAergic synapses precedes the formation of

glutamatergic synapses in most systems studied do far (Akerman and Cline, 2007; Ben-Ari, 2002).

GABA is not always an inhibitory neurotransmitter (Ben-Ari, 2002). As a classical neurotransmitter, GABA exerts its effects in part by activating ionotropic chloride ion channels, the $GABA_A$ and $GABA_C$ receptors. The direction of chloride flow - and therefore the intracellular concentration of chloride - determines whether the response to GABA will be hyperpolarizing or depolarizing (See **Fig. 1.8**). The inhibitory/hyperpolarizing effect of GABA is a result of the flow of chloride ions into neurons upon activation (Ben-Ari, 2002). The potassium chloride co-transporter, KCC2, plays a critical role in the establishment of this chloride gradient. Without it, the effect of GABA on ionotropic GABA receptors is excitatory (Rivera et al., 1999). Interestingly, the transition from a migratory state to a sedentary synaptogenic phase coincides with the up-regulation of KCC2 (Lu et al., 1999).

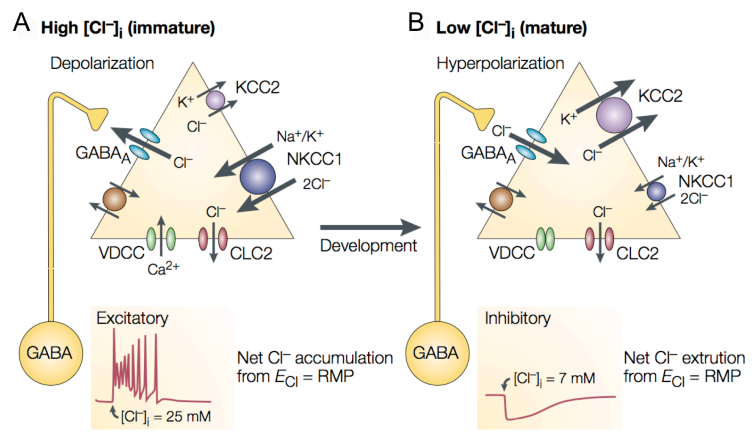

Figure 1.8 - Early expression of NKCC1 and late expression of KCC2 determines developmental changes in $[Cl–]_i$
Schematic diagram depicting the $Na^+–K^+–2Cl^-$ cotransporter NKCC1, the $K^+–Cl^-$ co-transporter KCC2 and voltage-gated calcium currents, as well as the gradients of chloride ions. **(A)** NKCC1 expression predominates in immature neurons, in which the intracellular concentration of chloride ($[Cl^-]_i$) is relatively high. **(B)** KCC2 expression predominates in mature neurons. Note that the activation of GABA (γ-aminobutyric acid) type A receptors generates an efflux of chloride and an excitation of immature neurons, and an influx of chloride and an inhibition of adult neurons. CLC_2, voltage-gated chloride channel 2; E_{Cl}, chloride reversal potential; RMP, resting membrane potential (V_{rest});VDCC, voltage-dependent calcium channel (copied from Ben-Ari, 2002).

Summary

One of the most astounding achievements in neuroscience is how much its founding fathers were able to determine about the nervous system simply by looking at it. Of this Edward Callaway and Joshua Sanes have written:

> *To a considerable extent, neurotechnology today can be viewed as the enterprise of building prosthetic devices that will enable mere mortals to demonstrate what Cajal intuited (Callaway and Sanes, 2006).*

Not to dispute the brilliance of these men, but humans are visual creatures with profound abilities to understand extremely complex phenomenon just by looking at them. Where the initial observations of neurons were made by labeling with Golgi staining and horseradish peroxidase, we can now electroporate cells with a variety of protein-based fluorescent markers, but the same necessity of simply observing developing neurons 'in the wild' remains the best way to determine with precision the developmental mechanisms leading to cortical circuit assembly. There are, however, limitations to our observational abilities.

My thesis consisted in developing new time-lapse confocal imaging and quantitative analysis tools to study some of the molecular and cellular mechanisms underlying: (1) the role of Neurogenin2 in the specification of the migration and morphology of pyramidal neurons (**Chapter 2** – Article 1) and (2) the role of GABA and KCC2 signaling in stopping the migration of cortical interneurons (**Chapter 3** – Article 2). Following the presentation of these two articles, I will synthesize these results and discuss their outcomes, their interpretation and potential future directions in **Chapter 4**.

CHAPTER TWO

Phosphorylation of *Neurogenin2* Specifies the Migration Properties and the Dendritic Morphology of Pyramidal Neurons in the Neocortex.

Randal Hand [1]*, DANTE BORTONE [2]*, Pierre Mattar [3], Laurent Nguyen [4], Julian Ik-Tsen Heng [4], Sabrice Guerrier [1], Elizabeth Boutt [1], Eldon Peters [1], Anthony P Barnes [1], Carlos Parras [4], Carol Schuurmans [3], François Guillemot [4] and Franck Polleux [1,2#]

* These two authors contributed equally to this work.
Doctoral student contributed figures: 2.2 A-B,K-N; 2.5; 2.6; 2.7; 2.8 A-H and N-P.
Doctoral student contributed supplemental figures: 2.1 C',C'',H-I; 2.2 M-R; 2.3, 2.4, 2.5, 2.6 and 2.8.

Published in Neuron (Hand and Bortone, et al., 2005)

[1] Univ. North Carolina - Neuroscience Center - Department of Pharmacology - Chapel Hill, NC 27599-7250-USA
[2] Univ. North Carolina - Neuroscience Center - Neurobiology Curriculum - Chapel Hill, NC 27599-7250-USA
[3] University of Calgary, Calgary, Alberta, Canada T2N 4N1
[4] Div. Mol. Neurobiol., NIMR- MRC, Mill Hill -UK

[#] Address correspondence to: polleux@med.unc.edu

Franck Polleux, Ph.D.
University of North Carolina
Neuroscience Center - Dept of Pharmacology
115 mason farm road –CB#7250
Chapel Hill, NC 27599
USA

Tel 919-966-1449
Fax 919-966-9605

SUMMARY

The developmental mechanisms specifying the dendritic morphology of different neuronal subtypes are poorly understood at the molecular level. Here we demonstrate that the bHLH transcription factor *Neurogenin2* (*Ngn2)* is both necessary and sufficient to specify the dendritic morphology of pyramidal neurons *in vivo* by specifying the polarity of its leading process outgrowth during the initiation of radial migration. The ability of Ngn2 to promote a polarized leading process outgrowth during the initiation of migration requires the phosphorylation of a tyrosine residue at position 241, an event that is neither involved in Ngn2 proneural function nor its direct transactivation properties. Interestingly, the migration defect observed in the *Ngn2* knockout and in progenitors expressing $Ngn2^{Y241F}$ can be significantly rescued by inhibiting the activity of the small-GTPase RhoA in cortical progenitors. Our results demonstrate that *Ngn2* coordinates the acquisition of the radial migration properties and the unipolar dendritic morphology characterizing pyramidal neurons through molecular mechanisms distinct from those mediating its proneural activity.

INTRODUCTION

The astonishing diversity of dendritic morphologies characterizing distinct neuronal subtypes underlies their sophisticated signal processing and computational properties (Hausser et al., 2000). Although an extensive amount of work performed over the past decade has identified the extracellular cues, the receptors and some of the corresponding signaling pathways controlling axon growth and guidance (Huber et al., 2003; Tessier-Lavigne and Goodman, 1996; Yu and Bargmann, 2001), the cellular and molecular mechanisms specifying the dendritic shape of distinct sub-classes of neurons is still poorly understood in vertebrates (Jan and Jan, 2003; Scott and Luo, 2001; Whitford et al., 2002). In particular, although substantial progress has been made in characterizing the late, activity-dependent phase of dendritic branching and adaptation of the size of the dendritic arbor relative to presynaptic inputs (Gaudilliere et al., 2004; Van Aelst and Cline, 2004; Wong and Ghosh, 2002), the early developmental mechanisms specifying the overall dendritic morphology of a given neuronal subclass has not been explored. One of the key unresolved questions is the relative importance of intrinsic versus extrinsic control in establishing the dendritic arborization characteristic of a given neuronal subtype (Scott and Luo, 2001).

The development of dendritic morphology conceptually involves at least four steps (Scott and Luo, 2001): (1) dendritic initiation, (2) dendritic outgrowth and guidance, (3) dendritic branching including spine or synapse formation and (4) limitation of dendritic outgrowth. The first step dictates whether dendritic outgrowth will be polarized or not and thereby determining whether the dendritic field of a neuron will sample the 'presynaptic space' uniformly or in a biased manner. In the neocortex and hippocampus, *pyramidal* neurons are initially characterized by a polarized outgrowth of one major dendrite i.e. the apical dendrite (Miller, 1981; Peters and Kara, 1985a), whereas the vast majority of cortical interneurons undergo an unpolarized dendritic outgrowth leading to a multipolar dendritic morphology that is by definition *non-pyramidal* (Miller, 1986; Peters and Kara, 1985b). Interestingly, it has been recently shown that pyramidal and non-pyramidal neurons represent two developmentally distinct neuronal lineages generated by specialized and distinct sets of progenitors. Pyramidal neurons (1) originate from progenitors located in the *dorsal telencephalon* and express region-specific

transcription factors that include *Emx1*, *Neurogenin* (*Ngn*) 1 and *Ngn2*, *Pax6* and *Tlx1/2* (2) migrate *radially* along a radial glial scaffold to reach their appropriate laminar position in an inside-first outside-last manner, (3) have an initially unipolar, unbranched pyramidal dendritic morphology characterized by an apical dendrite extending towards the pial surface, (4) generate axons that project over long distances to sub-cortical or to other cortical areas, and (5) use glutamate as an excitatory neurotransmitter. On the other hand, cortical interneurons (1) originate from progenitors located in the *ventral telencephalon* [medial and caudal ganglionic eminence (MGE and CGE respectively)] and express a different set of transcription factors such as *Mash1*, *Nkx2.1*, *Lhx6* and *Dlx1/2*, (2) migrate *tangentially* to reach the cortex, (3) display a variety of multipolar, non-pyramidal dendritic morphologies, (4) have locally-projecting axons and (5) use GABA as an inhibitory neurotransmitter (reviewed in Marin and Rubenstein, 2003; Schuurmans and Guillemot, 2002).

In *Drosophila*, proneural basic-helix-loop-helix (bHLH) transcription factors such as *atonal* or *achaete-scute* have been isolated based on their ability to promote neural fates in external sense organs models (Jarman et al., 1993; reviewed in Bertrand et al., 2002). Interestingly, in the fly central nervous system, *atonal* does not have proneural activity but is instead specifically required to control the pattern of axonal branching during larval and pupal development, an activity it carries out through interactions with Notch (Hassan et al., 2000). Furthermore, although the proneural activity of bHLH transcription factors has been demonstrated to reside in the DNA-binding basic region (Quan et al., 2004), there is evidence that neuronal subtype specification is controlled by residues outside the DNA-binding domain in both vertebrates and invertebrates (Huang et al., 2000b; Nakada et al., 2004). In mammals, recent evidence has also supported the notion that the bHLH protein *Ngn2* plays a critical role not only in the acquisition of pan-neuronal properties (Lee and Pfaff, 2003; Nieto et al., 2001; Scardigli et al., 2001; Sun et al., 2001) but also in the specification of neuronal subtypes (Fode et al., 1998; Fode et al., 2000; Lee and Pfaff, 2003; Ma et al., 1999; Mizuguchi et al., 2001; Parras et al., 2002; Ross et al., 2003; Scardigli et al., 2001; Schuurmans et al., 2004; Seibt et al., 2003). Specifically, a recent study demonstrated that *Ngn1* and *Ngn2* specify the expression of glutamate as the excitatory neurotransmitter in pyramidal cortical neurons (Schuurmans et al., 2004). These results raised the question of whether *Ngn2* function in cortical progenitors was limited to the specification of

neurotransmitter expression or whether *Ngn2* also participates to the specification of other phenotypic traits of cortical glutamatergic neurons, such as their radial migration properties and their pyramidal dendritic morphology?

Interestingly, recent time-lapse confocal analysis of the early initiation of radial migration of cortical progenitors has revealed that upon cell-cycle exit, immature neurons display a striking transition from a multipolar to a unipolar morphology at the level of the subventricular zone (Noctor et al., 2004). These results strongly suggest that molecular mechanisms operating during the initiation of radial migration are specifying the polarity of the leading process extension ultimately determining the unipolar dendritic morphology of pyramidal neurons in the cortex (Kriegstein and Noctor, 2004).

In the present study, we provide genetic evidence that the coordinated specification of the radial migration properties and the pyramidal dendritic morphology is controlled by the transcription factor *Ngn2* at least in part by functionally repressing the activity of the small GTPase RhoA. We combined *in vivo* and *in vitro* gain- and loss-of-function approaches to demonstrate that *Ngn2* specifies the dendritic morphology of pyramidal neurons by controlling their early polarization during the initiation of radial migration. Importantly, this activity is mediated by phosphorylation of a tyrosine residue at position 241 in the C-terminal domain of Ngn2, a residue that is not directly involved in mediating its transactivation properties or its proneural properties. Finally, we used time-lapse confocal microscopy of individual migrating neurons in slices and found that neurons expressing $Ngn2^{Y241F}$ display a strikingly leading process polarity defect and a failure to undergo proper nucleokinesis.

RESULTS

Neurogenin2 is expressed by cortical progenitors and transiently by post-mitotic neurons during the initiation of radial migration

It is well established that *Ngn2* mRNA is specifically expressed by cortical progenitors in both the ventricular zone (VZ) and sub-ventricular zone (SVZ) of the dorsal telencephalon throughout neurogenesis (Fode et al., 2000; Miyata et al., 2004; Schuurmans et al., 2004), while it is not expressed by progenitors located ventrally in the ganglionic

eminence (GE). Moreover, it has been recently shown that Ngn2 protein expression is regulated in a cell-cycle specific manner in the cortical VZ (Miyata et al., 2004). In particular, Ngn2 is expressed by cortical progenitors during the window of time when they commit to the neuronal lineage both in the 'surface', proliferative divisions in the VZ and the 'non-surface' neurogenic divisions in the SVZ (Miyata et al., 2004; Murciano et al., 2002).

We wanted to explore more carefully the spatial pattern of Ngn2 expression in the cortical germinal zones at E16 (when both the VZ and SVZ are prominent) by performing immunofluorescent staining directed against Ngn2 (**Fig. 2.1**). We confirmed that cortical progenitors located in the VZ express Ngn2 (**Fig. 2.1A** and **2.1J**). Interestingly, Ngn2 was also expressed by a subset of cells in the SVZ and in the intermediate zone (IZ), where early post-mitotic neurons exit the cell cycle and initiate radial migration (**Fig. 2.1A-C**). In order to test directly if these cells were indeed post-mitotic neurons, we performed double staining for Ngn2 and three distinct early post-mitotic neuronal markers: NeuN (**Fig. 2.1 D-E'''**), Microtubule Associated Protein-2 or MAP2 (**Fig. 2.1F-G'''**) and β-III tubulin or TuJ1 (**Fig. 2.1H-I'''**). This analysis showed unequivocally that Ngn2 is expressed by a sub-population of post-mitotic cells in the SVZ and IZ (**Fig. 2.1E-E'''**, **G-G'''** and **I-I'''**). The quantification shown in **Figure 2.1J** shows that although the majority of cells expressing Ngn2 (green bars) were located in the VZ, the bulk of Ngn2-NeuN double-labeled neurons (orange bars in **Fig. 2.1J**) were located primarily in the SVZ. The percentage of Ngn2+ cells expressing NeuN increased almost linearly as a function of the distance from the ventricle (**Fig. 2.1H**) reaching approximately 50% in the SVZ and 80% in the IZ. Interestingly, Ngn2 is

Figure 2.1 - Neurogenin2 is expressed both in neuronal progenitors and early postmitotic neurons in the developing cortex
(A–C) Double immunofluorescent staining performed at embryonic day (E) 16 on cryostat sections from mouse cortex against Ngn2 protein (A) and the early neuronal marker β III-tubulin (TuJ1) (B and C). **(D–D″ and E–Etriple prime)** Coexpression of Ngn2 (D) and NeuN (D′) in the SVZ (D–D″). Note the nuclear localization of Ngn2 in double immunopositive cells in the SVZ (arrows in [E]–[Etriple prime]). **(F–F″ and G–Gtriple prime)** Coexpression of Ngn2 (F and G) and MAP2 (F′ and G′) in the SVZ (arrow in [F″] and [G″]–[Gtriple prime]).

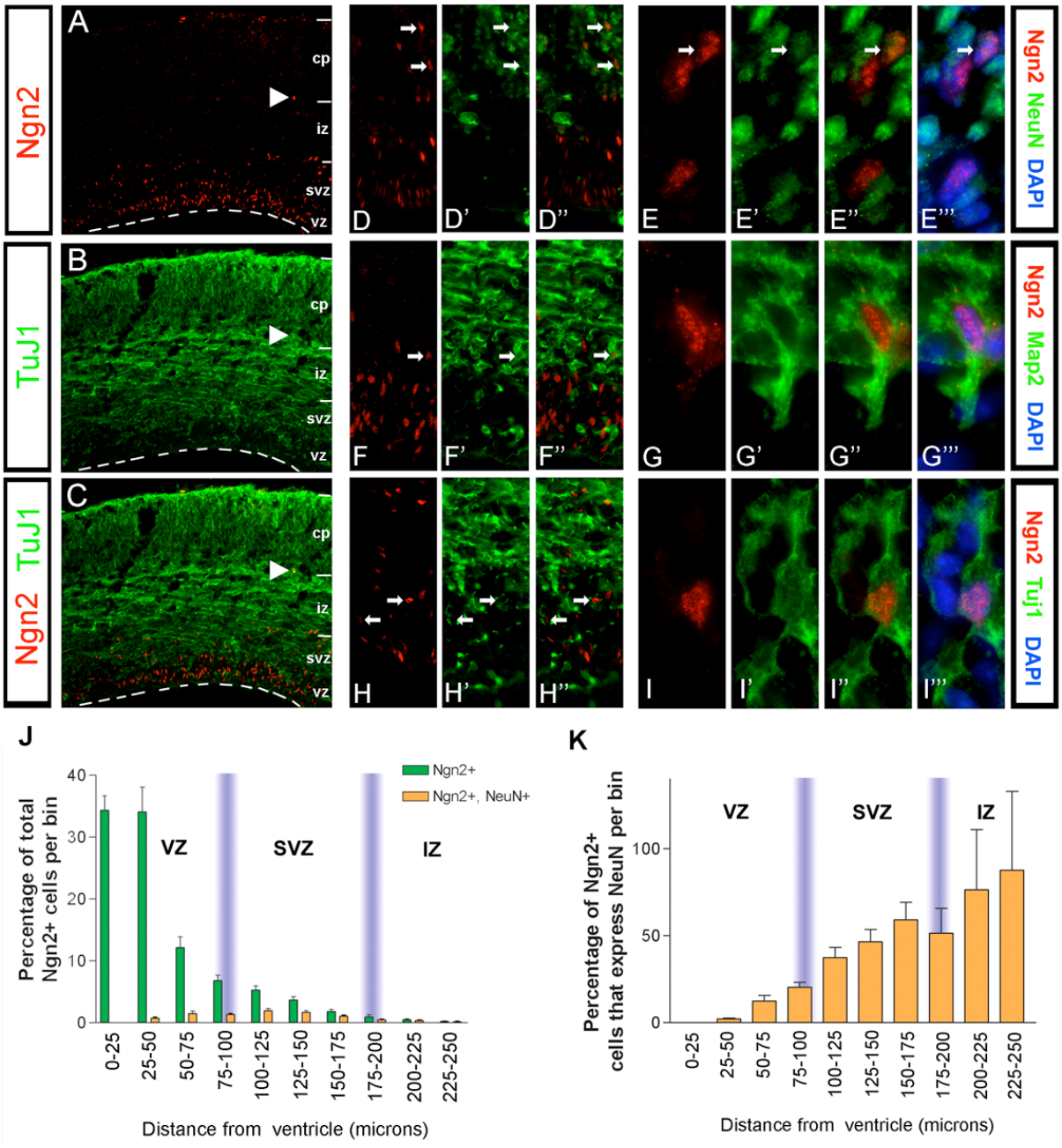

(H–H″ and I–Itriple prime) Coexpression of Ngn2 (H and I) and Tuj1 (H′ and I′) confirms the presence of Ngn2+ neurons in the SVZ (arrow in [F″] and [G″]–[Gtriple prime]). **(J)** Quantification of the distribution of Ngn2+ cells (green bars) and Ngn2/NeuN double-positive neurons (orange bars) expressed as a percentage of the total number of Ngn2+ cells found in 25 μm wide bins. **(K)** Quantification of the radial distribution of Ngn2-NeuN double-positive neurons calculated as a percentage of the total number of cells expressing Ngn2+ in each bin (CP, cortical plate; VZ, ventricular zone; SVZ, subventricular zone; IZ, intermediate zone).

very rapidly down-regulated at the protein level once neurons are reaching the top of the IZ and the CP. This analysis shows that Ngn2 is expressed transiently by post-mitotic neurons located in the SVZ and the IZ, coinciding with the time when these neurons engage in radial migration and display a morphological transformation from multipolar to unipolar (Noctor et al., 2004).

Neurogenin2 is necessary for the specification of the radial migration properties of cortical neurons

Recent BrdU birth-dating studies suggested that *Ngn2* knockout embryos were characterized by a pronounced migration defect in the cortex as suggested by the ectopic deep location of cells born between E12.5 and E14.5 in the germinal and intermediate zones of neonatal *Ngn2*-/- cortices (Schuurmans et al., 2004). We wanted to further explore the role of *Ngn2* in specifying the radial migration properties of cortical neurons. To do this we developed a new allele of *Ngn2* by replacing the entire *Ngn2* coding sequence with EGFP ([$Ngn2^{KIFGP}$; see Methods; Seibt, 2003). Throughout neurogenesis, EGFP faithfully reports the regional expression of *Ngn2* in the dorsal telencephalon of heterozygous $Ngn2^{KIGFP/+}$ embryos with the difference that EGFP is maintained much longer in neurons and acts as a lineage tracer (**Fig. 2.2A-B** at E14.5 and data not shown). Interestingly, homozygous $Ngn2^{KIGFP/KIGFP}$ embryos express approximately two-fold more EGFP compared to $Ngn2^{KIFGP/+}$ embryos (Compare **Fig. 2.2 A** and **C**). Similar to two previously described *Ngn2* null alleles, the majority of $Ngn2^{KIGFP/KIGFP}$ mice die shortly after birth (Fode et al., 1998; Fode et al., 2000). We will refer to mice homozygous for this EGFP allele as Ngn2-/- or Ngn2 knockout in the remainder of the study.

Figure 2.2 - Neurogenin2 is required *in vivo* for the proper migration of cortical neurons
(A and B) EGFP epifluorescence in live coronal organotypic slices isolated from E14.5 Ngn2KIGFP/+ mouse embryos (A) and Ngn2KIGFP/KIGFP mouse embryos (B) shows expression of Ngn2 in the dorsal telencephalon (D Tel.)

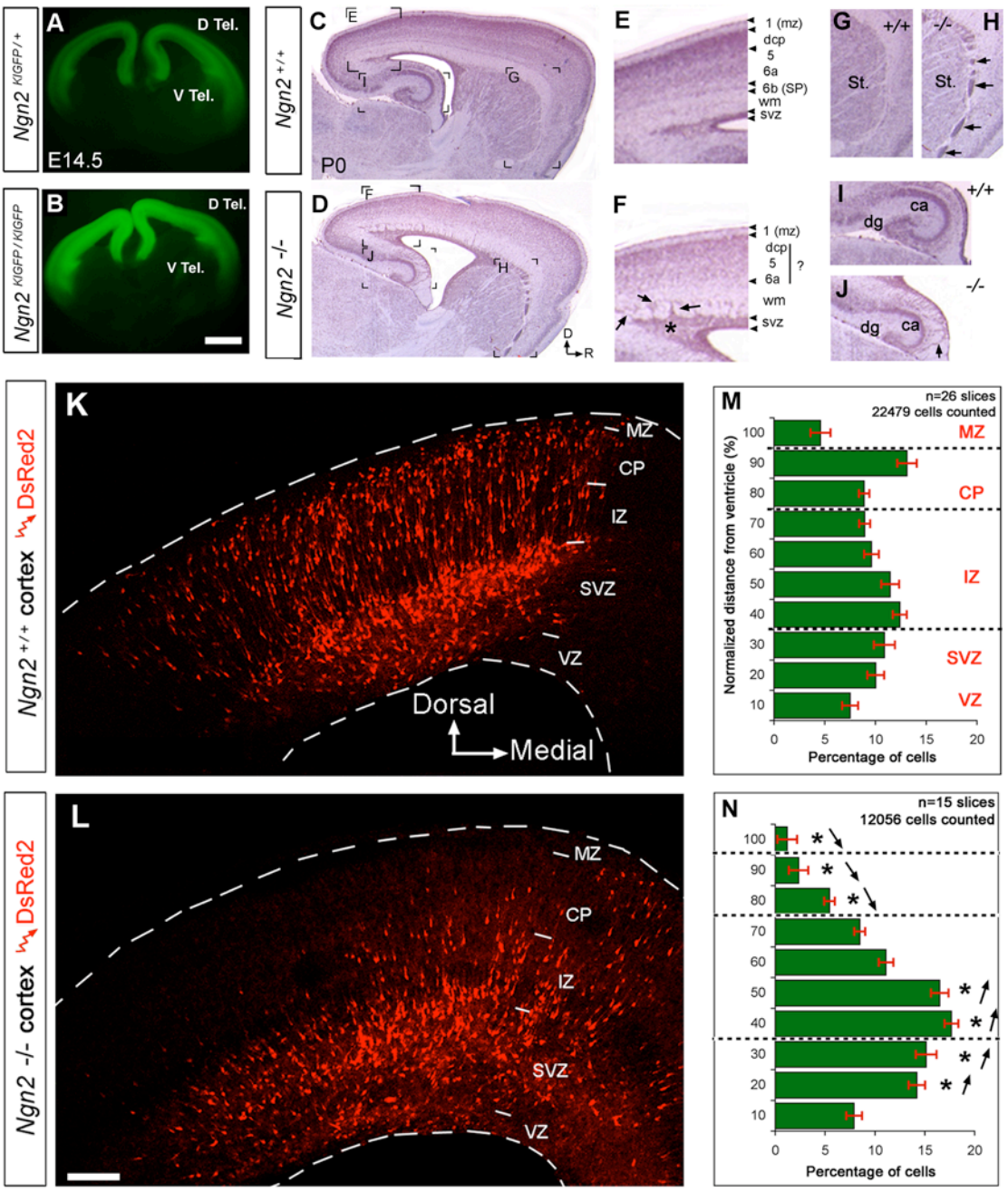

(C–J) Sagittal cryostat sections from postnatal day 0 (P0) Ngn2+/+ (C, E, G, and I) and Ngn2-/- (D, F, H, and J) mice counterstained with hematoxylin-eosin. At higher magnification, streams of ectopic cells (arrows in [F]) emerging from the SVZ (star in [F]) are detected in Ngn2-/- mice but not in control Ngn2+/+ mice (E). Heterotopic cell clusters are also found at the cortico-striatal boundary and underneath the developing CA regions of the hippocampus of the Ngn2-/- (arrows in [H] and [J], respectively) but not the Ngn2+/+ mice (G and I). **(K and L)** Ex vivo electroporation of pCIG2:DsRed2 in cortical progenitors of Ngn2+/+ (K) and Ngn2-/- (L) E14.5 embryos followed by organotypic culture for 4 days in vitro (DIV). (M and N) Quantification of the distribution of DsRed2-expressing cells along the radial axis of E14.5 Ngn2+/+ (M) and Ngn2-/- slices (N) after 4 DIV. *$p < 0.001$ $\chi 2$ test comparing corresponding bins (ca, Ammon's horn regions of the hippocampus; dg, dentate gyrus; MZ, marginal zone; St., striatum; wm, white matter. Scale bars, 100 μm (K and L).

Comparison of hematoxylin/eosin-stained sagittal sections from *Ngn2+/+* and *Ngn2-/-* neonatal cortices (**Fig. 2.2**) revealed the presence of large heterotopic cell clusters in the *Ngn2* mutants that are suggestive of a neuronal migration defect (arrows in **Fig. 2.2D-F**) but not in *Ngn2*+/+ controls (**Fig. 2.2C-E**). We also noticed a pronounced decrease in the cell density of the cortical plate of *Ngn2-/-* (**Fig. 2.2F**) compared to *Ngn2+/+* neonates (**Fig. 2.2E**) suggestive of a decreased level of migration in the Ngn2 knockout cortex. This is reinforced by the presence of streams of cells that seemed unable to exit the SVZ in the Ngn2-/- cortex (arrow in **Fig. 2.2F**). Other heterotopias are observed at the corticostriatal boundary and the hippocampus of the Ngn2-/- mice (arrows in **Fig. 2.2H** and **2.2J** respectively) but not in the control mice (**Fig. 2.2G** and **2.2I** respectively).

In order to test directly if radial migration was defective in *Ngn2-/-* embryos, we implemented a new technique that combines electroporation-mediated gene transfer and *in vitro* organotypic slice culture (see **Suppl. Fig. 2.1** for details). This *ex vivo* cortical electroporation technique allows the transfection of radial glial neural progenitors at reproducible efficiencies (up to 30% transfection efficiency among nestin+ VZ progenitors-Hand and Polleux-data not shown). After two days *in vitro* (2div), a cohort of post-mitotic neurons generated by the electroporated radial glial progenitors have engaged radial migration and are found in the IZ (**Suppl. Fig 2.1H**). By 4 div this single cohort of radially migrating neurons have reached their final position at the top of the cortical plate (**Suppl. Fig 2.1I**) recapitulating the same timing displayed *in vivo* as demonstrated by birthdating studies (Berry and Rogers, 1965) as well as using *in utero* electroporation technique (Hand, Bortone and Polleux, *manuscript in preparation*; see also Bai et al., 2003; Hasegawa et al., 2004; Hatanaka and Murakami, 2002; Kawauchi et al., 2003; Shu et al., 2004; Tabata and Nakajima, 2001). Therefore, this technique allows the modification of gene expression in a

synchronous cohort of cortical neurons and the subsequent examination of their migration properties and their final dendritic morphology *in vitro*.

Cortical progenitors electroporated at E14.5 (during the production layer 5 Polleux et al., 1997) give rise to neurons migrating radially into the intermediate zone and accumulating in the cortical plate of control cortex after 4 div (**Fig. 2.2K**). On the other hand, cortical electroporation of E14.5 *Ngn2*-/- littermate embryos revealed a pronounced migration defect resulting in the accumulation of transfected cells in the SVZ and IZ (**Fig. 2.2J**). Few cells successfully migrated into the cortical plate in the *Ngn2*-/- slices after 4 div (star in **Fig. 2.2J**). We quantified neuronal migration by using an automatized cell profile counting method where the total number of cell profiles along the radial axis of the cortical wall is expressed as normalized percentage of the total distance between the ventricle and the pial surface (**Fig. 2.2K-L** see Methods for details). This normalized distribution analysis demonstrates that after 4 div, approximately 30% of electroporated cells successfully migrated to the CP-MZ layers in *Ngn2+/+* slices whereas less than 10% of electroporated cells do so in the *Ngn2-/-* slices (**Fig. 2.2M-N**). In contrast a significantly higher percentage of electroporated cells remain in the lower IZ and SVZ regions of the *Ngn2-/-* slices compared to control *Ngn2+/+* slices (**Fig. 2.2M-N**).

This quantitative analysis suggests that *Ngn2* is required for the proper initiation of radial migration by cortical progenitors. However, a potential caveat of this analysis is due to the long-term consequences of the complete *Ngn2* loss-of-function on the fate of cortical progenitors. In fact, several studies have already demonstrated that *Ngn2* plays an essential role in the early specification of the molecular identity of dorsal telencephalic neurons (reviewed in Schuurmans and Guillemot, 2002). At E12.5 dorsal progenitors in *Ngn2* knockout upregulate *Mash1*, a bHLH transcription factor normally expressed predominantly by ventral progenitors of the GE which plays an important role in the specification of the phenotype of GABAergic neurons of the striatum and cortex (Fode et al., 2000; Parras et al.,

2002; Schuurmans et al., 2004). Therefore, there are long-term fate changes of knocking out *Ngn2* expression in dorsal telencephalic progenitors that could indirectly affect the migratory properties of their daughter neurons.

Acute conditional deletion of *Neurogenin2* in cortical progenitors alters the initiation of radial migration

In order to circumvent some of these long-term effects, we performed an acute deletion of *Ngn2* expression in cortical progenitors, using Cre-mediated deletion of *Ngn2* specifically in dorsal telencephalic progenitors. This was achieved by using *ex vivo* electroporation of a plasmid expressing Cre recombinase-IRES-EGFP in E14.5 cortical progenitors harboring a conditional allele of Ngn2 (*Ngn2*^{KIFloxNgn2Flox}; see Methods for detail). As shown in **Figure 2.3A-B**, our electroporation technique leads to a high co-expression of high levels of Cre-recombinase and EGFP in E14.5 cortical progenitors within the VZ in less than 24 hours *in vitro*. In order to demonstrate that this electroporation-mediated Cre-recombinase expression is efficiently knocking out Neurogenin2 protein expression, we performed anti-Ngn2 immunofluorescent staining of the slices electroporated with pCIG2:Cre-IRES-EGFP. As shown in **Figure 2.3C-D** Ngn2 immunoreactivity is markedly decreased in cells expressing Cre recombinase-IRES-EGFP. After 4 div, control (EGFP only) electroporation of *Ngn2*^{KIFloxNgn2Flox} E14.5 cortical slices results in a robust neuronal migration outside the VZ-SVZ into the IZ and up to the CP (**Fig. 2.3E** and **2.3G**). In contrast E14.5 *Ngn2*^{KIFloxNgn2Flox} cortical slices electroporated with Cre-recombinase present a pronounced neuronal migration defect with very few neurons reaching the CP (**Fig. 2.3F** and **2.3G**). These results reinforce our conclusion that *Ngn2* is necessary to specify the migration properties of cortical neurons.

One caveat of this interpretation is that this acute loss of Ngn2 function approach affects the percentage of electroporated EGFP-expressing cells expressing pan-neuronal

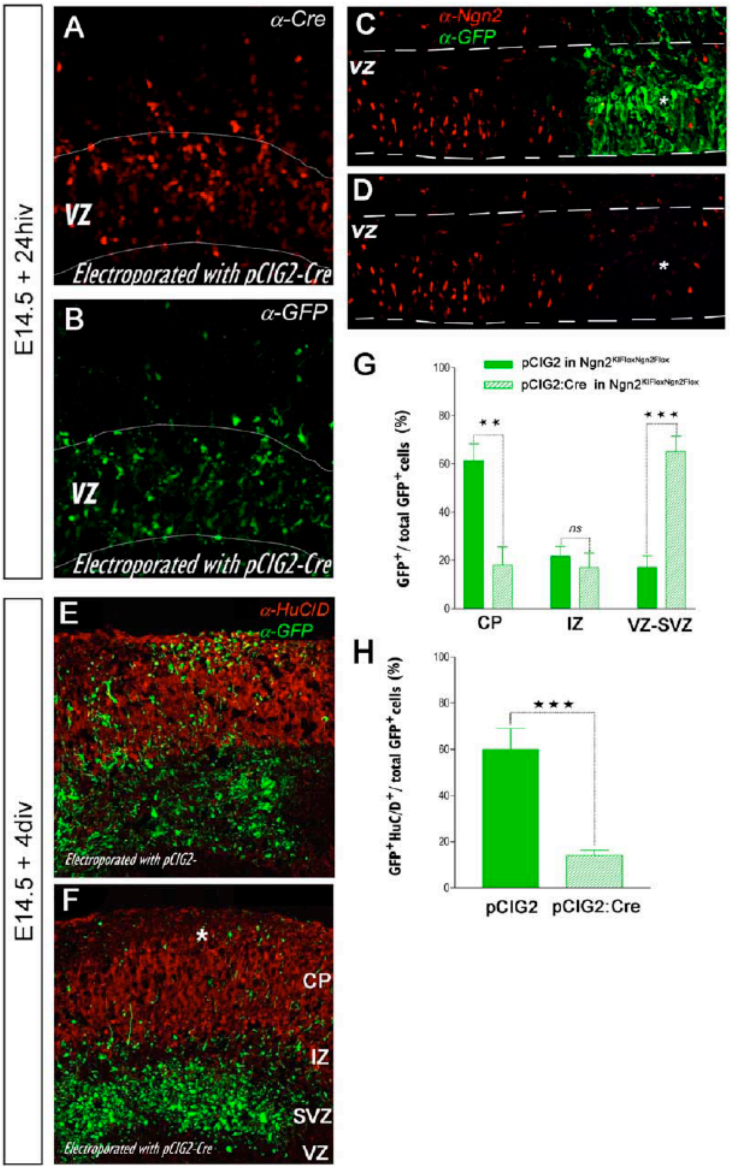

Figure 2.3 - Acute deletion of Ngn2 expression in E14.5 cortical progenitors impairs radial migration

(A and B) Ex vivo electroporation of E14.5 dorsal telencephalic progenitors using a pCIG2:Cre-recombinase-IRES-EGFP followed by in vitro organotypic slice culture for 24 hr in vitro results in high-level of coexpression of Cre-recombinase (A) and EGFP (B). **(C and D)** Electroporation of Cre-recombinase in cortical progenitors from Ngn2KIFloxNgn2Flox E14.5 embryos (C) results in a pronounced downregulation of Ngn2 protein expression (star in [C] and [D]) in the VZ. **(E and F)** Acute deletion of Ngn2 expression in cortical progenitors results in a pronounced decrease in the number of neurons reaching the CP (star in [F]) compared to control electroporation (EGFP only) in Ngn2KIFloxNgn2Flox E14.5 progenitors (E). Red: immunofluorescence against the neuronal marker HuC/D in (E) and (F). **(G)** Quantification of the percentage of EGFP+ cells located in the VZ-SVZ, IZ, or CP compartments. For both (G) and (H), n = 7 slices, unpaired t test, **p < 0.01, ***p < 0.001. **(H)** Quantification of the percentage of GFP+ cells expressing the neuronal marker HuC/D reveals a pronounced proneural defect in progenitors where Ngn2 was deleted (pCIG2::Cre) compared to control transfected progenitors (pCIG2).

markers such as HuC/D as an index of the proneural potential of cortical progenitors (**Fig. 2.3H**). This quantification reveals that after 4 div, only 15% of cells electroporated with Cre-expressing vector in *Ngn2*^{KIFloxNgn2Flox} slices expressed the neuronal marker HuC/D against approximately 60% in *Ngn2*^{KIFloxNgn2Flox} slices electroporated with control (EGFP only). This result suggests a strong proneural defect due to the acute inactivation of Ngn2 expression in cortical progenitors which is compatible with the well-documented function of *Neurogenins* (reviewed in Bertrand et al., 2002). Therefore, the migration defect characterizing both the complete and the conditional loss of *Ngn2* function could be a secondary consequence of the inability of cortical progenitors to initiate neuronal differentiation and possibly exit the cell cycle. The dominant proneural function of this class of transcription factors represents one of the main limitations in the exploration of their other potential functions in neuronal subtype specification. To overcome this limitation, we decided to perform a structure-function analysis of Ngn2 in order to isolate potential residues that could uncouple the proneural activity of Neurogenin2 from its potential function in the phenotypic specification of neuronal subtypes.

Neurogenin2 is tyrosine phosphorylated *in vivo*

The alignment of chick (*Gallus gallus*), mouse (*Mus musculus*) and human (*Homo sapiens*) Ngn2 protein sequences revealed a complete conservation of the bHLH domains and a partial conservation of domains of unknown function in the amino- (N-) and carboxy- (C-) terminal domains (**Fig. 2.4A**). Interestingly, the N- and C-terminal domains of Ngn2 are also highly divergent from Ngn1 and Ngn3, two of its most closely related homologues in the mouse genome (**Fig. 2.4B**). In order to isolate potential residues of Ngn2 outside the DNA-binding domain that might mediate neuronal subtype specification, we first sought to determine if Ngn2 was post-translationally modified and specifically if it was phosphorylated in cortical progenitors. Using electroporation of myc-tagged Ngn2 in E14.5 cortical

progenitors followed by 24 hours of cortical wholemount culture *in vitro* in the presence of $^{\gamma 32}$P-labeled ATP (**Fig. 2.4C**) we found that Ngn2 is phosphorylated in cortical precursors (**Fig. 2.4D**).

To examine the putative phosphorylation sites in Ngn2, we used a sequence- and structure-based prediction program (Blom et al., 1999; see Experimental Procedures) which predicted 15 potential serine residues, 4 threonine residues and 3 tyrosine residues displaying a significant ($p>0.90$) probability of phosphorylation (data not shown). Using electroporation of a GST-Ngn2 fusion protein in cortical precursors followed by GST-pulldown and thrombin cleavage of Ngn2 from GST, we found that Ngn2 is tyrosine phosphorylated *in vivo* using anti-phosphotyrosine immunoblotting (**Fig. 2.4E**). Using GST-pulldown in undifferentiated P19 cells in order to increase the protein yield we were able to confirm that Ngn2 is tyrosine phosphorylated (**Fig. 2.4F**). Furthermore we found that tyrosine 241 is the major site for tyrosine phosphorylation in Ngn2 since its mutation into a non-phosphorylatable phenylalanine residue ($Ngn2^{Y241F}$) drastically reduced the signal detected by phosphotyrosine immunoblotting.

Therefore we focused our effort on the effects of mutating tyrosine 241. In addition, mutations of the two other tyrosine residues presenting a high probability to get phosphorylated (Y226F and Y252F) did not produce any detectable effects on the acquisition of neuronal migration properties or dendritic morphologies (see **Suppl. Fig. 2.5** and data not shown). Interestingly, tyrosine 241 (i) is part of a proline-rich motif (YWQPPPP, boxed in **Fig. 2.4A**) that constitutes a predicted binding site for SH3-containing proteins, (ii) is mammalian-specific (not conserved in chick but perfectly conserved in human) and (iii) is specific to Ngn2 (not present in mouse Ngn1 or mouse Ngn3; see box in **Fig. 2.4B**).

In order to test the requirement of the DNA-binding properties of Ngn2 in mediating some of its biological functions, we also produced a DNA-binding incompetent form of Ngn2 by substituting the last two basic/polar residues of the basic domain (position 123-124

Figure 2.4 - Neurogenin2 is tyrosine phosphorylated in cortical precursors

(A) Alignment of human (Homo sapiens NP_076924), mouse (Mus musculus NP_033848), and chick (Gallus gallus NP_990127) Ngn2 protein sequences. The asterisks indicate the position of the four tyrosine residues conserved in mouse and human Ngn2 proteins. The arrowheads indicate the tyrosine residues presenting a high probability of phosphorylation that we mutated into phenylalanine residues.

(B) Alignment of mouse Ngn2 (MATH4A; NP_033848), Ngn1 (MATH4C; NP_035026), and Ngn3 (MATH4B; NP_033849) protein sequences reveals a high level of conservation of their bHLH domains but a low level of conservation of the N- and C-terminal domains including the YWQPPPP motif in the C-terminal domain of Ngn2 (boxed in [A] and [B]), which is not found in Ngn1 or Ngn3.

(C) Photomicrograph showing the high electroporation efficiency of myc-tagged Ngn2 (myc-Ngn2-IRES-EGFP) obtained by ex vivo electroporation of E14.5 dorsal telencephalic progenitors subsequently cultured as wholemount for 24 hr in vitro (HIV).

(D) Anti-myc immunoprecipitation (IP) of Ngn2 in E14.5 cortical progenitors as shown above. Minus lane: control (EGFP only) electroporation. Right panel: 32P autoradiogram of telencephalic wholemount cultures performed in the presence of γ 32P-labeled ATP reveals the presence of a phosphorylated protein corresponding to myc-Ngn2 (arrowhead at 36–40 kDa; n = 3).

(E) A GST-Ngn2 fusion protein was expressed using cortical electroporation at E14.5 followed by 24 hr of wholemount in vitro culture as shown in (C). GST-pulldown using glutathione-beads (line 1) leads to the detection of a product corresponding to GST-Ngn2 (65 kDa) using anti-GST immunoblotting. Cleavage of the GST-Ngn2 fusion protein bound to the beads by thrombin releases a small amount of GST (lane 2 at 25 kDa) and a product corresponding to Ngn2, which is detected by using an anti-phosphotyrosine antibody (Recombinant PY20 i.e., RC20 lane 5). Note that GST is efficiently released by glutathione elution (lane 3) and is not tyrosine phosphorylated (lane 6).

(F) Transfection of undifferentiated P19 cells with GST-, GST-Ngn2 fusion, or GST-Ngn2Y241F fusion followed by GST-pulldown using glutathione-beads, elution, and immunoblotting with anti-GST antibody (left blot) or anti-phosphotyrosine antibody (RC20) demonstrates that tyrosine 241 is the major tyrosine phosphorylation site in Ngn2.

(G) Mapping of the transcriptional activation domain of mouse Ngn2 in HEK 293T cells using the Gal4-UAS-Luciferase system. Gal4-Ngn2[181-213] fusion protein (but not Gal4-Ngn2[214-263]) is able to transactivate a UAS-Luciferase reporter to a similar extent as Gal4-Ngn2[181-263], suggesting that the minimal transactivation domain is located between residues 181 and 213. *p < 0.01 Mann-Whitney nonparametric test (n = 6); n.s., nonsignificant.

(H) Full-length Ngn2 as well as Ngn2Y241F induces a robust 20-fold increase (compared to control, **p < 0.001 Mann-Whitney test) in transactivation of the 1.7 kB NeuroD promoter (Huang et al., 2000a). Both Ngn2NR->AQ and Ngn2Δbasic (complete deletion basic domain) fail to transactivate this promoter in undifferentiated P19 cells.

(I–K) Immunofluorescence staining for EGFP (I) and MAP2 (J) was used to assess the proportion of E14.5 cortical progenitors differentiating into postmitotic neurons in different experimental conditions after culturing dissociated E14.5 progenitors for 5 DIV.

(L) Histogram of the percentage of neurons (MAP2+) derived from EGFP+ precursors expressing the indicated constructs. A minimum of 200 cells from four independent experiments were counted for each construct; **p < 0.01; n.s., nonsignificant; χ2 analysis.

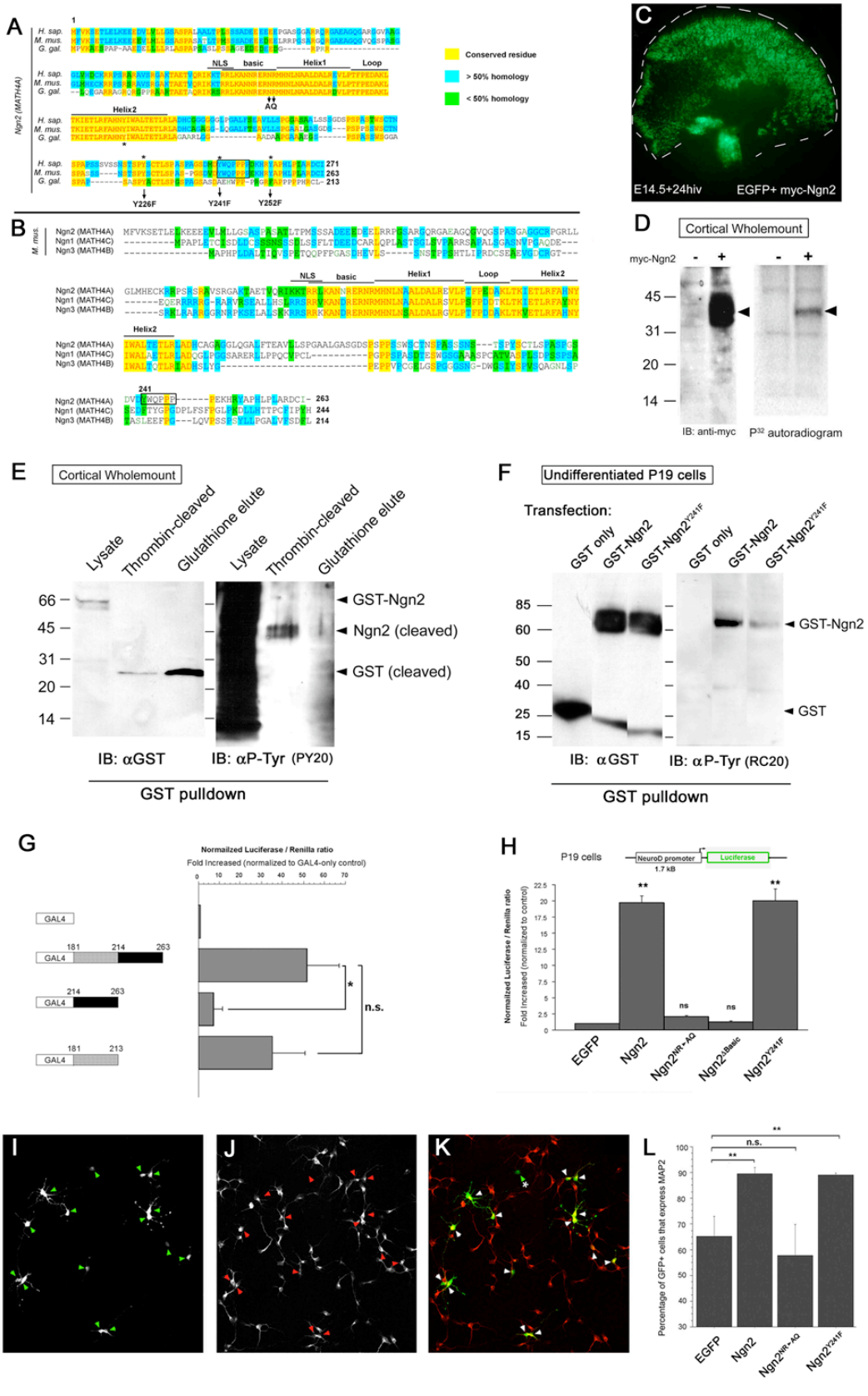
A
Ngn2 (MATH4A)
H. sap.
M. mus.
G. gal.
NLS
basic
Helix1
Loop
Helix2
AQ
Conserved residue
> 50% homology
< 50% homology
Y226F
Y241F
Y252F
B
M. mus.
Ngn2 (MATH4A)
Ngn1 (MATH4C)
Ngn3 (MATH4B)
Helix2
241
263
244
214
C
E14.5+24hiv
EGFP+ myc-Ngn2
D
Cortical Wholemount
myc-Ngn2
45
31
20
14
IB: anti-myc
P32 autoradiogram
E
Cortical Wholemount
Lysate
Thrombin-cleaved
Glutathione elute
66
45
31
20
14
GST-Ngn2
Ngn2 (cleaved)
GST (cleaved)
IB: αGST
IB: αP-Tyr (PY20)
GST pulldown
F
Undifferentiated P19 cells
Transfection:
GST only
GST-Ngn2
GST-Ngn2Y241F
85
60
50
40
25
15
GST-Ngn2
GST
IB: αGST
IB: αP-Tyr (RC20)
GST pulldown
G
Normalized Luciferase / Renilla ratio
Fold Increased (normalized to GAL4-only control)
GAL4
181
214
263
213
*
n.s.
H
P19 cells
NeuroD promoter
1.7 kB
Luciferase
Normalized Luciferase / Renilla ratio
Fold Increased (normalized to control)
**
ns
EGFP
Ngn2
Ngn2NR+AQ
Ngn2ΔBasic
Ngn2Y241F
I
J
K
L
Percentage of GFP+ cells that express MAP2
n.s.
**
EGFP
Ngn2
Ngn2NR+AQ
Ngn2Y241F

respectively NR; arrows in **Fig. 2.4A**) into non-polar residues (AQ). This double substitution (e.g. $Ngn2^{NR->AQ}$) was previously shown to abolish Ngn1- and Ngn2-mediated DNA-binding and therefore the transactivation of its direct target promoter sequences in a dominant-negative manner (Lee and Pfaff, 2003; Sun et al., 2001) without interfering with its nuclear translocation (see **Suppl. Fig. 2.2**).

We first wanted to determine if tyrosine 241 was located within the transcription-activation (transactivation) domain (TAD) of Ngn2. To our knowledge, the TAD of Ngn2 has never been mapped before. Therefore we performed a standard TAD mapping using a modified Gal4-UAS system (**Fig. 2.4G**). The TAD of most proneural bHLH transcription factors lies in the proximal or the distal portion of the C-terminal domain of the protein (Sharma et al., 1999). Therefore, we designed three Gal4 fusion proteins containing respectively (1) the entire C-terminal tail of Ngn2 (residues 181 to 263), (2) the proximal part of the C-terminal tail (residues 181 to 213; hatched in **Fig. 2.4G**) and (3) the distal domain of the C-terminal tail (residues 214-263; black in **Fig. 2.4G**). Using a normalized UAS-Luciferase reporter assay, we found that the first half of the C-terminal tail proximal to the second helix (181-213) displays transactivation properties comparable to the entire C-terminal tail (**Fig. 2.4G**). Interestingly, the distal portion encompassing residues 214 to 263 (including tyrosine 241) did not have any significant transactivation properties (**Fig. 2.4F**).

To assess more directly the transactivation properties of the mutant forms of Ngn2 used in this study, we used the 1.7 kB promoter region of *NeuroD* previously shown to be strongly transactivated by Ngn3 (Huang et al., 2000a). We subcloned this portion of the *NeuroD* promoter upstream of a luciferase reporter system and used constitutive Renilla expression to normalize for transfection efficiency in undifferentiated P19 cells. We found that Ngn2 strongly transactivates the *NeuroD* promoter (**Fig. 2.4H**; on average 20 fold $p<0.01$ Mann Whitney test n=3), whereas $Ngn2^{NR->AQ}$ and $Ngn2^{\Delta basic}$ (presenting a complete

deletion of the basic domain) both failed to transactivate the *NeuroD* promoter (**Fig. 2.4H**). Interestingly, the mutation of tyrosine 241 did not interfere with Ngn2-mediated transactivation of the *NeuroD* promoter (**Fig. 2.4H**).

Taken together with the transactivation mapping, these results suggest that tyrosine 241 does not affect the ability of Ngn2 to heterodimerize with class-I bHLH transcription factors such as E12 or E47, a function primarily mediated by the HLH domains, or to bind DNA, a function primarily mediated by the basic domain (Bertrand et al., 2002; Puri and Sartorelli, 2000).

Tyrosine 241 of Neurogenin2 is not involved in mediating its proneural activity

Next we wanted to assess the functional effect of mutating tyrosine 241 on the proneural function of N*gn2*. To do this, E14.5 cortical progenitors were electroporated, dissociated and cultured for 5 days *in vitro* at medium cell density (**Fig. 2.4I-K**). The proneural activity of Ngn2 was assessed quantitatively by scoring the percentage of Ngn2-transfected progenitors that express MAP2 after 5 div. This analysis revealed that under our serum-free culture conditions, over-expression of Ngn2 significantly increased the bias of progenitors to differentiate into MAP2+ neurons (approximately 90%; n=481 cells from 3 independent experiments; **Fig. 2.4L**) compared to control EGFP-only transfected progenitors (63%; n=357 from 3 independent experiments; **Fig. 2.4L**). Importantly, expression of $Ngn2^{NR->AQ}$ was unable to promote neuronal differentiation (n=509 cells; 4 independent experiments; **Fig. 2.4L**) whereas expression of $Ngn2^{Y241F}$ had a proneural activity that was undistinguishable from wild-type Ngn2 (n=377 cells; 4 independent experiments; **Fig. 2.4L**). These results demonstrate that the proneural activity of Ngn2 is (1) at least partially dependent on its DNA-binding properties as previously shown (Lee and Pfaff, 2003; Sun et al., 2001), and (2) importantly the proneural activity of Ngn2 does not require the integrity of tyrosine 241.

Ngn2 specifies the radial migration properties of cortical progenitors in a DNA-binding independent manner

We used the *ex vivo* cortical electroporation technique to study the radial migration properties of neurons generated by cortical progenitors forced to express various mutant forms of Ngn2. As shown above, control electroporations performed at E14.5 resulted in the radial migration of a synchronous cohort of neurons, with approximately one third of the total number of cells electroporated accumulating at the top of the cortical plate after 4 div (**Fig. 2.5A** and **2.5E**). Overexpression of wild-type Ngn2 in E14.5 cortical progenitors, increases significantly the proportion of cells recruited to the SVZ and the proportion of neurons initiating radial migration and accumulating in the CP (**Fig. 2.5B** and **2.5F**).

Surprisingly, the radial distribution of cells expressing $Ngn2^{NR->AQ}$ did not differ significantly from the distribution observed after expression of full length Ngn2 and certainly did not impair the radial migration properties of E14.5 cortical neurons (**Fig. 2.5C** and **2.5G**). Importantly, expression of $Ngn2^{Y241F}$ in E14.5 cortical progenitors almost completely abolished the radial migration of cortical neurons into the cortical plate, with the majority of neurons accumulating in the IZ and being unable to penetrate into the CP (**Fig. 2.5D** and 2.**5H**). None of the differences in migration exhibited following forced expression of $Ngn2^{Y241F}$ could be attributed to defects in neuronal differentiation as the same proportion of EGFP+ expressed the post-mitotic markers TuJ1 and MAP2 in the IZ of electroporated slices (RH, DB and FP data not shown; see also **Fig. 2.4H-K**). It is worth emphasizing that the forced expression of $Ngn2^{Y241F}$, but not expression of $Ngn2^{NR->AQ}$, phenocopies the complete and the conditional loss of *Ngn2* function (see **Fig. 2.2** and **Fig. 2.3**). The radial migration arrest in the IZ due to expression of $Ngn2^{Y241F}$ by cortical progenitors is unlikely to be due to an indirect effect on the structure of the radial scaffold since both at short-term (36 hiv) and long-term (4 div) time points, radial glial processes are unaffected by expression of $Ngn2^{Y241F}$ (**Suppl. Fig. 2.3**).

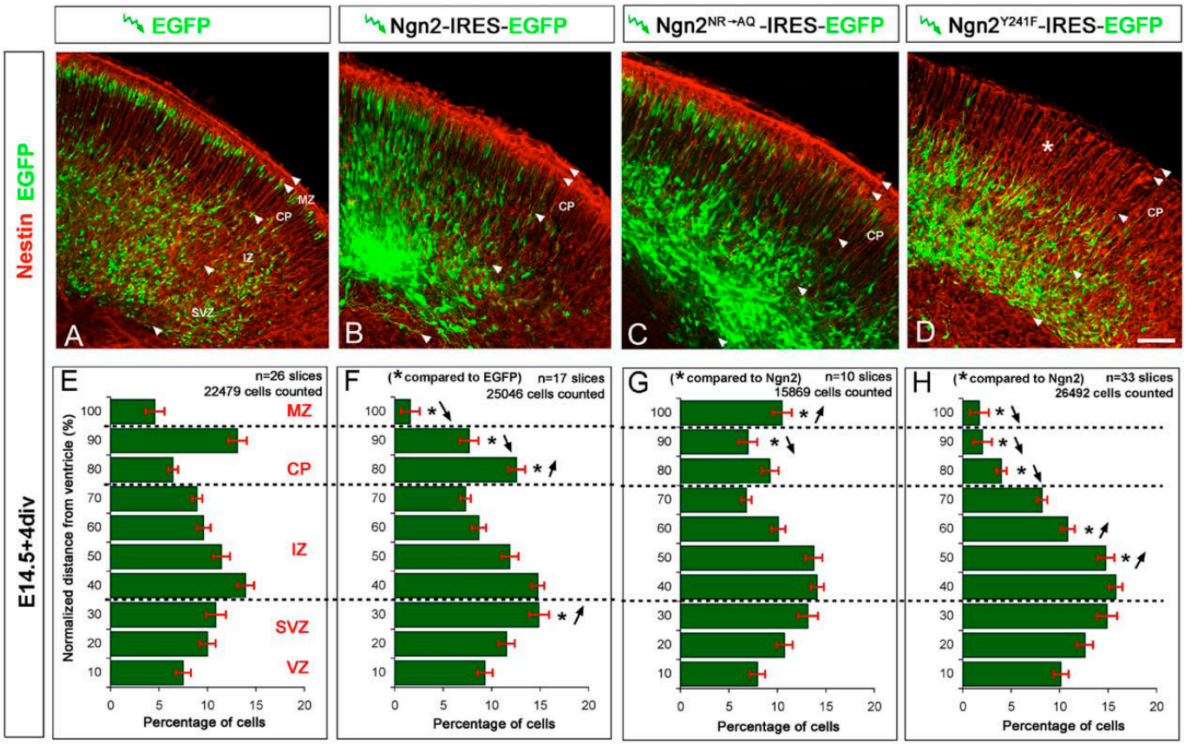

Figure 2.5 - Phosphorylation of tyrosine 241 in Ngn2 is necessary to specify the radial migration properties of cortical progenitors
(A) Ex vivo electroporation of E14.5 cortical progenitors followed by organotypic slice culture for 4 DIV (see also Figure S1) allows the visualization of the radial migration properties of a single cohort of neurons to the top of the CP. Red counterstaining is anti-Nestin immunofluorescence revealing the intact structure of the radial glial scaffold in all four conditions. **(B and C)** Electroporation of full-length Ngn2 or Ngn2NR->AQ increases the number of cortical progenitors engaging in radial migration in the IZ and reaching the CP. **(D)** Electroporation of Ngn2Y241F results in a premature arrest of migration in the IZ (star) beneath the CP. **(E–H)** Histograms of the distribution of EGFP+ cells along the radial extent of the cortical wall (normalized as a percentage). Error bars represent standard error to the mean. *p < 0.01; $\chi 2$ comparing equivalent bins (Scale bar value in (A)–(D), 200 μm).

These results strongly suggest that the inhibition of radial migration resulting from the expression Ngn2^{Y241F} in cortical progenitor is dominant over endogenously expressed Ngn2 in cortical progenitors (see **Fig. 2.1**). In order to test directly if Ngn2^{Y241F} acts as a dominant-negative over Ngn2, we performed a set of co-electroporations aimed at expressing different ratios of full length Ngn2 and Ngn2^{Y241F} (**Suppl. Fig. 2.4**). When expressed at a 1:1 or even a 10:1 ratio over full length Ngn2, Ngn2^{Y241F} (**Suppl. Fig. 2.4B** and **2.4C** respectively) is still inhibiting significantly radial migration compared to control electroporation of wild-type Ngn2 alone (**Suppl. Fig. 2.4A**). Therefore, we conclude that Ngn2^{Y241F} acts as a dominant-

negative over Ngn2, probably by binding competitively to rate-limiting effectors and therefore preventing wild-type Ngn2 to interact with these effectors that could be necessary to transactivate specific target promoters of genes involved in regulating radial migration and/or neuronal polarity (see below and **Fig. 2.2.9**).

Expression of Ngn2^{Y241F} impairs the polarity and nucleokinesis of radially migrating neurons

In order to gain insights into the cellular mechanisms underlying the function of the Y241 residue in Ngn2, we coupled *ex vivo* cortical electroporation with slice culture and time-lapse confocal microscopy to document the dynamics of radial migration of neurons expressing endogenous wild-type Ngn2 (**Fig. 2.6A**) or Ngn2^{Y241F} (**Fig. 2.6B**). This analysis reveals that progenitors expressing Ngn2^{Y241F} are able to transit from the SVZ into the IZ but when they should engage radial migration these cells display a striking loss of the polarity of their leading process outgrowth (red arrow in **Fig. 2.6B**) as well as failure to undergo nucleokinesis (three cells pointed in **Fig. 2.6B**). Our quantification demonstrate that cells expressing Ngn2^{Y241F} display a significant decrease of the rate of cell body translocation (**Suppl. Fig. 2.5A**) and a significant increase of the rate of leading process branching (**Suppl. Fig. 2.5B**) compared to progenitors expressing endogenous wild-type Ngn2.

Rescue of the migration defect due to *Neurogenin2* loss-of-function by inhibition of RhoA function

In order to improve our understanding of the molecular mechanisms underlying the role of *Ngn2* in specifying the radial migration properties of pyramidal neurons, we took advantage of a recent substractive hybridization screen (Mattar et al., 2004) that led to the identification of several Ngn2-target genes in the developing cortex. Interestingly, several of these putative Ngn2-target genes have been previously shown to be critical for radial migration such as *Doublecortin* (*Dcx*; Bai et al., 2003; des Portes et al., 1998; Gleeson et al.,

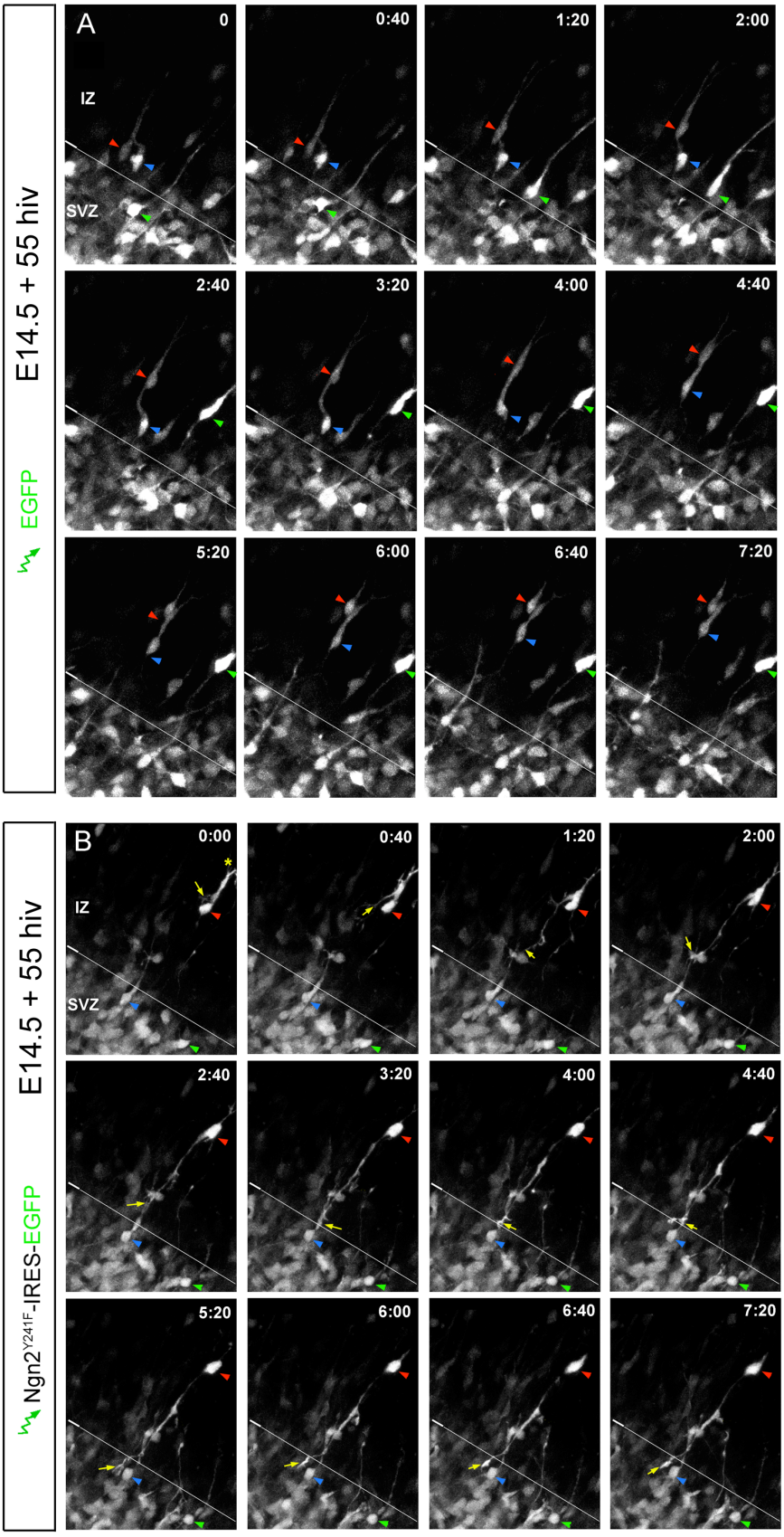

Figure 2.6 – Expression of Ngn2Y241F impairs the polarity of neu-rons initiating during radial migration in the intermediate zone

(A) Time-lapse confocal microscopy images showing the dynamics of radial migration for neurons transitioning from the SVZ to the IZ (time stamp in hours: minutes). Colored arrows (red, green, and blue) point to individual control cells electroporated with EGFP, which display the characteristic unipolar morphology of migrating neurons with a single leading process directed toward the pial surface (top of the pictures).

(B) In contrast, neurons expressing Ngn2Y241F display a striking polarity defect where some cells (red arrow) lose their pre-existing leading process (pointed by asterisk in [B]) and extend a process toward the ventricle instead (yellow arrow). In addition, all three cells pointed to by arrows fail to translocate their nucleus toward the leading process and as a result fail to move during the entire duration of the movie.

1998). However, several other target genes have no known function in regulating neuronal migration. Among those, two genes encode two distinct Rho-family of GTPase Activating Proteins (Rho-GAPs) called *RhoGAP5* (also called *ARHGAP5* or *p190 Rho-GAPb*) and *Formin Binding Protein 2* (*FNBP2*; Katoh, 2004; also called *srGAP2* Coyle et al., 2004; Wong et al., 2001). Interestingly, *FNBP2* is specifically down-regulated in cortical progenitors of E13.5 Ngn2 knockout mice compared to wild-type littermates (Mattar et al., 2004). Rho-GAPs act as negative regulators of small-GTPase activity by increasing GTPase catalytic activity therefore promoting the GTP to GDP exchange (Ridley et al., 2003). Interestingly, the small-GTPase RhoA itself is specifically expressed at high levels by cortical progenitors but is sharply down-regulated during the initiation of radial migration in the IZ (Olenik et al., 1999). Given the known function of activated-RhoA in inhibiting non-neuronal cell migration (Arthur and Burridge, 2001) and the down-regulation of two Rho-GAPs in Ngn2 knockout cortical progenitors, we hypothesized that (1) inhibition of RhoA activity is normally a pre-requisite to initiate radial migration outside the VZ/SVZ into the IZ and therefore that (2) a failure to up-regulate the expression of RhoGAPs such as *RhoGAP5/ARHGAP5* or *FNBP2/srGAP2* could lead to reduced inhibition of RhoA activity in Ngn2-/- cortical progenitors impairing their ability to initiate radial migration upon cell-cycle exit.

In order to test directly if cortical progenitors failed to initiate migration in Ngn2-/- cortex at least partially because of an inability to inhibit RhoA activity, we used the electroporation technique in order to rescue the migration phenotype characterizing the Ngn2-/- cortical progenitors by expressing a dominant-negative form of RhoA ($RhoA^{N19}$; Olson et al., 1995). Expression of $RhoA^{N19}$ in E14.5 cortical progenitors of *Ngn2* knockout embryos is sufficient to rescue partially the migration defect and induces a significant proportion of neurons to leave the VZ/SVZ and migrate into the IZ (**Fig. 2.7A-D**). However,

this rescue was only partial as most migrating neurons stopped sharply at the boundary between the IZ and the CP after 4 div (**Fig. 2.7B** and **2.7D**).

Because the expression of many different genes might be altered in *Ngn2*-/- cortical progenitors that might directly or indirectly affect their migration properties, we wanted to determine if we could rescue more specifically the migration phenotype due to the expression of $Ngn2^{Y241F}$ in cortical progenitors by inhibiting RhoA activity. As shown in **Suppl. Fig. 2.7**, co-electroporation of two constructs expressing $RhoA^{N19}$-IRES-DsRed2 and $Ngn2^{Y241F}$-IRES-EGFP leads to the very high rate of co-expression of both construct.

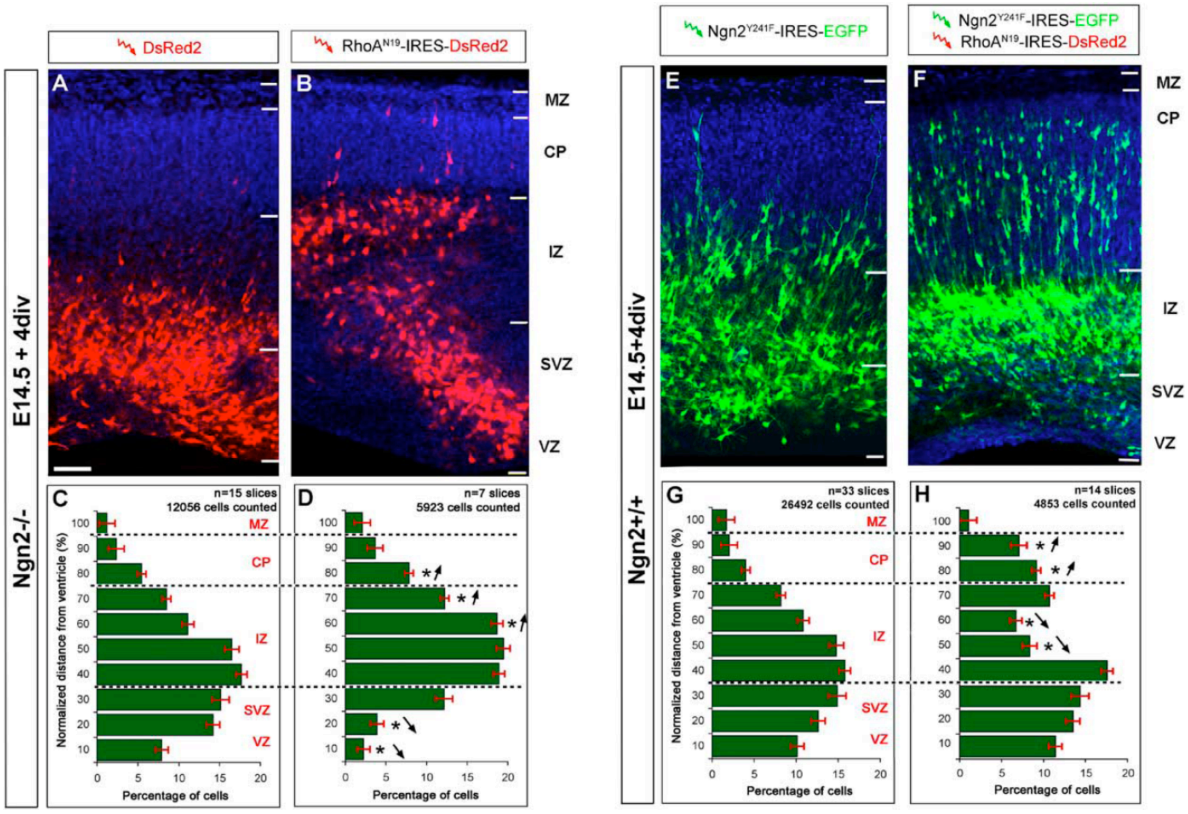

Figure 2.7 - Inhibition of RhoA activity rescues the migration defect due to Ngn2 loss of function

(A–D) Ex vivo electroporation of dominant-negative RhoA (RhoAN19-IRES-DsRed2; [B and D]) in E14.5 Ngn2-/- cortical progenitors increases the number of cells initiating migration into the IZ compared to control DsRed2 electroporation in Ngn2-/- progenitors (A and C). Note that this is a partial rescue because the majority of cells expressing RhoAN19 in the Ngn2-/- slices fail to enter the CP. **(E–H)** Coexpression of dominant-negative RhoAN19-IRES-DsRed2 and Ngn2Y241F-IRES-EGFP (F–H) almost completely rescues the migration defect caused by expression of Ngn2Y241F alone (E–G).

*$p < 0.01$ $\chi 2$ test comparing equivalent bins. Scale bar in (A), (B), (E), and (F), 50 μm.

Importantly, expression of $RhoA^{N19}$ is sufficient to rescue very significantly the inhibition of migration due to expression of $Ngn2^{Y241F}$ in cortical progenitors (**Fig. 2.7F-H**) to a level comparable to control electroporation of EGFP only (see **Fig. 2.5A** and **2.5E**) or wild-type Ngn2 (see **Fig. 2.5B** and **2.5F**).

These results demonstrate that tyrosine 241 in Ngn2 is required for the specification of the radial migration properties of cortical progenitors at least partially by inhibiting RhoA activity.

Neurogenin2 is sufficient to specify cell-autonomously the unipolar dendritic morphology of pyramidal neurons

In slices expressing EGFP only (**Fig. 2.8A**) or full length *Ngn2* (**Fig. 2.8B**), the vast majority of neurons accumulate at the top of the cortical plate after completion of their radial migration where they displayed a unipolar morphology with their leading process/apical dendrite directed towards the marginal zone (**Fig. 2.8E-F** respectively). Interestingly, expression of $Ngn2^{NR->AQ}$ resulted in a significant disorganization of the CP (**Fig. 2.8C**), even though the total number of neurons that successfully reached the upper cortical plate was comparable to full length *Ngn2*-electroporated slices (**Fig. 2.8B**). Moreover, $Ngn2^{NR->AQ}$ expressing neurons seem to ignore the upper limit of the CP and abnormally invade the MZ (**Fig. 2.5G** and see also **Fig. 2.8C**).

Importantly, expression of both $Ngn2^{NR->AQ}$ and $Ngn2^{Y241F}$ led to more severe disruption of the dendritic morphology of neurons in the CP (**Fig. 2.8G-H**). Expression of either mutations of Ngn2 affected the unipolar the dendritic morphology of immature pyramidal neurons reaching the CP in fact, a significant number of cells expressing $Ngn2^{NR->AQ}$ or $Ngn2^{Y241F}$ displayed a non-pyramidal morphology defined by the outgrowth of multiple primary dendrites from the cell body (red arrows in **Fig. 2.8G-H**). We specifically quantified the effect of expression of $Ngn2^{Y241F}$ on the dendritic morphology of cortical neurons in slices

using an computerized approach described below (see **Fig. 2.8N-P**) called the Pyramidal Morphology Index (**Suppl. Fig. 2.8**). These results suggested that the integrity of tyrosine 241 in Ngn2 is necessary to specify the polarity of leading process/apical dendrite outgrowth, one of the defining features of pyramidal neurons.

The interpretation of the effects we observed on the polarity of dendritic outgrowth in neurons expressing $Ngn2^{Y241F}$ in slices is complicated by the fact that this defect could be a secondary consequence of migration defects as previously observed in the developing cortex of the *reeler* mutant mouse for example (Pinto Lord and Caviness, 1979; Pinto-Lord et al., 1982). In other words, the unipolar dendritic morphology of pyramidal neurons in the cortical plate may depend on the ability of these neurons to respond to appropriate extracellular cues, which may not be the case for neurons expressing $Ngn2^{Y241F}$ given that their migration is abnormal or retarded.

In order to determine if *Ngn2* plays a direct role in the specification of the dendritic morphology of pyramidal neurons in the cortex, we took advantage of the fact that previous studies have shown that when cortical progenitors are dissociated and cultured from 5 to 7 days *in vitro* at low to medium cell density to minimize cell-cell contacts, these progenitors give rise to neurons that fail to display the unipolar morphology characterizing pyramidal neurons *in vivo* (Peters and Kara, 1985a; Peters et al., 1985) and instead display multipolar morphologies (Hayashi et al., 2002; Threadgill et al., 1997). Interestingly, *Ngn2* transcription is significantly down-regulated in dissociated cortical cultures (data not shown), raising the possibility that maintenance of proper level of *Ngn2* expression in cortical progenitors requires cell-cell contacts. As previously reported (Threadgill et al., 1997), cortical progenitors in dissociated cultures give rise to neurons displaying multipolar dendritic morphologies characterized by multiple dendrites emerging from the cell body (arrowheads in **Fig. 2.8I**), and therefore failed to establish a polarized dendritic outgrowth *in vitro*. Quantification using observer-based categorization (**Fig. 2.8M**) revealed that only 30% of

the neurons in control cultures displayed a unipolar morphology characteristic of pyramidal neurons *in vivo* (i.e. one large apical dendrite emerging from the cell body), approximately 10% displayed a bipolar morphology (i.e. 2 equally wide dendrites emerging from the cell body) and approximately 60 % displayed multipolar, non-pyramidal morphologies (i.e. more than 2 dendrites emerging from the cell body). Strikingly, constitutive expression of *Ngn2* by electroporation in cortical progenitors resulted in a dramatic switch in the polarity of dendritic outgrowth, causing 60% of all MAP2-positive neurons to display a unipolar dendritic morphology characterized by one large apical dendrite and a single axon emerging from the opposite side of the cell body (**Fig. 2.8J** and **2.8M**). Importantly, neither $Ngn2^{NR->AQ}$ (**Fig. 2.8K**) nor $Ngn2^{Y241F}$ (**Fig. 2.8L**) exerted the same activity as wild-type Ngn2 as both failed to promote a unipolar morphology in cortical neurons (**Fig. 2.8M**), suggesting that both the DNA-binding properties and tyrosine 241 of Ngn2 are necessary to specify the polarized dendritic outgrowth characterizing cortical pyramidal neurons.

Figure 2.8 - Ngn2 expression is sufficient to specify a pyramidal dendritic morphology

(A–D) Confocal micrographs illustrating cell organization of the CP of slices electroporated with EGFP (control; [A]), wild-type Ngn2 (B), Ngn2NR->AQ (C), or Ngn2Y241F (D). **(E–H)** Precursors expressing Ngn2NR->AQ (G) or Ngn2Y241F (H) but not EGFP (E) or full-length Ngn2 (F) give rise to neurons displaying nonpyramidal, multipolar dendritic morphologies in the CP (red arrows point to nonpyramidal neurons; white arrow to pyramidal neurons). Small arrowheads point to the axon. **(I–L)** E14.5 cortical progenitors electroporated with a control plasmid (EGFP) and maintained for 5 DIV in dissociated culture fail to establish a pyramidal morphology and instead display nonpyramidal morphologies with multiple, relatively thin dendritic processes (arrowheads; identified using MAP2, data not shown) and a unique, long and thin axonal process (arrow; MAP2 negative but neurofilament 165 kDa positive; data not shown). Expression of full-length Ngn2 (J) (but not Ngn2NR->AQ [K] or Ngn2Y241F [L]) is sufficient to restore the unipolar pyramidal dendritic morphology characterized by a unique large apical process tapering away from the cell body (arrowhead in [J]) and a unique axon (arrow in [J]). **(M)** Qualitative categorization of dendritic morphologies of cortical postmitotic neurons emerging from E14.5 progenitors electroporated by the constructs indicated in panels (I)–(L). *$p < 0.05$ and **$p < 0.01$; $\chi 2$ analysis. A minimum of 200 randomly sampled neurons from four independent experiments were examined for each treatment. **(N and O)** Definition of the Pyramidal Morphology Index (PMI) as a tool allowing unbiased categorization of dendritic morphology. The PMI is defined as the ratio between the width of the largest process and the total number of processes (as depicted in [O]) crossing a sampling circle of fixed diameter (25 μm). **(P)** Box plots of PMI values computed for a minimum of 150 neurons per experimental set (from four independent experiments). The expression of Ngn2 (but not Ngn2NR->AQ or Ngn2Y241F) increases significantly the PMI values of neurons derived from control EGFP-expressing progenitors. *$p < 0.01$ ANOVA one-way test. Box plots indicate the median (bottleneck), the 25th, and 75th percentiles (main box) as well as the 90th and 10th percentiles (top and bottom bars, respectively). Scale bars, 40 μm (A–D), 20 μm (E–H),and 30 μm (I–L).

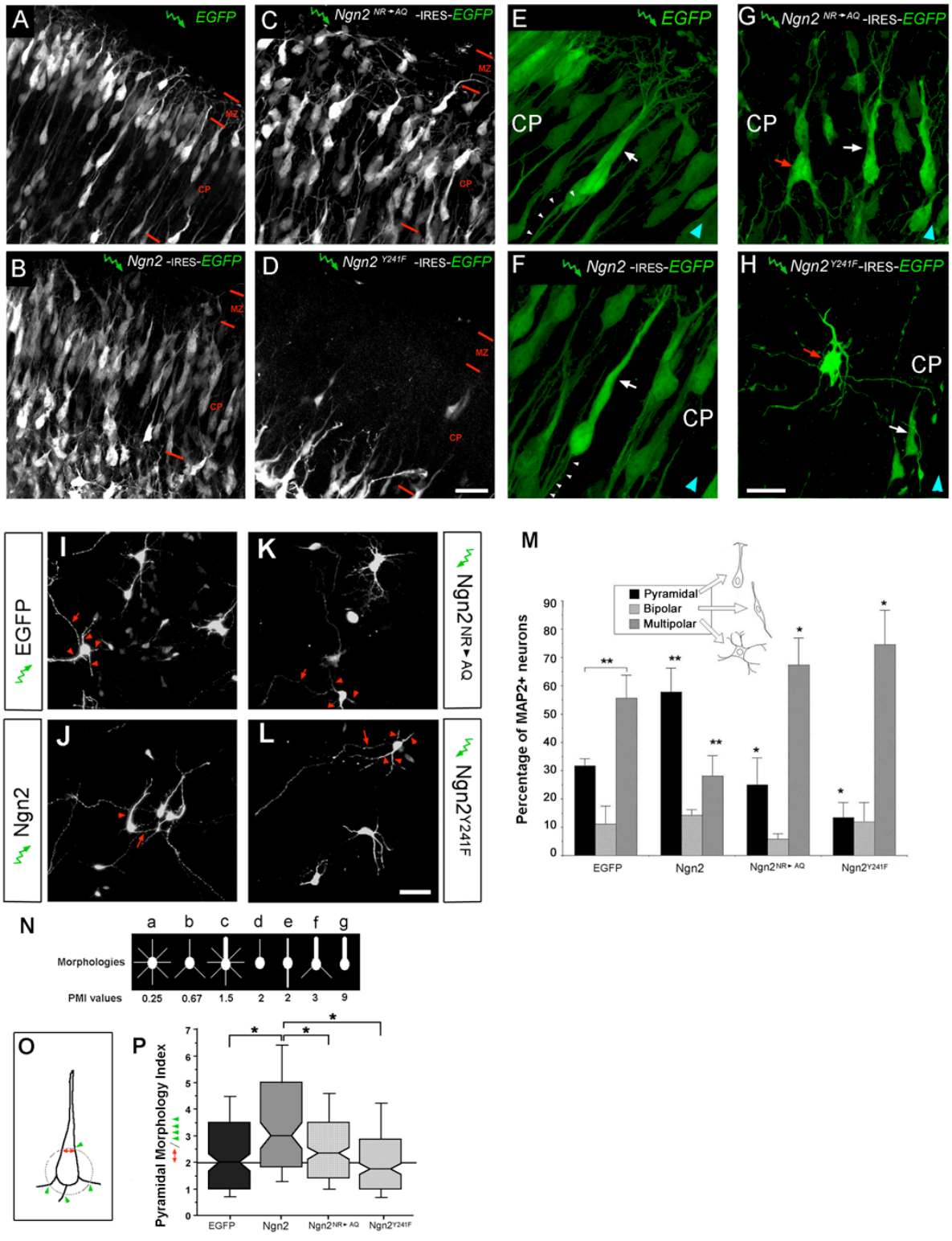
A
EGFP
MZ
CP
C
Ngn2 NR→AQ -IRES-EGFP
E
G
B
Ngn2 -IRES-EGFP
D
Ngn2 Y241F -IRES-EGFP
F
H
I
K
J
L
EGFP
Ngn2
Ngn2NR→AQ
Ngn2Y241F
M
Pyramidal
Bipolar
Multipolar
Percentage of MAP2+ neurons
N
a b c d e f g
Morphologies
PMI values
0.25 0.67 1.5 2 2 3 9
O
P
Pyramidal Morphology Index

The categorization of the dendritic morphologies of neurons is subjective and therefore heavily observer-dependent (see Discussion in Threadgill et al., 1997). In order to circumvent this general problem of qualitative and therefore potentially biased categorization, we developed a quantitative, unbiased index called the Pyramidal Morphology Index (PMI). We defined the PMI as the ratio between the width of the largest process and the total number of processes emerging from the cell body (**Fig. 2.8O**). As shown in **Figure 2.8N** on model cells, the PMI value obtained for a population of cells ranging from purely multipolar (cell a) to purely unipolar (cell g) increases with the polarity of dendritic outgrowth. The PMI index thus allows us to distinguish between two cells each of which has 3 dendrites emerging from the cell body (cells b and f), but one of which (cell f) has one apical-like dendrite process that makes it 'more pyramidal' than cell b. The measure of the width and number of processes was automatized using an Image J-based macro that we developed. This program enables to draw a 'sampling' circle of fixed diameter (25 microns) centered on the cell body, allowing the extraction of the width of each dendritic process and the total number of dendrites crossing the sampling-circle (**Fig. 2.8O**). As shown in **Figure 2.8P**, the PMI turns out to be a reliable measurement of the shift between multipolar morphologies observed in control (EGFP) cultures and unipolar morphologies observed in neurons constitutively expressing Ngn2 ($p=0.0014$; ANOVA-test). The increase in PMI values obtained in Ngn2-electroporated neurons compared to EGFP-control neurons actually corresponds to a doubling of the percentage of neurons displaying PMI values superior to 4 i.e. to most unipolar neurons.

Importantly, expression of both $Ngn2^{NR->AQ}$ and $Ngn2^{Y241F}$ failed to increase the average PMI values observed when over-expressing wild-type Ngn2 (**Fig. 2.8P**) demonstrating that both the DNA-binding properties and the tyrosine 241 residue of Ngn2

are necessary to specify the polarity of dendritic outgrowth characterizing immature pyramidal neurons.

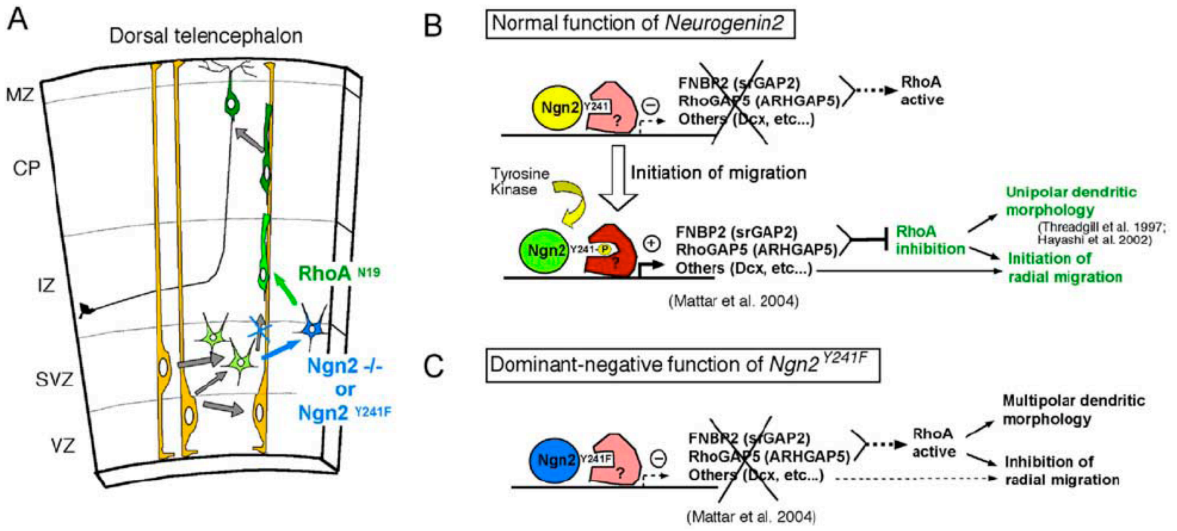

Figure 2.9 - Proposed model for Ngn2 function in the specification of the migration properties and the dendritic morphology of pyramidal neurons
(A) Radial glial cells (yellow) are proliferating and producing neurons through both asymmetrical division in the VZ and symmetrical neurogenic divisions in the SVZ (Kriegstein and Noctor, 2004; Malatesta et al., 2000; Miyata et al., 2004; Noctor et al., 2001, Noctor et al., 2002 and Noctor et al., 2004). Progenitors expressing Ngn2Y241F generate postmitotic neurons that fail to migrate past the IZ and present unpolarized, multipolar dendritic morphologies. These defects are significantly (but not completely, see Discussion) rescued by inhibiting RhoA activity.
(B) Potential mechanisms underlying the function of Ngn2 in the specification of the radial migration properties and the dendritic morphology of pyramidal neurons. We hypothesize that during the initiating radial migration (B), Ngn2 is phosphorylated on tyrosine 241, which converts one of its putative interactors from a transcriptional repressor into a transcriptional activator regulating the transcription of genes that could regulate neuronal migration and dendritic polarity such as RhoGAP proteins (FNBP2 or RhoGAP5) or Doublecortin (see Mattar et al., 2004).

Ngn1 promotes radial migration but does not promote unipolar dendritic morphology to the same extent than Ngn2

As mentioned previously the tyrosine 241 and its surrounding proline-rich motif (YWQPPPP) are not present in Ngn1 or Ngn3. We wanted to determine if Ngn2 function in the specification of the migration properties and the dendritic morphology of pyramidal neurons was specific to Ngn2 of if this is a property shared by other Neurogenins. In order to test this we electroporated both mouse Ngn1-IRES-EGFP at E14.5 to assess the migration

properties of cortical progenitors in organotypic slice culture. Our quantitative analysis demonstrate that Ngn1 (**Suppl. Fig. 2.9A** and **2.9C**) promotes the radial migration of cortical progenitors to the same overall extent than Ngn2 (**Suppl. Fig. 2.9B** and **2.9D**) despite minor differences in the actual distribution of post-mitotic neurons in the CP and MZ.

However, we found that Ngn1 does not specify the pyramidal neuronal morphology in dissociated culture of E14.5 cortical progenitors to the same extent than Ngn2 (**Suppl. Fig. 2.9E-F**). In fact the Pyramidal Morphology Index values obtained for progenitors overexpressing Ngn1 were not significantly different from control EGFP-electroporated cortical progenitors (**Suppl. Fig. 2.9F**) suggesting that Ngn2 is unique with regard to its ability to promote pyramidal dendritic morphology.

DISCUSSION

In the present study, we identified *Ngn2* as a critical element in the specification of the radial migration properties and the polarized dendritic outgrowth characterizing immature pyramidal cortical neurons. In particular, we showed that specification of the radial migration properties of cortical neurons and specifically their ability to migrate through the intermediate zone into the upper cortical plate, is controlled by Ngn2 largely through a DNA-binding-independent mechanism, but that these functions are instead critically dependent on the phosphorylation of tyrosine 241 in its C-terminal domain (**Fig. 2.4**). Interestingly, we found that tyrosine 241 is not required for Ngn2-mediated transactivation of the *NeuroD* promoter and therefore this residue is unlikely to be involved in Ngn2 DNA-binding properties, transcriptional activation (e.g. ability to recruit the general transcription machinery such as RNA polymerase II complex) or the ability to hetero-dimerize with E box proteins or Class I bHLH transcription factors (such as E12 or E47), all of which are required to transactivate Ngn2-target promoters (Bertrand et al., 2002; Puri and Sartorelli, 2000; Skowronska-Krawczyk et al., 2004). We also found that the inhibition of neuronal migration due to the

expression of Ngn2^{Y241F} can be largely rescued by inhibition of the small-GTPase RhoA. The third important finding in the present study is that Ngn2 specifies the polarized outgrowth of the apical dendrite, a characteristic feature of cortical pyramidal neurons. In contrast to Ngn2 function in migration, the ability of Ngn2 to specify a polarized dendritic outgrowth requires both the integrity of its DNA-binding properties and phosphorylation of tyrosine 241.

Coordinated specification of the radial migration properties and dendritic morphology of pyramidal neurons

Using time-lapse analysis of the morphology of single neuronal progenitors exiting the cell-cycle, several studies recently demonstrated that newly-generated neurons transiently display a multipolar, exploratory morphology in the SVZ before achieving a polarized morphology at the point when neurons initiate radial translocation into the IZ (Noctor et al., 2004; Tabata and Nakajima, 2003). The molecular cues and signaling pathways triggering this striking transition are unknown at present. Our results show for the first time that the coordinated initiation of radial migration and the acquisition of a unipolar leading process/apical dendrite outgrowth is dynamically controlled by Ngn2. Interestingly, the constitutive (**Fig. 2.2**) or the acute (**Fig. 2.3**) loss-of-Ngn2 function in cortical progenitors leads to a defect in the initiation of radial migration. However, we demonstrate that part of this defect is likely due to the proneural function of Ngn2 resulting in a pronounced defect of neuronal differentiation or cell cycle exit, which precluded the analysis of other functions of bHLH proneural transcription factors. The expression of Ngn2^{Y241F} uncouples for the first time the neuronal-subtype specification functions of *Ngn2* from its generic proneural function. Interestingly, a recent study in chick spinal cord has also shown that the proneural and the subtype specification functions of bHLH transcription factors such as Mash1 and Math1 are actually dependent on residues located outside the basic DNA-binding region, in the second Helix region (Nakada et al., 2004). These results strongly suggest that (1) bHLH

transcription factors such as Ngn2 are coordinating the acquisition of pan-neuronal properties through the control of the transcription of genes allowing cell cycle exit and initiation of generic (non-subtype specific) neuronal differentiation program involving expression of pan-neuronal markers (MAP2, βIII-tubulin, etc…) but (2) at the same time these bHLH TFs regulate the transcription of region-specific genes specifying neuronal subtype identity including migration properties (radial vs tangential) or the dendritic morphology (unipolar vs multipolar). The main finding of this study is that these two distinct functions involve different molecular modules within Ngn2.

New classification of dendritic morphology: polarized versus unpolarized initiation of dendrite outgrowth

We propose a model in which the unipolar dendritic morphology of pyramidal neurons represents a cellular consequence of their radial migration properties. Our results from dissociated cultures of cortical progenitors demonstrate that when progenitors give rise to neurons *in vitro*, the absence of appropriate cell-cell contacts (and maybe decreased Notch receptor activation), such as those that occur normally between radial glial cells and early post-mitotic neurons, results in a failure to establish a polarized, pyramidal morphology, with neurons instead acquiring a multipolar, non-pyramidal morphology characterized by an unrestricted number of primary dendrites emerging from the cell body (see **Figure 2.9** in present study and Threadgill et al., 1997). Interestingly, dissociated cortical progenitors are able to differentiate into unipolar pyramidal neurons when plated onto cortical slices in the slice overlay assay (unpublished observations; Polleux et al., 2000). Taken together these results strongly suggest that extracellular cues present in the environment of cortical progenitors during and after completion of radial migration are required for the establishment of a polarized dendritic outgrowth (Whitford et al., 2002). These results also strongly suggest that the molecular machinery specifying the migration

properties of cortical neurons (radial vs tangential) also regulate their dendritic morphology (unipolar/pyramidal vs mutlipolar/non-pyramidal). Future experiments will be aimed at determining the molecular basis linking the migration properties to the dendritic morphology of pyramidal glutamatergic and non-pyramidal interneurons in the cortex.

Candidate genes underlying the role of *Neurogenin2* in the specification of pyramidal dendritic morphology

What are the signaling pathways underlying the ability of *Ngn2* to promote radial migration and a pyramidal dendritic morphology? As mentioned earlier, a hint comes from a recent subtractive hybridization screen performed in order to identify direct and indirect downstream targets of *Ngn2* in mouse cortical progenitors (Mattar et al., 2004). Several candidate genes that might explain the effects of Ngn2 on neuronal migration and dendritic morphology were found to be downregulated in *Ngn2* knockout cortical progenitors, including the microtubule-binding protein *Doublecortin* and known regulators of Rho-like small GTPase activity involved in cell polarity and cytoskeleton dynamics, such as *Forming-Binding Protein 2* (*FNBP2* also annotated as *srGAP2* (slit-Robo GAP2; Coyle et al., 2004; Katoh, 2004) as well as *RhoGAP5* (also called *ARHGAP5* and *p190-RhoGAPb*; Mattar et al., 2004). Our results provide strong evidence that at least one of the pathway downstream of Ngn2 that regulate radial migration involves inhibition of the activity of the small-GTPase RhoA. Therefore, down-regulation of FNBP2 and/or RhoGAP5 in cortical progenitors could actually be causal to the migration defect characterizing Ngn2 loss-of-function. Future experiments will test directly the involvement of these two genes in the control of neuronal migration and dendritic morphology.

Our results also provide novel insights into the molecular control of neuronal migration and dendritic polarity in the cortex because in both rescue experiments (Ngn2 knockout and $Ngn2^{Y241F}$ electroporation), expression of dominant-negative RhoA is sufficient

to recruit the migrating neurons into the IZ but a lot of migrating neurons are stalled beneath the CP and seem to be unable to enter their final environment by bypassing their predecessors. This suggests a two step model of radial migration with a first step when early post-mitotic neurons exit the VZ/SVZ neuroepithelium and migrate into the IZ which requires phosphorylation of Ngn2 at tyrosine 241 leading to transient inhibition of RhoA activity (and maybe expression of Doublecortin; Mattar et al., 2004) and a second step controlled by Rac1/Cdc42 activity (Kawauchi et al., 2003) where neurons migrate through from the IZ into the CP (reviewed in Gupta et al., 2002).

Potential signaling pathways involved in the DNA-binding independent function of Ngn2

Several studies have already illustrated the importance of protein-protein interactions and post-translational modifications in mediating some of the biological functions of bHLH transcription factors (Lee and Pfaff, 2003; Moore et al., 2002; Olson et al., 1998; Sun et al., 2001; Talikka et al., 2002; Vojtek et al., 2003; reviewed in Puri and Sartorelli, 2000). Our results show that the DNA-binding independent function of Ngn2 in the specification of the neuronal migration properties and dendritic morphology of cortical neurons is mediated by phosphorylation of tyrosine 241. This tyrosine residue is part of a larger proline rich domain (YWQPPPP) motif that constitutes a putative SH2-binding site for non-receptor tyrosine kinase of the Tec family. This includes Interleukin-2 regulated Tyrosine Kinase (ITK; Smith et al., 2001) which is expressed by immature cortical neurons at E14.5 (Hand and Polleux, data not shown). Future experiments will be aimed at determining if ITK or other non-receptor tyrosine kinases phosphorylate tyrosine 241 of Ngn2 and how the potential phosphorylation of Y241 regulates Ngn2 function.

We hypothesize that the subtype specification activity mediated by phosphorylation of tyrosine 241 in Ngn2 involves protein-protein interaction, for example by converting a

transcriptional repressor into an activator thereby inducing the transcription of downstream target genes regulating neuronal migration and dendritic polarity such as specific Rho-GAPs (**Fig. 2.9**). This is actually the only model that would explain why $Ngn2^{Y241F}$ is acting as a dominant-negative over Ngn2 since this dominant-negative activity must involve some interaction between $Ngn2^{Y241F}$ that cannot be competed by the wild-type Ngn2. Current experiments are aimed at identifying phosphorylation-dependent interactors of the tyrosine 241 residue of Ngn2.

Is the phosphorylation of Y241 in Ngn2 a mammalian-specific feature?

The tyrosine residue in position 241 of Ngn2 that we characterized in the present study is conserved in mammals (human, rat and mouse) but not in non-mammalian vertebrates such as birds (chick). Interestingly, neurons in the dorsal telencephalon of birds (and reptiles also) accumulate according to a loose 'outside-first, inside-last' sequence (Tsai et al., 1981a, b), a pattern opposite to the inside-first, outside-last pattern characterizing all mammals (Sidman and Rakic, 1973), leading to a loosely laminated structure that lacks the six layers characteristic of the mammalian neocortex. Furthermore, studies examining the dendritic morphology of neurons in the avian telencephalic cortex revealed that very few if any neurons display a pyramidal morphology (Molla et al., 1986), contrasting to the mammalian neocortex where approximately 70 to 80% of all cortical neurons are pyramidal (Peters and Kara, 1985a; Peters et al., 1985). The ability of migrating pyramidal neurons to develop a unipolar morphology, invade the cortical plate and therefore bypass its predecessors by perforating the cell-dense cortical plate (leading to an inside-out accumulation pattern) is therefore a mammalian-specific feature (Bar et al., 2000; Gupta et al., 2002). It is tempting to speculate that tyrosine 241 belongs to a molecular motif (YWQPPPP) representing a mammalian-specific protein-protein interaction module that

might have enabled the coordinated appearance of a pyramidal unipolar morphology and the inside-out laminar accumulation of neurons during brain evolution.

Finally, this motif is specific to mammalian *Ngn2* as it is not found in the closely related mouse *Ngn1* or *Ngn3* (**Fig. 2.4B**). Interestingly, expression of mouse *Ngn1* promotes radial migration just as efficiently as Ngn2 but we found that Ngn1 does not promote pyramidal dendritic morphology of E14.5 cortical progenitors. Therefore, this implies that Ngn1 might be able to control the transactivation of RhoGAPs genes using a mechanism distinct from phosphorylation of Y241, which is not present in Ngn1. However, Ngn2 is unique in its ability to promote unipolar dendritic morphology and therefore, the phosphorylation of tyrosine 241 in cortical progenitors might represent a unique molecular mechanism among Neurogenins. Future experiments will determine the molecular basis underlying the potential differences between chick *Ngn2*, mouse *Ngn1*, mouse *Ngn3* and mouse *Ngn2* functions in the specification of cortical neurons phenotype.

EXPERIMENTAL PROCEDURES

Animals

Mice were used according to a protocol approved by the Institutional Animal Care and Use Committee at the University of North Carolina, and in accordance with NIH guidelines. All experiments were performed on wild-type C57Bl6/J mouse strain (JAX) or on Ngn2 EGFP-knockin allele backcross with C57Bl6/J mouse strain. Time-pregnant females were obtained by overnight breeding with males of the same strain and the morning following the breeding is considered as E0.5.

Immunofluorescence on cryostat sections

See supplementary Experimental Procedures.

Constructs

All Ngn2 cDNAs were subcloned into a pCIG2 vector that we modified from the pCIG vector (kind gift of Dr Andy Mc Mahon; Harvard University), which contains a (cDNA)-IRES-EGFP or a (cDNA)-IRES-DsRed2 cassette expressed under the control of a CMV-enhancer and a chicken β-actin promoter (Megason and McMahon, 2002). pCIG2 differs from pCIG in that the SV40 nuclear localization sequence 3' of the EGFP coding sequence was removed. The Cre recombinase coding sequence fused to SV40 nuclear localization sequence was obtained from pSK-Cre1 (a generous gift from Malcom Logan) and inserted into pCIG2.

Ex vivo electroporation and organotypic slice culture

A detailed protocol describing the combination of *ex vivo* electroporation of embryonic mouse cortex and organotypic slice culture will be published separately (Hand and Polleux, manuscript in preparation) and is available upon request. Briefly, electroporation of dorsal telencephalic progenitors was performed by injecting pCIG2 plasmid DNA into the lateral ventricles of isolated E14.5 embryonic mouse heads that were decapitated and placed in complete HBSS (**Supp. Fig. 2.1**; Polleux et al., 2002. Injections were performed using a Picospritzer III (General Valve) injector with 20 psi input pressure and one to four 4 msec long pulses as needed to fill the lateral ventricles. To visualize the DNA-containing solution we add 0.5% Fast Green (Sigma) at a 1:20 ratio with a high-titer plasmid DNA solution (3μg/μl endotoxin-free plasmid DNA; MEGA-Prep kit from Clontech). Electroporations were performed on the whole head with gold-coated electrodes (GenePads 5x7mm BTX; **Supp. Fig. 2.1**) using an ECM 830 electroporator (BTX) and the following parameters: two to four 100 ms-long pulses separated by 100ms-long intervals at 55V. In our transfected areas, we obtained transfection rates of close to 30% of all Nestin+ progenitors in the cortical ventricular zone of E14.5 mouse (Hand and Polleux, data not shown). Immediately after electroporation, the brain was extracted and 250 microns thick

slices were cut using a LEICA VT1000S vibratome with special care towards the integrity of the pial surface. The resulting slices were maintained in organotypic slice cultures, fixed and stained for immunofluorescence as previously described (Polleux and Ghosh, 2002). The primary antibodies used for immunofluorescence on slices were: mouse monoclonal anti-Nestin (Rat 401 Developmental Hybridoma Bank; 1:10); mouse monoclonal anti-MAP2 (Sigma); rabbit polyclonal anti-EGFP and chicken polyclonal anti-EGFP (Molecular Probes); rabbit polyclonal anti-Ngn2 that we developed [directed against amino-acid 35-49:C-SSADEEEDEELRRPG, BioGenes GmbH, Germany; used in **Suppl. Fig. 2.2**] and another rabbit polyclonal anti-Ngn2 antibody (kind gift of Dr. M. Nakafuku; used in **Figure 2.1**), rabbit polyclonal anti-Cre recombinase (Covance Research Product, 1:3000), mouse anti-HuC/D (Molecular probes, 1:200).

Dissociated cortical cultures

Dissociated E14.5 cortical cultures were performed using a papain-based enzymatic dissociation method as previously described (Polleux and Ghosh, 2002; Polleux et al., 2000). Dissociated and electroporated cortical progenitors were cultured on glass-bottom dishes coated with Laminin and Poly-L-Lysine for 5 days in serum-free culture medium (NeuroBasal +B27+N2 supplements).

Confocal microscopy

Fluorescent immunostaining was observed using a LEICA TCS-SL laser scanning confocal microscope equipped with an Argon laser (488 nm), green Helium-Neon laser (546nm) and red Helium-Neon laser line (633nm) for observation of Alexa488-, Alexa-546 conjugated secondary antibodies (Molecular Probes) and Draq5 nucleic acid staining (Alexis), respectively.

Acknowledgements

We are grateful to K. Burridge, A. McMahon, M.J. Tsai and A. Ghosh for providing constructs and Dr Nakafuku for providing the polyclonal anti-Ngn2 antibody. We also thank P. Vanderhaeghen for his comments on an earlier version of the manuscript. The Nestin (Rat-401) monoclonal antibody developed by Dr Susan Hockfield was obtained through the Developmental Studies Hybridoma Bank developed under the auspices of the NICHD and maintained by The University of Iowa, Department of Biological Sciences, Iowa City, IA 52242. We thank all members of the Polleux lab for fruitful discussions and comments on the manuscript. This project was partially funded by the National Institute of Neurological Disorders and Stroke (NIH-NINDS NS047701-01) (FP), by the Confocal and Multiphoton Imaging Facility of the NINDS Institutional Center Core Grant to Support Neuroscience Research (P30 NS45892-01) and the March of Dimes Foundation for Birth Defects (FP). PM is a recipient of a CIHR Doctoral award, LN is supported by a EMBO long-term fellowship, JITH is supported by a Postdoctoral training fellowship from Australian NHMRC. FG's lab contribution was supported by MRC core funding and an European Commission RTD Program grant.

SUPPLEMENTAL FIGURES

Supplementary Figure 2.1 - *Ex vivo* electroporation of cortical progenitors coupled to organotypic slice culture is a powerful technique to study the migration properties and dendritic morphology of cortical neurons

(A-C') Intact head of E14.5 mouse embryos where a solution containing a pCIG2 plasmid mixed with 0.5% Fast Green has been injected into the lateral ventricles (labeled LV in A). After electroporation, the brain is isolated (B) and immediately sliced using a vibratome (see Method for details). 250 μm thick sections are then plated onto a semi-permeable organotypic membrane (C) as described previously (Polleux and Ghosh, 2002). After 12 hours *in vitro*, robust EGFP expression is specifically observed in cortical progenitors here shown on five slices (live picture in C-C'). Note that the plasmid expression is precisely targeted dorsally and therefore does not transfect ventral progenitors in the ganglionic eminence.
(D-G) Confocal micrograph of a triple stained slice fixed 24 hours after electroporation showing that at this point, the vast majority of EGFP expressing cells (D) display radial glial morphologies with their cell bodies located in the VZ or SVZ and their radial glial process reaching the pial surface (arrowheads in G). The vast majority of EGFP expressing cells at 24 hiv express Nestin, a radial glial marker (E and data not shown). Nucleic acid dye Draq5 (blue) was systematically used to reveal the slices cytoarchitecture (F).
(H) After 2 days *in vitro*, EGFP+ neurons are found in the intermediate zone and start to invade the cortical plate displaying a typical unipolar morphology with a leading process directed towards the pial surface (red arrow). Arrowheads points to EGFP+ radial glial process still visible at this stage.
(I) After 4 days *in vitro*, EGFP+ neurons have reached the top of the cortical plate accumulating beneath the marginal zone (MZ). These pyramidal neurons already started differentiating with their apical dendrite branching in the MZ (arrowhead) and their axon growing ventrally towards the intermediate zone (arrow).
Abbreviations: CP: cortical plate; H: hippocampal anlage; LGE: lateral ganglionic eminence; MZ: marginal zone; IZ: intermediate zone; SVZ: subventricular zone; VZ: ventricular zone.
Scale bar values: D-G: 50 microns; H-I: 10 microns.

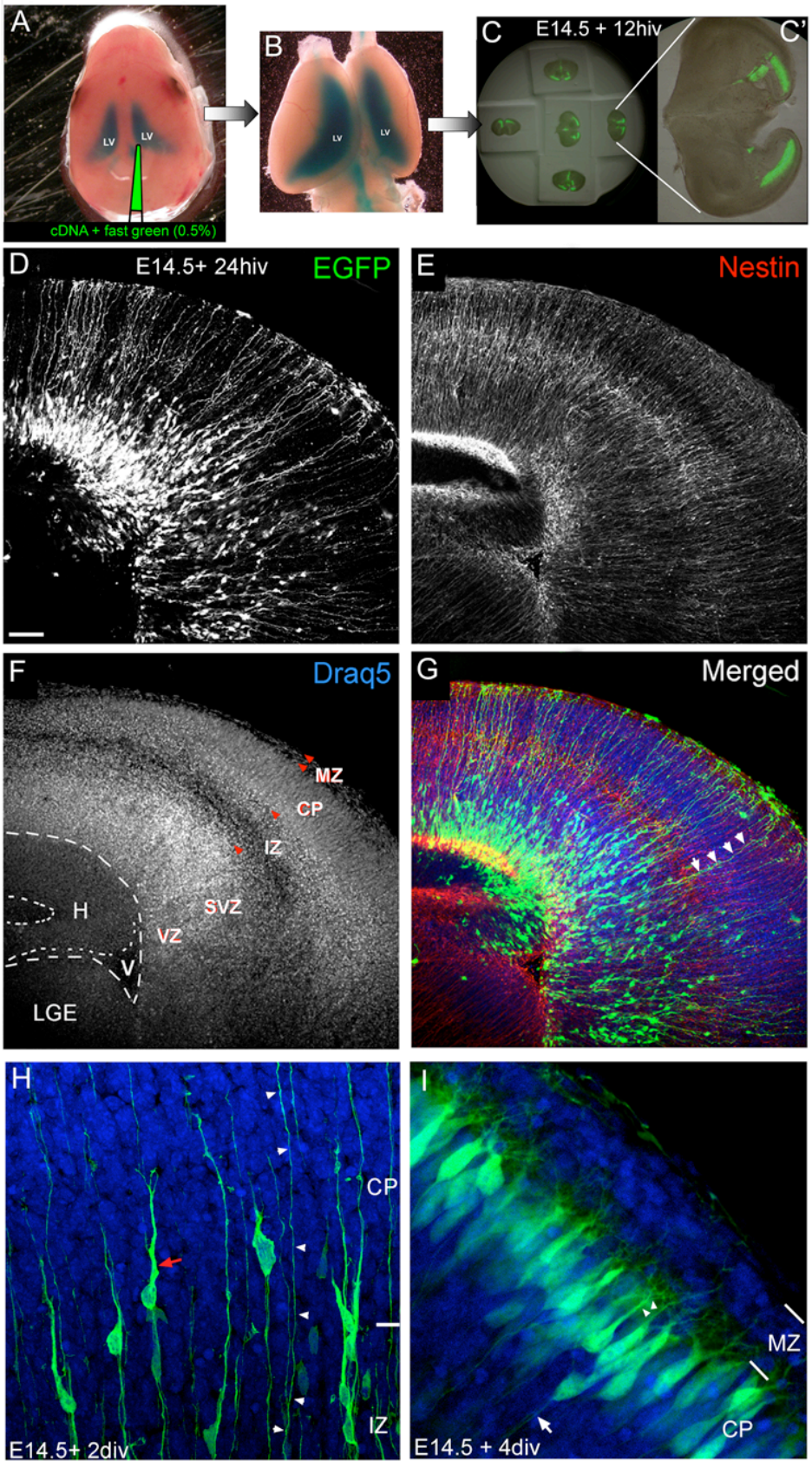
A
LV
LV
cDNA + fast green (0.5%)
B
LV
LV
C
E14.5 + 12hiv
C'
D
E14.5+ 24hiv
EGFP
E
Nestin
F
Draq5
MZ
CP
IZ
H
SVZ
VZ
V
LGE
G
Merged
H
CP
IZ
E14.5+ 2div
I
MZ
CP
E14.5 + 4div

Supplementary Figure 2.2 - Ngn2$^{NR->AQ}$ and Ngn2^{Y241F} are targeted normally to the nucleus

(**A-D)** Neurons derived from E14.5 progenitors successfully electroporated with a Flag epitope-tagged version of Ngn2 are identified by EGFP expression after 4 div (A). Immunofluorescence directed against the Flag-epitope reveals a prominent nuclear localization of Ngn2-Flag (arrowheads in B) as confirmed by the identification of the nucleus using Draq5 (C).
(E-L) Expression of Flag-tagged Ngn2$^{NR->AQ}$ (E-H) or Flag-tagged Ngn2^{Y241F} (I-L) also shows a prominent nuclear localization of Ngn2 (arrowheads in F and J respectively) demonstrating that these mutations do not interfere with nuclear targeting of Ngn2.
(M-R) Single confocal optical section (<1 microns z-section) showing that overexpression of wild-type Ngn2 or Ngn2^{Y241F} by electroporation results in physiological levels of protein expression in cortical neurons in slice culture after 3 div. Immunofluorescence against Ngn2 using a polyclonal antibody allows comparison of the endogenous level of Ngn2 expression (blue arrows in N-O and Q-R) to the level of Ngn2 overexpression in electroporated cells identified by expression of DsRed2 (arrowheads in M-O for Ngn2 and P-R for Ngn2^{Y241F}). Note again the prominent nuclear localization of both endogenous Ngn2 and ectopically expressed Ngn2 or Ngn2^{Y241F}. These cells are migrating through the IZ after 3div and were imaged using single optical section (<1 microns z-section) by confocal microscopy.
Scale bar values: A-D: 30 microns; E-H: 15 microns; I-L: 20 microns; M-R: 10 microns.

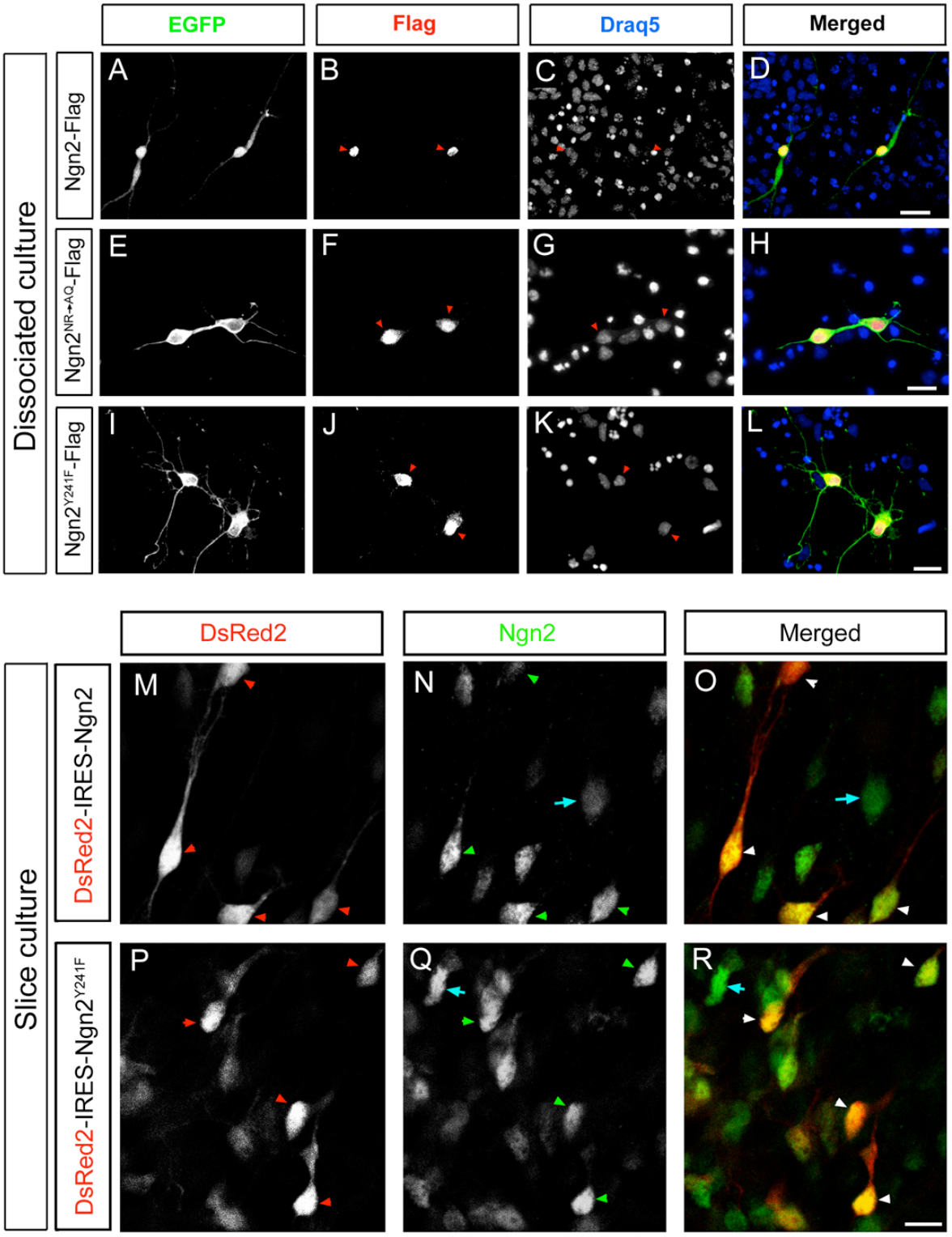
EGFP
Flag
Draq5
Merged
Dissociated culture
Ngn2-Flag
Ngn2NR→AQ-Flag
Ngn2Y241F-Flag
A
B
C
D
E
F
G
H
I
J
K
L
DsRed2
Ngn2
Merged
Slice culture
DsRed2-IRES-Ngn2
DsRed2-IRES-Ngn2Y241F
M
N
O
P
Q
R

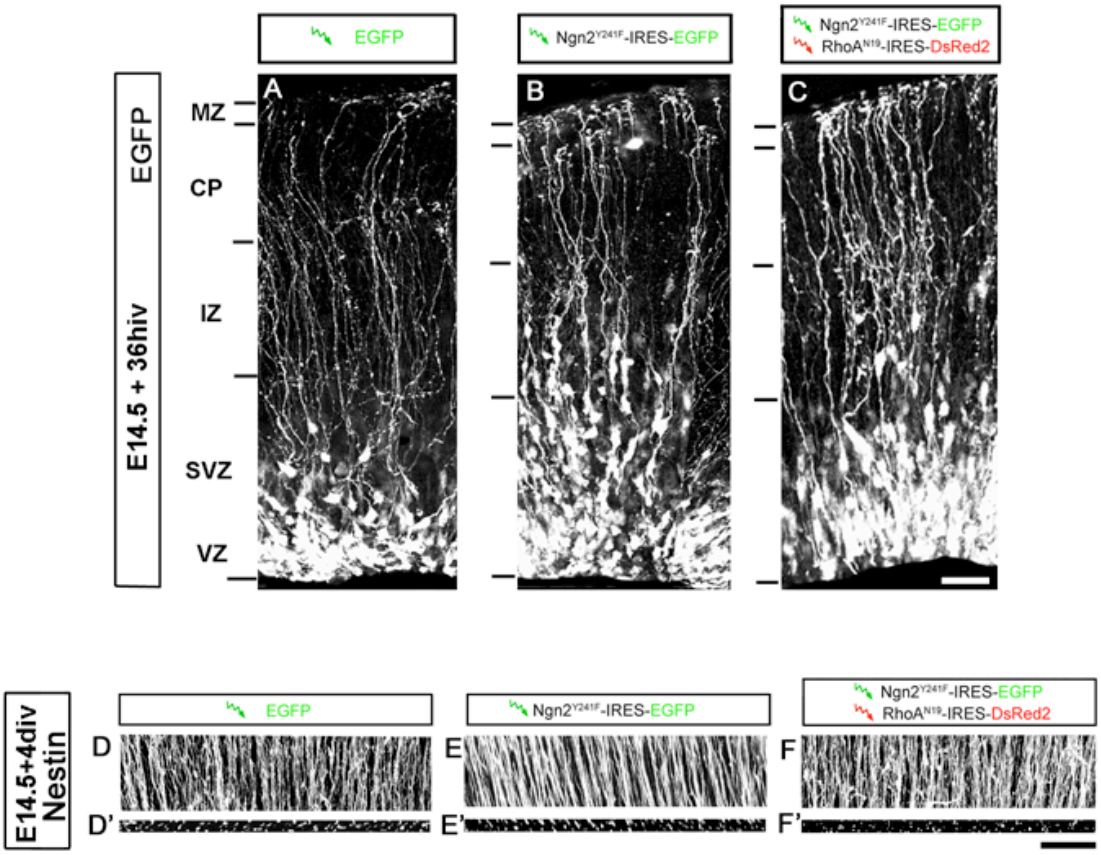

Supplementary Figure 2.3 - Expression of Ngn2^{Y241F} and/or RhoA^{N19} does not affect the structure of the radial glial scaffold

(A-C) Cortical electroporation of E14.5 progenitors with EGFP (A) Ngn2Y241F or Ngn2Y241F and RhoAN19 expressing constructs does not alter the morphology of radial glial cells after 36 hours *in vitro*. Cells still display long their radial process (green arrows) with attachment to the basal membrane of the pia (red arrowheads).
(D-F') After 4 days *in vitro* the radial glial scaffold integrity was assessed more globally using anti-Nestin immunofluorescence followed by examination using laser-scanning confocal microscopy. Both maximum projection of 10 microns stacks (D-F) and orthogonal Z-sections (D'-F') of slices electroporated with the 3 sets of constructs indicated in panels A-C did not have any significant effect on the morphology or the number of radial glial processes.
Scale bar values: 50 microns in A-C; 25 microns in D-F'.

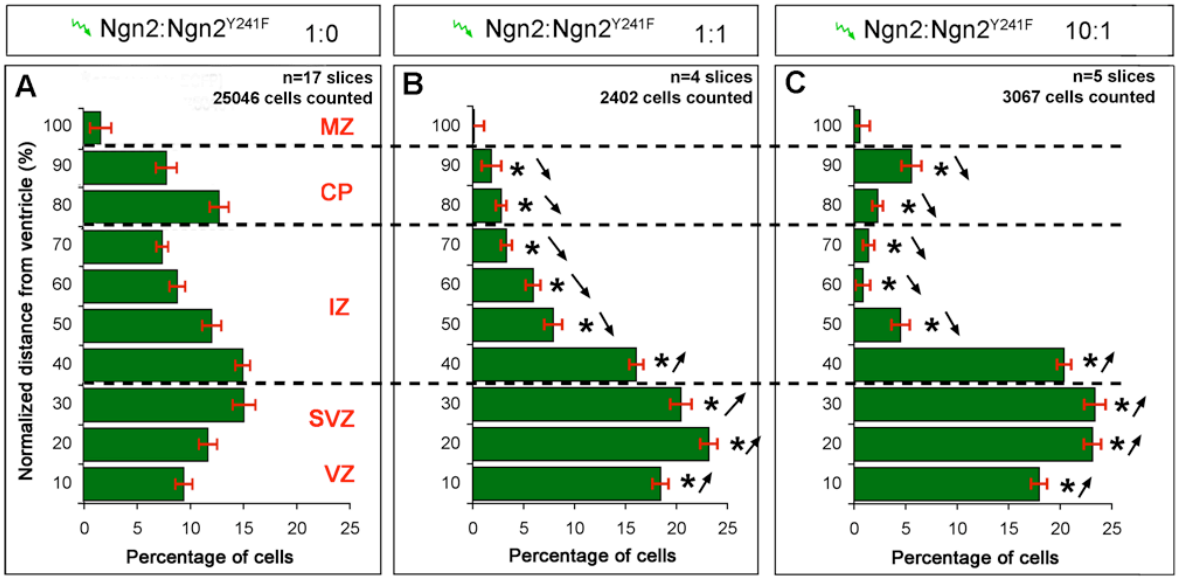

Supplementary Figure 2.4 - Demonstration of the dominant-negative nature of Ngn2^{Y241F} over full-length Ngn2

(A-C) Histograms of the radial distribution of cells derived from progenitors co-electroporated with different ratios of Ngn2 versus Ngn2^{Y241F} (1:0 in A; 1:1 in B and 10:1 in C). Note that at a 1:1 ratio or a 10:1 ratio, cortical progenitors are still strongly inhibited in their ability to migrate radially suggesting that Ngn2^{Y241F} is playing a dominant-negative function over Ngn2.
Error bars represent standard error to the mean. Stars indicate significant ($p<0.01$- Chi square) differences of the proportion of neurons find in similar bins in B or C compared to A.

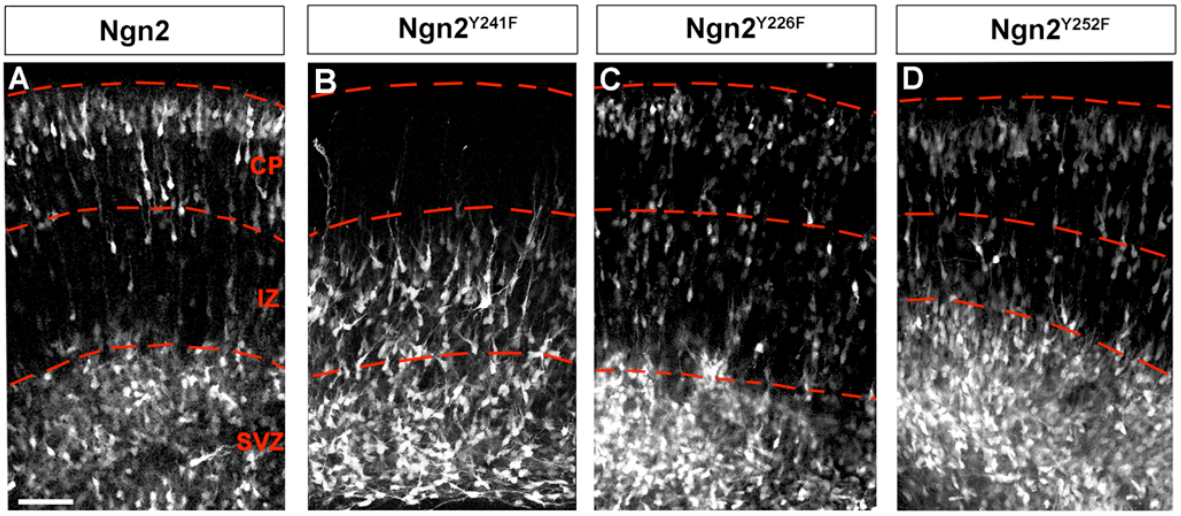

Supplementary Figure 2.5 - Specificity of tyrosine 241 in inhibiting the radial migration properties of cortical progenitors

(A-D) Confocal micrograph of wild-type E14.5 slices electroporated *ex vivo* with full-length Ngn2 (A), $Ngn2^{Y241F}$ (B), $Ngn2^{Y226F}$ (C) and $Ngn2^{Y252F}$ (D). Only expression of $Ngn2^{Y241F}$ inhibits the radial migration of cortical progenitors, expression of either $Ngn2^{Y226F}$ (C) or $Ngn2^{Y252F}$ has no effect on the migration properties of cortical progenitors with a similar proportion of neurons reaching the cortical plate (C-D) compared to full-length Ngn2 electroporation (A).

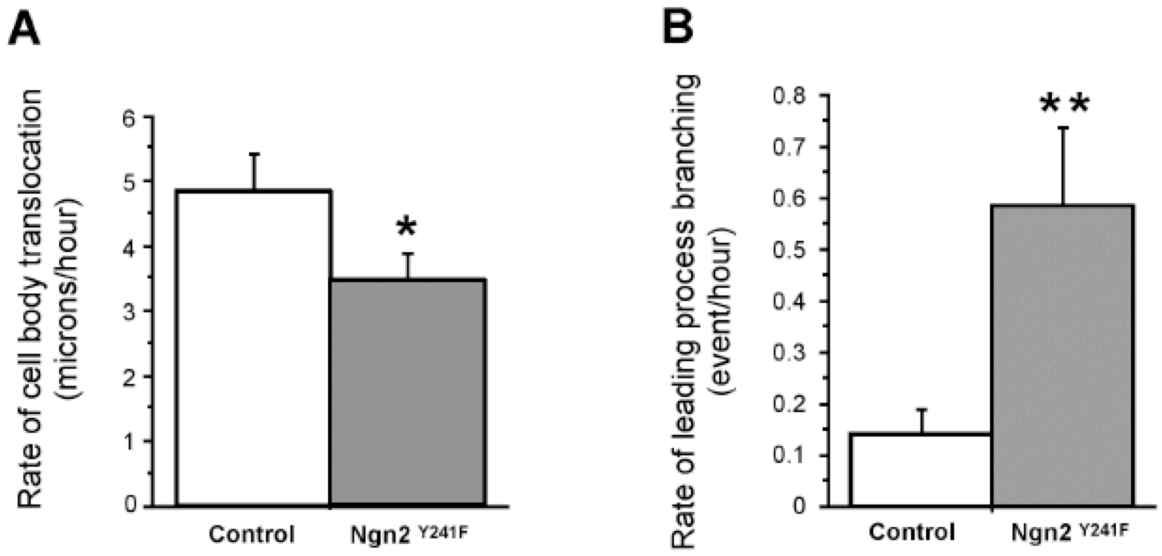

Supplementary Figure 2.6 - Expression of Ngn2^{Y241F} decreases rate of cell body translocation and increases the rate of leading process branching of radially migrating neurons

(A-B) Quantification of the rate of cell body translocation (expressed in microns/hour, A) and the rate of leading process branching (event/hour, B) in neurons located in the intermediate zone and electroporated with control EGFP only (endogenously expressing Ngn2; white bars; n=17 cells from independent experiments) or Ngn2^{Y241F} (grey bars; n=12 cells from 3 independent experiments). * $p<0.05$ and ** $p<0.001$ according to a Mann-Whitney non-parametric test.

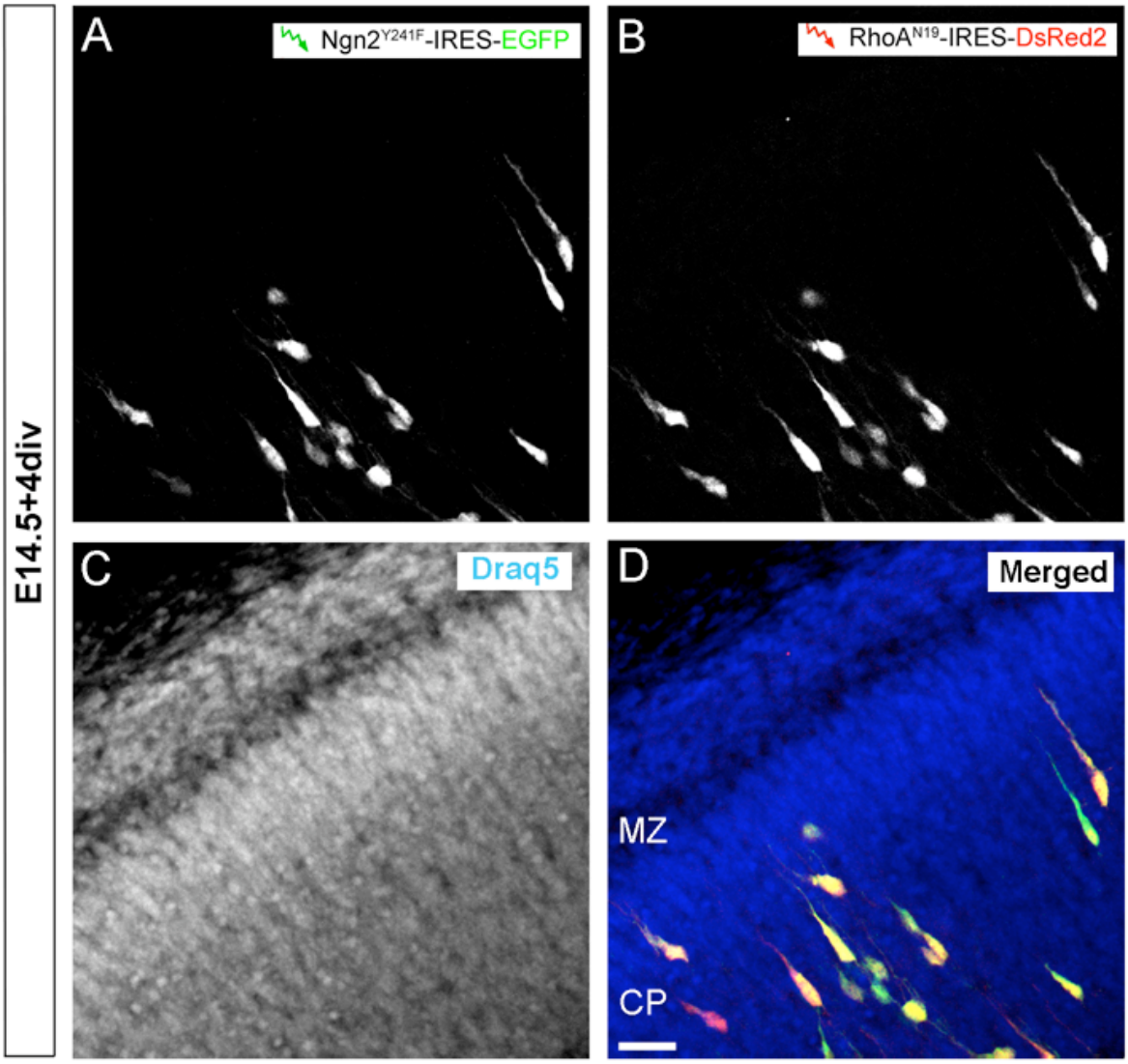

Supplementary Figure 2.7 - High percentage of co-expression of two constructs following cortical co-electroporation

(A-D) E14.5 cortical slices co-electroporated with 1:1 ratio of Ngn2^{Y241F}-IRES-EGFP (A, green in D) and RhoA^{N19}-IRES-DsRed2 (B, red in D) are almost perfectly co-expressed in all neurons present in the cortical plate (merged in D). Slices were counterstained with nuclear staining Draq5 to reveal the cytoarchitecture (C).

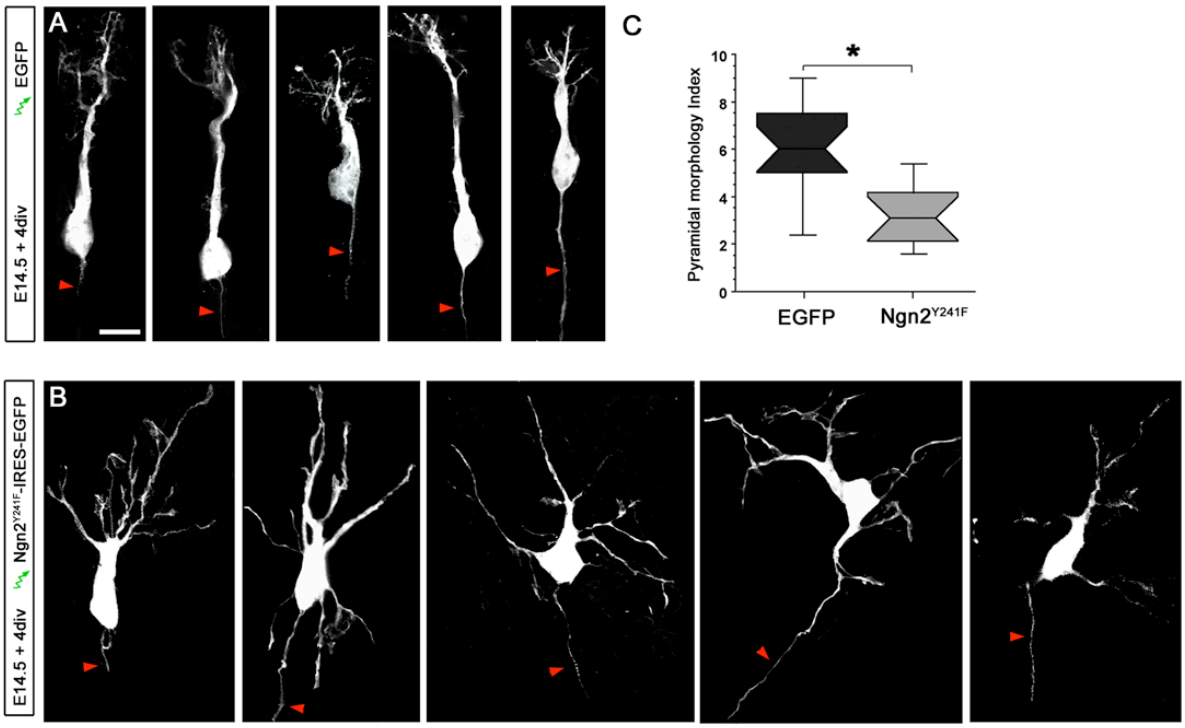

Supplementary Figure 2.8 - Quantification of the dendritic morphology of electroporated neurons in the cortical plate

(A-B) Five representative dendritic morphologies of individual neurons located in the cortical plate after 4 div following progenitors electroporation at E14.5 with control EGFP (A) or Ngn2^{Y241F} (B) constructs. Note the prominent multipolar dendritic morphologies of neurons expressing the Ngn2^{Y241F} mutation. The pial surface is systematically oriented towards the top of the picture. Interestingly, the red arrowheads point to morphologically identified axons that do not seem to be affected by expression of Ngn2^{Y241F} at least with regard to their direction of outgrowth towards the ventricle.

(C) Box plot representation of the Pyramidal Morphology Index values obtained for EGFP-expressing neurons (n=17) and Ngn2^{Y241F} expressing neurons (n=12) in the cortical plate of E14.5 + 4 div. * $p<0.001$ Mann-Whitney non-parametric test. See Figure 8P for details regarding the box plot representation.

Scale bar value: 15 microns for A-B.

Supplementary Figure 2.9 - Ngn1 induces radial migration but is not promoting unipolar neuronal morphologies to the same extent than Ngn2

(A-B) Low magnification confocal micrographs illustrating the radial distribution of cell emerging from progenitors electroporated with Ngn2 (A) and Ngn1 (B).
(C-D) Histograms of the distribution of EGFP+ cells along the radial axis of the cortical wall (normalized as a percentage). Error bars represent standard error to the mean. Stars indicate significant ($p<0.01$- Chi square) differences of the proportion of neurons find in similar bins (for example comparing the 50% normalized distance bins between Ngn2 and Ngn1 over-expression). Ngn1 produces similar increase in the percentage of cells migrating to the cortical plate than Ngn2 when compared to control electroporation (EGFP only, see Figure 5). Note a slight but significant re-distribution of cells within the cortical plate and marginal zone in Ngn1 compared to Ngn2 electroporation.
(E-F) Electroporation of EGFP (not shown) Ngn1-IRES-EGFP and Ngn2-IRES-DsRed2 (E) in two distinct sets of E14.5 cortical progenitors followed by dissociation and co-culture for 6 div reveals than Ngn2 but not Ngn1 is sufficient to promote pyramidal dendritic morphologies compared to control EGFP expressing progenitors (quantified in F). See Figure 8P for details about the box plot representation.
* $p<0.001$ according to ANOVA one-way test and Fisher PLSD post-hoc test; n.s.: non significant according to the same analysis.
Scale bar values: 100 microns A-B; 30 microns E.

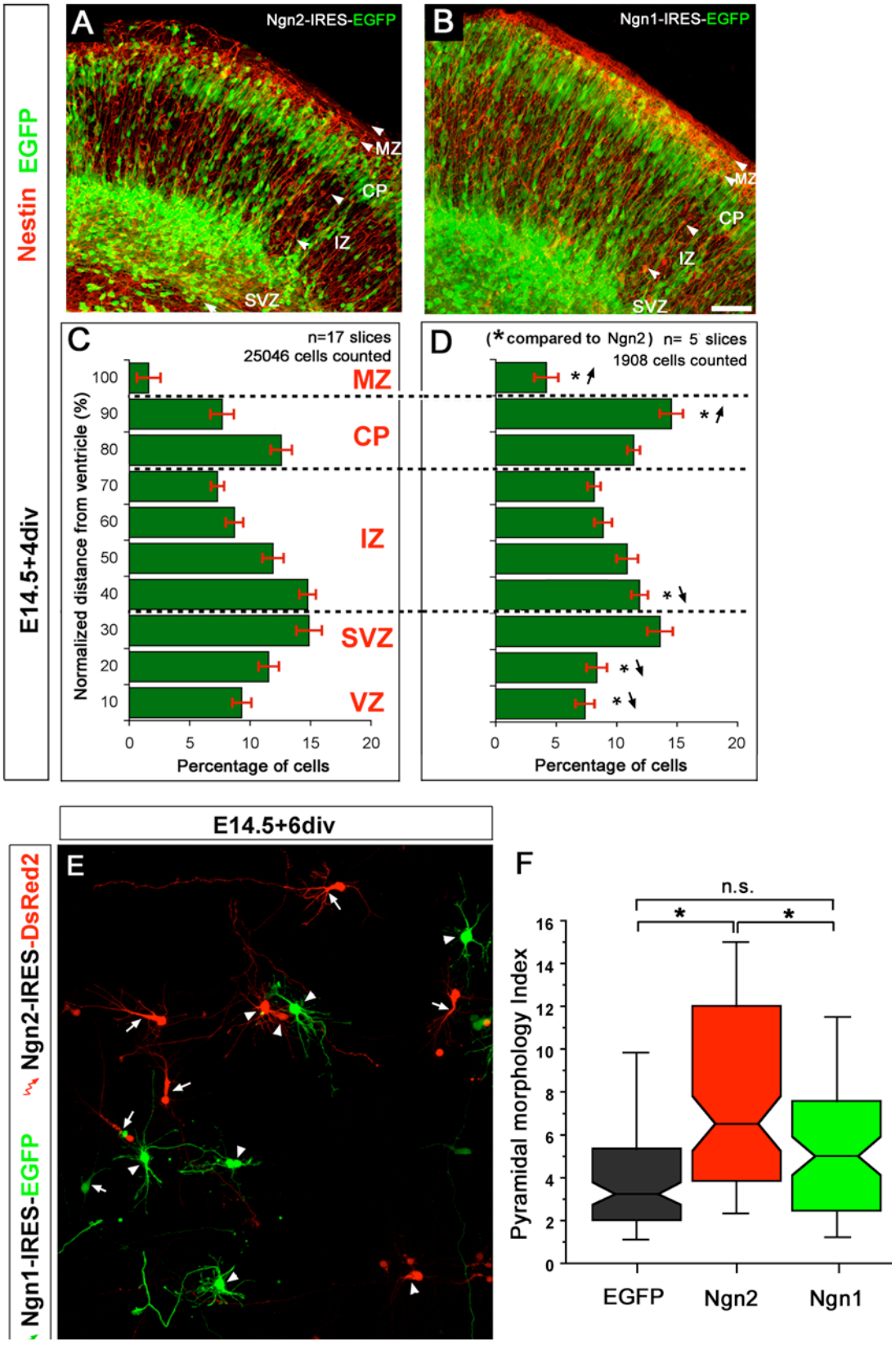
Nestin EGFP
E14.5+4div
A
Ngn2-IRES-EGFP
MZ
CP
IZ
SVZ
B
Ngn1-IRES-EGFP
MZ
CP
IZ
SVZ
C
n=17 slices
25046 cells counted
MZ
CP
IZ
SVZ
VZ
Normalized distance from ventricle (%)
Percentage of cells
D
(*compared to Ngn2) n= 5 slices
1908 cells counted
Percentage of cells
E14.5+6div
Ngn1-IRES-EGFP
Ngn2-IRES-DsRed2
E
F
n.s.
Pyramidal morphology Index
EGFP
Ngn2
Ngn1

SUPPLEMENTARY EXPERIMENTAL PROCEDURES

Immunofluorescent staining of cryostat sections

Ngn2 immunofluorescence was performed on freshly dissected brains were fixed in 4% paraformaldehyde/PBS for two hours, cryoprotected in 20% sucrose/PBS overnight, and cryopreserved in OCT. Ten micron thick sections were washed 3 times in TBST (25 mM Tris pH 7.5, 0.14 M NaCl, 0.1% Triton X-100), and blocked at room temperature for 1 hr in TBST supplemented with 5% goat serum (Invitrogen, Burlington ON) and 3% Bovine Serum Albumin (Sigma, St. Louis MO). Primary antibodies were co-incubated overnight at 4ºC with rabbit anti-Ngn2 (obtained from Dr Masato Nakafuku, Cincinnati Children's Hospital Research Foundaton, Cincinnati, OH, USA) diluted 1:2000 as follows: mouse anti-MAP2 (Clone HM-2; Sigma;1:500); mouse anti-NeuN (MAB377; Chemicon, Temecula CA; 1:500); mouse anti-Tuj1 (Covance, Berkeley CA; 1:1000). Sections were washed 3 times in TBST, and incubated with donkey anti-rabbit Cy3-conjugated (Jackson Immunoresearch, West Grove PA) and goat anti-mouse Alexa-488-conjugated (Molecular Probes, Eugene OR) secondary antibodies, diluted 1:500 in blocking solution for 2 hrs at room temperature. Sections were washed 3 times in TBST, incubated with TBST supplemented with 1 µg/ml DAPI (Santa Cruz Biotechnology, Santa Cruz CA) for 10 min at room temperature, washed 3 times in TBST, and coverslipped using Aqua Polymount (Polysciences Inc., Washington PA).

Sections stained for Ngn2 (n=20) were visualized using a Leica DMRXA2 microscope fitted with a Q Imaging Retiga EX camera under constant imaging conditions. Bins were generated by drawing lines at 100 µm intervals from the surface of the ventricle, extending into the cortical plate using Adobe Photoshop. Ngn2-positive cells were counted and scored for the presence or absence of NeuN immunofluorescence.

Automatic quantification of radial cell distribution in slice culture

Using a tile-scan function on a Leica TCS-SL confocal microscope (mounted on a DM-IRE2 inverted microscope stand) and equipped with a X-Y motorized Märzhäuser stage, assembly of multiple 20x fields (15 microns Z-stacks) were acquired to reconstruct the entire neocortical region electroporated along the radial and the latero-medial axis. Using ImageJ (http://rsb.info.nih.gov/ij/), the entire montage was run through a Bandpass Filter to segment and isolate cell-sized shapes. The image was then thresholded and segmented into radial regions of interest were individual cell position along the radial axis was recorder relative to the distance between the ventricle and the pial surface. Cell coordinates were recorded using ImageJ's Analyze Particles feature. These coordinates were imported into Excel along with the top (pial) and bottom (ventricle) boundaries coordinates obtained using ImageJ's Path Writer plugin. From these top and bottom boundaries, 200 boundary points were taken at regularly spaced intervals leading to a sampling of approximately 10 microns wide. All of this processing was done using an Excel macro.

Time Lapse confocal microscopy

Using a Leica TCS-SL confocal microscope (mounted on a DM-IRE2 inverted microscope stand) and equipped with a X-Y motorized Märzhäuser stage, time-lapse confocal microscopy was performed by imaging multiple Z-stacks at different positions on a given set of electroporated slices (using X-Y motorized stage) repetitively at a frequency of 1 picture every 20 minutes. Slight drifts of the slices were corrected using an image registration tool developed in ImageJ (Turboreg and Stackreg; Thévenaz et al., 1998).

Automatic categorization of dendritic morphology using the Pyramidal Morphology Index (PMI)

The width of dendrites and the number of dendrites emerging from the cell body were automatically sampled using a sampling circle of fixed diameter (25 microns; see Fig. 7O) around a cell body from confocal images taken E14.5 cortical cultures maintained for 5 days in vitro. The java program used to record these values was adapted from William O'Connell's ImageJ plugin, Oval Profile Plot. Changes to this program were made with the gracious help of William O'Connell (Department of Radiology, University of California-San Diego) enabling the program to quickly record data from multiple cells into a single table. The coordinates of the pixel values along the sampling circle were then imported into Excel (v. X- Microsoft). A macro in Excel was written to normalize 8-bit pixel values (0-255) and binarized them (>50% of max equal 1) so that contiguous positive pixels were counted as one process. The sum of adjacent positive points was used to calculate the relative width of each process. For each cell the PMI was recorded as the width of the largest process divided by the total number of processes that crossed the sampling circle.

Protein sequence analysis

Complete amino-acid sequences from human (NP_076924), mouse (NP_033848) and chick (NP_990127) Neurogenin2 (Ngn2) were aligned using Vector NTI suite 9.0.0. Putative phosphorylation sites were compared between chick, mouse and human Ngn2 using a structure- and conformation-based program (Blom, et al., 1999); NetPhos2; http://www.cbs.dtu.dk/services/NetPhos/).

Myc pull-downs and biochemistry

E14.5 cortical wholemounts electroporated with N-terminal pCIG2::cMyc-Ngn2-IRES-EGFP (Fig. 3B) were harvested at 48hiv and washed once in cold 1X PBS (containing protease and phosphatase inhibitors) and then lysed on ice for 15min in 1% NP40 buffer

(containing protease and phosphatase inhibitors). The lysate was passed twice through a fine gauge needle, and cell debris was then pelleted by centrifugation (10,000 rpm for 15min at 4°C). The supernatant was removed and used for immunoprecipitations: 250-500mg of protein lysate was mixed with 2ml of anti c-Myc antibody (final 1:250; Cell Signalling) plus 1% NP40 buffer (with protease and phosphatase inhibitors) to reach a final volume of 500 ml. Pull-downs were performed with pre-washed protein A agarose beads. Supernatants from pull-downs were denatured by boiling at 95°C for 5 minutes in the presence of SDS and proteins were separated electrophoretically on an 10% SDS-PAGE gel.

For phosphorylation experiments, cortical dissociated cells were cultured for 20 hours in vitro as described above. Cultured neurons were exposed to a thirty minutes 'phosphate purge' (cultured in phosphate-free, serum-free medium) and for 6 hours in the same medium containing 300mCi [g32P]-labeled ATP. After myc-pulldowns were performed, proteins were separated by electrophoresis and the blots were imaged using a Typhoon PhosphorImager (ImageQuant v1.1 Molecular Dynamics).

GST Pulldown from E15.5 cortex

Eight E15.5 embryos were electroporated ex vivo with pCIG2::GST-Ngn2-IRES-EGFP (N-terminal fusion; approx. 65kDa). After electroporation, the cortices were dissected from the embryos and cultured as cortical whole mounts for 48hrs in vitro. EGFP expressing regions of the cortices were removed and lysed in RIPA lysis buffer. 10% of the lysate was saved for analysis. Glutathione sepharose beads were added to the remaining 90% of the lysate, and the lysate+beads were rotated at 4°C for 1hr. The beads were then pelleted by centrifugation, the supernatant was removed, and the beads were washed with 1XPBS (0.1M pH 7.4) three times. After washing with PBS, thrombin was added to the beads to cleave Ngn2 from GST. After 1hr, the supernatant containing the cleaved Ngn2 was removed and stored for analysis. Then 10mM of glutathione was added to elute GST from

the glutathione sepharose beads. After 10min, the supernatant containing cleaved GST was removed and saved for analysis.

Luciferase-Renilla assay

A 1.7kB promoter sequence of NeuroD (also called BETA2; kind gift of Dr MJ Tsai-Baylor Coll. Med. (Huang et al., 2000a)) was subcloned upstream of a promoterless firefly luciferase plasmid (pGL3; Dual-Luciferase®; Promega). Freshly plated P19 cells (ATCC) were transfected using Lipofectamine® 2000 (Invitrogen), with the appropriate combination of four constructs: (1) the NeuroD-Luciferase reporter, (2) a control plasmid expressing Renilla under the control of a constitutive mammalian promoter (TK-pRL; Promega), (3) an IRES-EGFP plasmid (pCIG2) expressing (or not; control empty vector) the following cDNAs: full-length mouse Ngn2, Ngn2NR->AQ, Ngn2Dbasic where the entire basic domain was deleted (amino-acid 113-124), and Ngn2Y241F; (4) a plasmid expressing the ubiquitous bHLH protein E47 under the control of a CMV promoter (kind gift of Dr Anirvan Ghosh). Cell lysates were harvested 24 hours after transfection and the Luciferase-Renilla normalized chemiluminescence (ratio pGL3 over TK-pRL) were assayed using a multiple fluorescence (FluoScan) plate reader as per the manufacturer's instructions (Promega).

Transactivation domain mapping

Transactivation mapping of mouse Neurogenin2 (mNgn2) was performed as above using the Dual Luciferase Assay (Promega). PCR fragments of mNgn2 (containing aa180-213, aa214-263, aa180-263) were subcloned into a GAL4 fusion protein plasmid (pFA, Stratagene). Human Embryonic Kidney (HEK) 293T cells were transiently co-transfected in triplicate with the respective GAL4-fusion constructs, pFRLuc (pFR-Luc, Stratagene), and Renilla plasmid (TK-pRL) using Lipofectamine® 2000. Twenty-four hours after transfection cells were lysed and assayed as mentioned above.

CHAPTER THREE

$GABA_A$ Receptor Activation Closes the Window of Cortical Interneuron Migration in a KCC2 Dependant Manner

Dante Bortone [1] and Franck Polleux [1#]

[1] Univ. North Carolina- Neuroscience Center - Neurobiology Curriculum - Chapel Hill, NC 27599-7250-USA

[#] Address correspondence to: polleux@med.unc.edu

Franck Polleux, Ph.D.
University of North Carolina
Neuroscience Center - Dept of Pharmacology
115 mason farm road –CB#7250
Chapel Hill, NC 27599
USA

Tel 919-966-1449
Fax 919-966-9605

Summary

The extracellular cues and signaling pathways that control the termination of cortical interneuron migration are unknown. In the present study, we use a BAC-transgenic mouse line (Lhx6-EGFP) reporting expression in approximately 50% of parvalbumin-positive interneurons (adult basket cells and chandelier cells) and combinations of *ex vivo* co-culture assay, time-lapse confocal microscopy, manipulation of gene expression by electroporation and pharmacology to explore the signaling pathways the stop interneuron migrating in the developing cortex. We found that activation of $GABA_A$ receptors by GABA acts as a paracrine stop signal for interneuron migration but only after interneurons up-regulate the potassium-chloride exchanger KCC2. Expression of KCC2 by migrating interneurons is both necessary and sufficient to confer responsiveness to GABA as a stop signal by decreasing the frequency of intracellular calcium transients. Before or concomitant with using GABA as a neurotransmitter to hyperpolarize their post-synaptic partners, GABA first specifies the timing of a key transition between the end of migration and the onset of inhibitory synaptogenesis.

INTRODUCTION

The balance between excitation and inhibition in cortical circuitry is dictated in part by the relative number of glutamatergic pyramidal neurons and GABAergic interneurons. This balance is of critical importance for the proper function of the adult neocortex. Developmental neuropathologies such as schizophrenia (Pierri et al., 1999) and Autism Spectrum Disorders (ASD) (Belmonte et al., 2004; Polleux and Lauder, 2004) are often hypothesized to be caused, at least in part, by an imbalance between inhibition and excitation in specific cortical circuits. More generally, even a modest decrease of this interneurons:pyramidal neuron ratio (20-80%; Braak and Braak, 1986; DeFelipe et al., 2002; Sloper, 1973; Sloper et al., 1979; Tombol, 1974; Winfield et al., 1980) can lead to cortical hyper-excitability leading to epilepsy (Cobos et al., 2005). In mammals, pyramidal glutamatergic neurons are generated by progenitors located in the dorsal telencephalon that migrate along the radial glial scaffold to reach the cortical plate (Marin and Rubenstein, 2003; Noctor et al., 2004; Rakic, 1972). On the other hand, the vast majority of cortical GABAergic interneurons are generated by a specialized populations of progenitors located in the ventral telencephalon, precisely in the medial and caudal parts of the ganglionic eminence (MGE and CGE respectively) and migrate tangentially towards the dorsal telencephalon where they will invade the cortical plate and terminally differentiate into specific sub-populations of interneurons in a given layer (Marin and Rubenstein, 2003).

The mechanisms guiding or stimulating cortical interneuron migration from the ventral to the dorsal telencephalon are beginning to be made known (Flames et al., 2004; Marin et al., 2001; Polleux et al., 2002; Pozas and Ibanez, 2005). On the other hand, the factors terminating interneuron migration and precisely dictating where and when cortical interneurons should stop migrating are unknown. Identifying these signaling mechanisms would greatly improve our ability to study critical features of the development of the

GABAergic circuitry such as synaptogenesis, balancing inhibitory/excitatory drive and setting up the critical period (Ben-Ari et al., 2004; Hensch, 2005; Markram et al., 2004).

The phenotype of cortical interneurons is genetically specified by the expression of several transcription factors including *Dlx1/2*, *Nkx2.1* and *Lhx6* (Anderson et al., 1997; Lavdas et al., 1999; Sussel et al., 1999). Lhx6-expressing interneurons originate from the medial ganglionic eminence (MGE) and will primarily become the parvalbumin-positive subpopulation of cortical interneurons (Cobos et al., 2005; Cobos et al., 2006). This subpopulation mainly comprises large basket cells and chandelier cells that make restricted synaptic contacts at the soma and axon initial segment of pyramidal neurons, respectively. These interneurons present fast spiking firing patterns (Butt et al., 2005; Kawaguchi and Kondo, 2002) and are thought to control oscillatory patterns of neural activities such as theta and gamma waves (Freund, 2003).

Tangentially migrating interneurons migrate in a stuttered, start-stop fashion (termed 'saltatory locomotion') to the dorsal telencephalon, whereupon these interneurons undergo tangential migration through the marginal zone and intermediate zone (DeDiego et al., 1994; O'Rourke et al., 1995; Polleux et al., 2002). This tangential migration is distinct from the radial migration of pyramidal cells, born in the ventricular or sub-ventricular zones of the dorsal telencephalon which specifically adhere to a radial glial process and migrate radially using this fiber as substrate (Noctor et al., 2004; Rakic, 1972). Upon reaching the top of the cortical plate radial migration is terminated by the detachment of the pyramidal cell from this substrate (Dulabon et al., 2000; Pinto-Lord et al., 1982) allowing subsequent generations of pyramidal cells to pass forming the cortex in an inside out manner. Although interneurons transiently fasciculate with radial glial fibers during their invasion of the cortical plate (Polleux et al., 2002), they can rapidly detach and are most frequently seen moving tangentially to the direction of radial glia even within the cortical plate (O'Rourke et al., 1995; Polleux et al., 2002; Bortone and Polleux – unpublished observations) suggesting that radial

glial processes are not a required substrate for interneurons migration in the cortex. There is some evidence that axons may be involved in the process of tangential migration (Denaxa et al., 2001; McManus et al., 2004). However, the observation that interneurons can move independent of axons as a guide (Polleux et al., 2002; Wichterle et al., 2001) argues against axons as the sole substrate of cortical interneurons. Since no essential substrate has yet been identified in interneurons, determining when tangential migration ends is not as simple as observing when they detach as observed for radially migrating neurons (Anton et al., 1996).

Gamma-aminobutyric acid (GABA), the primary inhibitory neurotransmitter of the central nervous system, may play a role in this termination of tangential migration. GABA receptors are generally categorized into three types: $GABA_A$, $GABA_B$, and $GABA_C$. $GABA_A$ and $GABA_C$ are ionotropic receptors composed of 5 heteromeric subunits and are predominantly permeable to chloride ions. These two ion channels can be distinguished pharmacologically as $GABA_C$ receptors are not inhibited by bicuculline, a $GABA_A$ antagonist. $GABA_B$ receptors are metabotropic (G-protein coupled) and are therefore not thought to be dependent on the electrochemical equilibrium of chloride ions for their function. Tangentially migrating interneurons contain GABA, the means to release it (Conti et al., 2004), and the capacity to respond to it through both ionotropic $GABA_A$ and metabotropic $GABA_B$ receptors during their migration (Cuzon et al., 2006; Lopez-Bendito et al., 2003; Lujan et al., 2005), yet no function is ascribed to GABA in migrating interneurons.

The neurotransmitter GABA has been suggested to play diverse, sometimes conflicting, roles on neuronal proliferation, migration and differentiation during development of the central nervous system. Here we report that GABA acts as a pause signal for cortical interneurons through activation of $GABA_A$ receptors. Interestingly, GABA's ability to pause interneuron migration in the cortex requires expression of the K+/Cl- exchanger KCC2, which controls the reversal potential of chloride and therefore determines the switch of

$GABA_A$ receptor activation from depolarizing to hyperpolarizing. Expression of KCC2 is both necessary and sufficient for stop cortical interneuron migration by negatively regulating the frequency of spontaneous intracellular calcium transients in these migrating cells. These results provide a new important function of GABA in the regulation of a key transition during interneuron migration.

RESULTS

Cortical interneurons terminate migration during the first postnatal week in a cell autonomous manner

To first document when interneurons stop migrating *in vivo* in the developing mouse cortex, we performed time-lapse analysis in acute cortical slices isolated from a BAC-transgenic mouse line where enhanced green fluorescent protein (EGFP) is expressed under the control of the regulatory elements of LIM homeobox 6 (Lhx6), a transcription factor expressed specifically in MGE progenitors (Lavdas et al., 1999). In this mouse line obtained from the GENSAT consortium (Gong et al., 2003), EGFP is expressed in approximately 65% of cortical interneurons *in vivo*. Most of these Lhx6-positive interneurons will become parvalbumin-positive large basket cells or chandelier cells (Cobos et al., 2006). These time-lapse experiments revealed a gradual reduction in interneuron migration from E15 to P7 as shown in **Figures 3.1B-D**.

Although some interneurons have terminated migration in the cortical plate (CP) by E15 (15.1% ± 2.8%; n = 388 cells, 8 movies; **Fig. 3.1E**), the vast majority continue to translocate. By P1, 57.8 ± 1.9% (n = 970 cells, 10 movies) of interneurons have stopped migrating and almost all cortical interneurons have terminated migration by P7 (91.6 ± 1.4%; n = 366 cells, 12 movies).

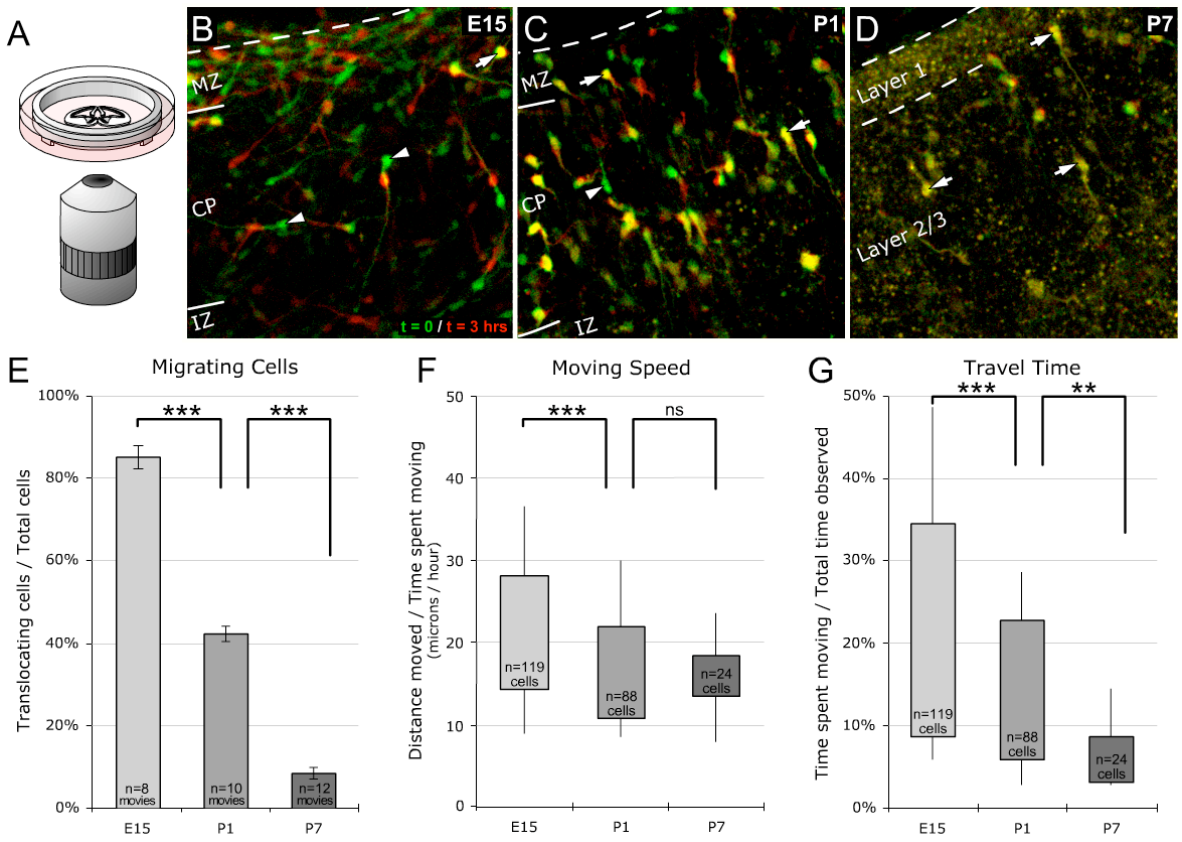

Figure 3.1 - Characterizing the termination of cortical interneuron migration
(**A**) Illustration of time-lapse set-up. Cell culture media has access to slice from below, while temperature, humidity and CO_2 levels are controlled by incubation chamber from above.
(**B-D**) Images show decrease in movement of Lhx6-EGFP+ interneurons in cortical slices between embryonic day (E)14.5 and post-natal day (P)5 after culturing *ex vivo* for 1-2 days to allow settling. Frame corresponding to the start of imaging (t=0) is pseudo-colored in green. Image taken three hours later is pseudo-colored in red. Yellow cell bodies correspond to interneurons that did not migrate. (**E-G**) Movements of interneurons in the cortical plate were quantified. (E) By P7 the majority of interneurons have shown no detectable somal translocations after 6 hours of observation. (F) The average moving speed showed an initial decrease, but showed no decline at older ages. (G) The primary means of slowing and stopping interneuron migration was therefore due to a steady decrease in the percentage of time spent traveling.

The quantitative assessment of interneuron migration was performed by computing two parameters: (1) we defined the *moving speed* as the rate of translocation (microns/hour) when the interneuron is moving i.e. not including the time when the cell pauses and (2) the *travel time* indicates the proportion of time that the interneuron is moving during recording. Most time-lapse investigations report only the average speed as defined by distance traveled over a certain period of time (Cuzon et al., 2006). However, this measure is ambiguous due to the saltatory nature of interneuron migration, changes in *average speed*

can be caused either by change in the stalling frequency and/or a change in moving speed. By separating these two components, we were able to uncover significant changes that would not be apparent otherwise. Most importantly, although the moving speed of cortical interneurons declines from 23.0 ± 1.2 microns/hour at E15 to 18.5 ± 1.3 microns/hour at P1 (**Fig. 3.1F**) there is no significant decline found from P1 to P7. While moving speed levels off modestly, travel time is found to decrease significantly between all ages dropping from 24.7 ± 1.6% at E15 to 7.6 ± 1.1% by P7 (**Fig. 3.1G**). This analysis shows that interneurons stop migrating, not by decreasing their moving speed, but largely by increasing the stalling frequency.

Figure 3.2 - GABA decreases motility of interneurons expressing high levels of KCC2 via $GABA_A$ receptor activation

(A) Wild-type neocortex was dissociated providing a 2-D substrate for EGFP migrating interneurons. **(B-D)** Time-series of migrating interneurons pseudo-colored at equally spaced time-frames before (B, white 180 minutes after start of imaging i.e. 180 minutes before application of GABA; C, blue 360 minutes after start of imaging corresponding to time of GABA application) and after extracellular application of GABA (20μM; D, red, 540 minutes after start of imaging i.e. 180 minutes after GABA application; E, green 720 minutes after start of imaging i.e. 360 minutes after GABA application). These cell cultures where fixed immediately after the last frame, and immunofluorescently stained with anti-EGFP and anti-KCC2 antibodies (J). This technique allows the matching of individual interneuron responses to GABA treatment (G) and the segregation of these responses based on individual levels of KCC2 expression found by measuring the optical density of KCC2 immunofluorescence (L). Interneuron responses to GABA application were binned into low and high KCC2 populations (green and red, respectively), indicating a large negative shift in the high KCC2-expressing population of interneurons.
(M-N) Box plots show quantification of binned interneuron responses to drug application.
No significant changes in moving speed were detected in either sub-population following GABA (M) or 20μM GABA with concurrent application of $GABA_A$ receptor antagonist bicuculline methiodide (BMI; 10μM; data not shown). (N) Low KCC2 interneurons showed no significant decrease in travel time upon GABA application, while high KCC2 interneurons showed a significant (p=0.0004) decline after GABA application. BMI co-application with GABA significantly disinhibited the effect of GABA alone (p=0.0308), leaving no significant difference between pre and post-drug travel times.

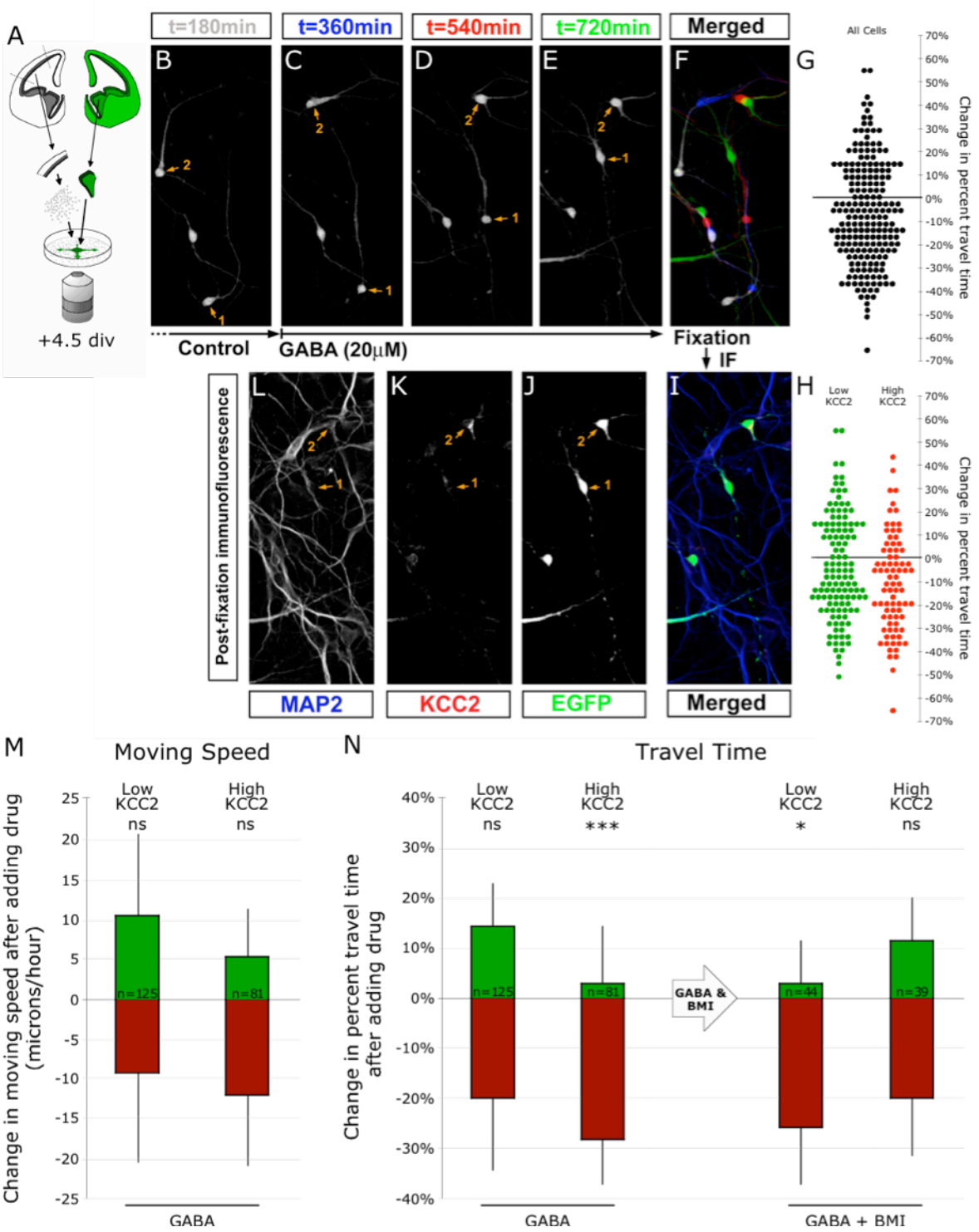
A
+4.5 div
t=180min
t=360min
t=540min
t=720min
Merged
B
C
D
E
F
G
All Cells
Change in percent travel time
Control
GABA (20μM)
Fixation
IF
Post-fixation immunofluorescence
L
K
J
I
H
Low KCC2
High KCC2
MAP2
KCC2
EGFP
Merged
M
Moving Speed
Change in moving speed after adding drug (microns/hour)
Low KCC2 ns
High KCC2 ns
n=125
n=81
GABA
N
Travel Time
Change in percent travel time after adding drug
Low KCC2 ns
High KCC2 ***
Low KCC2 *
High KCC2 ns
GABA & BMI
n=125
n=81
n=44
n=39
GABA
GABA + BMI

GABA application induces pausing behavior in a subset of migrating interneurons expressing KCC2.

Difficulty in time-lapsing acute slices of brain tissue arises from tracking a single interneuron for long periods of time as they dive into the slice and out of the focal plane. This complication compromises not only the number and length of single neuron observations, but all movements occurring in the Z-axis are lost as well. Since the imaging of stacks in the Z-plane at the resolution, depth and speed necessary to enable longer and more accurate observations of these cells was not possible without introducing unacceptable levels of phototoxicity, a novel *in vitro* 2D migration assay was developed. By dissociating and plating E14.5 wild-type isochronic dorsal telencephalic neurons immediately before explanting MGE isolated from EGFP-expressing littermates (**Fig. 3.2A**), longer observations at higher temporal frequencies are made possible onto this 2D substrate. This assay also enables efficient and rapid application of pharmacological treatments to migrating interneurons, which is difficult to optimize in slices due to limited diffusion of the drugs into the tissue.

Using this two-dimensional assay, we tested the hypothesis that GABA plays a role in terminating the migration of cortical interneurons. The exact nature of GABA's effect on interneuron migration, specifically through ionotropic receptors, remains unclear in spite of much evidence that GABA can modulate the migration of cortical neurons (Behar et al., 1996; Behar et al., 1998; Cuzon et al., 2006).

Interneurons from EGFP-expressing MGE explants were allowed to migrate on a substrate of dissociated isochronic wild-type cortical neurons for 4.5 div and were time-lapsed for 6 hours (**Fig. 3.2B-C**) prior to addition of GABA (20μM) and time-lapsed for 6 more hours (**Fig. 3.2D-E**). This method allowed us to quantify the migration properties of

individual interneurons before and after drug addition (**Fig. 3.2B-F**). Interneurons that were not present for the entirety of the 12-hour imaging sessions were excluded from the analysis. Interestingly, the moving speed did not decline significantly while the proportion of time these interneurons spent traveling dropped slightly but significantly (-7.0 ± 1.5%; p=0.0002; n=206 cells; data not shown). This significant decline, specifically in travel time, while maintaining stable moving speeds upon GABA addition strikingly resembles the attributes of the age-related termination of migration measured *in situ*. In other words, a significant increase in the stalling frequency was observed both during maturation of cortical interneurons in slices and upon exogenous addition of GABA to interneurons migrating on dissociated cortical cultures.

Although a significant trend was observed at the population level i.e. slightly more interneurons showing decrease of travel time than increase upon GABA addition, our analysis mainly unravels a significant level of variability in the response of individual interneurons to GABA addition. Some interneurons within this group responded by reducing the frequency of pauses (decrease percentage of time travel), while others show the opposite response upon GABA addition (**Fig. 3.2G**).

What could account for this important variability in the migratory response of interneurons to GABA? These results strongly suggest that interneurons have different intrinsic properties underlying their differential responsiveness to GABA. *In vivo*, we determined that most interneurons stop migrating sometime around birth i.e. approximately 7 days after interneurons start invading the cortex (E13.5; Bortone and Polleux unpublished observation). To test if interneurons responsiveness to stop signals (including ambient GABA) is due to cell-autonomous or cell non-autonomous changes, we first performed isochronic and heterochronic co-cultures where the age of the cortical substrate for migration varies from 2div versus 7div (see **Supp. Fig. 3.1**). Our results demonstrate that after 2div, most interneurons migrate readily (**Supp. Fig. 3.1A**), but when both interneurons

and their cortical substrate have matured for 7div (**Supp. Fig. 3.1B**), interneurons stop migrating. Interestingly, heterochronic experiments reveal that when 'immature' interneurons (E14.5+ 2div) are plated on 'mature' cortical substrate (7div), interneuron migrate at the same rate as in isochronic conditions (**Supp. Fig. 3.1C**, quantified in **Supp. Fig. 3.1D-E**). This strongly suggests that interneurons responsiveness to stop signals requires intrinsic maturation maybe necessary for upregulation of an intrinsic 'gating' factor.

Responsiveness of interneurons to GABA via $GABA_A$ receptors correlates with KCC2 expression.

There are two intrinsic factors that could contribute to this differential response of migrating interneurons towards GABA: 1) the differential expression of GABA receptors subunits and 2) the nature of the chloride gradient across the membrane dictating the direction of chloride ion flow upon opening of ionotropic GABA receptors. Metabotropic GABA receptors, $GABA_B$ receptors, are present on interneurons, but appear to have consistent expression from interneuron to interneuron (Lopez-Bendito et al., 2003). Differential expression of ionotrophic GABA receptor subunits could alter the cell's responsiveness to GABA (Cuzon et al., 2006). Although differential subunit compositions can confer distinctive properties including cellular localization, agonist affinity, rates of ion permeability and desensitization, $GABA_A$ receptors are the most diverse ligand-gated ion channel composed of a staggering 21 subunits (Fritschy and Brunig, 2003). Systematically addressing the effect of each of these subunits may not be feasible.

Another critical modulator of ionotropic GABA function is the reversal of chloride's electrochemical driving force in neurons, which could completely reverse the effect of GABA from hyperpolarizing to depolarizing. This reversal is predominantly controlled by the expression of one protein, the potassium chloride co-transporter, KCC2 (Rivera et al., 1999). Early in development the expression of this chloride extruder is low, resulting in a high

intracellular concentration of chloride. The driving force of this gradient causes a depolarizing efflux of chloride upon the binding of GABA to ionotropic GABA receptors. As a neuron matures, the up-regulation of KCC2 extrudes chloride, which leads to a reversal of its chloride electrochemical driving force (Ben-Ari, 2002; Payne et al., 1996; Rivera et al., 1999). The same neurotransmitter, GABA, acting on the same ionotropic GABA receptors then leads to a hyperpolarizing influx of chloride ions, underlying the inhibitory function of GABA as a neurotransmitter in the adult CNS.

To test this hypothesis, we took a refined approach, combining individual tracking of migrating interneuron by confocal time-lapse microscopy with pharmacological treatment and post-hoc immunofluorescent staining of KCC2 in the same interneurons. 2D co-cultures time-lapsed for 12 hours as described above (**Fig. 3.2A-F**) were fixed immediately after the last frame and stained for KCC2, MAP2 and EGFP. Each interneuron tracked during time-lapse and pharmacological treatment was then re-located, enabling the optical density of KCC2 to be correlated to the response of individual cells to GABA addition (**Fig. 3.2K-H**). The individual data points of percentage change in travel time before and after GABA addition shown in **Figure 3.2G** could then be retrospectively split into bins of high and low KCC2 expression (**Fig. 3.2L**). The results revealed two strikingly different sub-populations of interneurons. Interneurons expressing low levels of KCC2 showed no significant changes moving speed or percent travel time in response to GABA (**Fig. 3.2L**, green dots, whereas interneurons expressing high levels of KCC2 (red dots) responded to GABA addition with a significant reduction in the time they spent migrating (Mann-Whitney test $p=0.0004$ when compared to pre-drug measurements; $n=81$ cells). As seen when characterizing the termination of migration *in situ*, this GABA-induced depression in travel time occurs without a significant decrease in moving speed (data not shown).

Is this response to GABA as a ause signal mediated by activation of $GABA_A$ receptors? Co-application of 20μM GABA with 10μM bicuculline methiodide (BMI), a $GABA_A$

receptor competitive antagonist, significantly blocked GABA's effect on the travel time specifically in interneurons expressing high levels of KCC2 (-2.8 ± 3.0%; n=39; p=0.0308 compared to change elicited by GABA application alone; p=0.6312 compared to control observation period; **Fig. 3.2N**). Where co-application of GABA and BMI increased the travel time of the high KCC2-expressing interneurons relative to GABA application alone, it significantly depressed the travel times of interneurons expressing low levels of KCC2 (-8.12 ± 3.1%; n=44; p=0.0271 with respect to pre-drug observations; data not shown). These results are also evident when viewing the frame-by-frame data (**Supp. Fig. 3.2**) for interneurons subdivided into high and low KCC2 expressing interneurons. Our results identified that expression of KCC2 is coinciding with the ability of interneurons to respond to GABA as a stop signal.

To determine the relevance of increased KCC2 expression to a termination of migration, as opposed to a GABA-induced pausing, KCC2 expression was measured in older (E14.5 + 7div) interneurons and correlated with their motility. Explanted E14.5 EGFP+ interneurons were cultured for 7 div on a dissociation of wild-type E14.5 dorsal telencephalon, time-lapsed for 6 hours, fixed, and immunostained for KCC2 (**Supp. Fig. 3.3**). Interneurons showing no movement during the course of this 6-hour observation had 44.4% higher KCC2 expression than those that moved (±7.1%; n=51; p<0.0001). The correlation of high KCC2 expression with those interneurons exhibiting no movement in the absence of artificial GABA application suggest that KCC2 up-regulation is tightly coupled with the termination of interneuron migration.

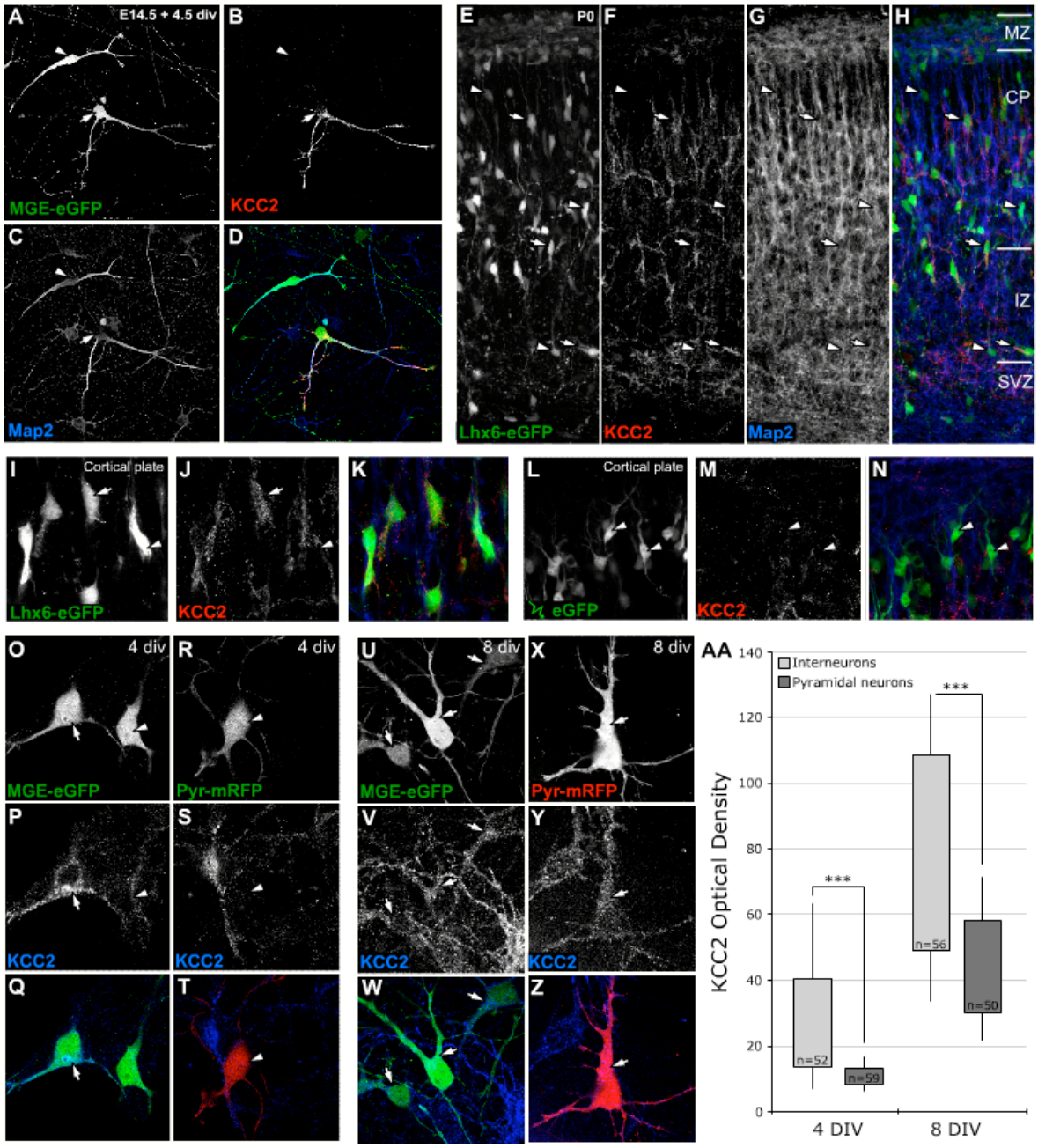

Figure 3.3 - KCC2 expression is highly variable among cortical interneurons.
(A-D) Explanted E14.5 EGFP-MGE interneurons show drastically different KCC2 expression after 4 div. Throughout the figure, arrowheads identify cells expressing low levels of KCC2. Arrows indicate high KCC2 expressing cells. **(E-K)** Disparity in cortical interneuron KCC2 expression is also found *in vivo*. **(L-M)** E14.5 pyramidal cell progenitors were electroporated with GFP and stained for KCC2 after 4.5 div. No KCC2 was observed. **(O-Z)** Interneurons up-regulate KCC2 earlier than pyramidal cells *in vitro*. Variability of interneuron KCC2 expression was also much higher at early ages.
(**AA**) Quantification of KCC2 optical density (OD) in cortical pyramidal cells was significantly lower than interneurons at 4 and 8 div ($p<0.0001$ for both).

KCC2 expression is highly variable among migrating interneurons and precedes KCC2 expression in pyramidal cells.

To confirm the *in vivo* relevance of the variability of KCC2 expression observed *in vitro* (**Fig. 3.3A-D**), we performed immunofluorescent staining for KCC2 on Lhx6-EGFP cortical interneurons *in vitro* and *in vivo*. These results were consistent with intracellular variability observed *in vivo* (**Fig. 3.3E-H**). Surprisingly, this variability was observed in every layer of the neocortex at P0 including the cortical plate (**Fig. 3.3E-K**). If KCC2 up regulation contributes toward the termination of migration in interneurons specifically, one might expect to see KCC2 expression occur in interneurons much sooner than in pyramidal cells.

The pyramidal cell population was labeled by dorsal electroporation. This electroporation technique specifically labels pyramidal cells with no cross-labeling of interneurons (**Supp. Fig. 3.4A-C**). After culturing for 4 days these slices were fixed and immunostained for KCC2 (**Fig. 3.3L-N**), showing little to no KCC2 expression in pyramidal cells *in situ* at an age when a large proportion of interneurons are already highly expressing the co-transporter.

The 2D *in vitro* assay was adapted to more directly isolate and compare KCC2 expression in these two distinct neuronal sub-populations. Cortical pyramidal cells were electroporated with monomeric red fluorescent protein (mRFP) at E14.5, dissociated and cultured *in vitro* with MGE-EGFP explants (**Supp. Fig. 3.4D**). The cultures were processed for immunofluorescence against KCC2 at 4 and 8 div allowing a comparison of optical densities between interneurons and pyramidal cells (**Fig. 3.3O-Z**). The quantification of the staining showed KCC2 is up-regulated in interneurons much sooner than pyramidal cells (**Fig. 3.3AA**). At E14.5 + 4 div interneurons had an average optical density of 32.5 ± 4.3 (n = 52), which was about three times higher than pyramidal cells at the same age (average optical density of 11.8 ± 0.7; n = 59; $p < 0.0001$). By 8 div the optical density of interneurons (82.9 ± 5.5; n=56) was still twice that of pyramidal cells (46.9 ± 2.9; n=50; $p<0.0001$). Also

of note, the standard error to the mean (SEM) for interneurons at 4 div comprised a much higher percentage (± 13.2%) of its measurement compared to that of pyramidal cells (± 5.9%). In other words, up-regulation of KCC2 in pyramidal cells appeared uniform compared to the highly variable and precocious expression in interneurons.

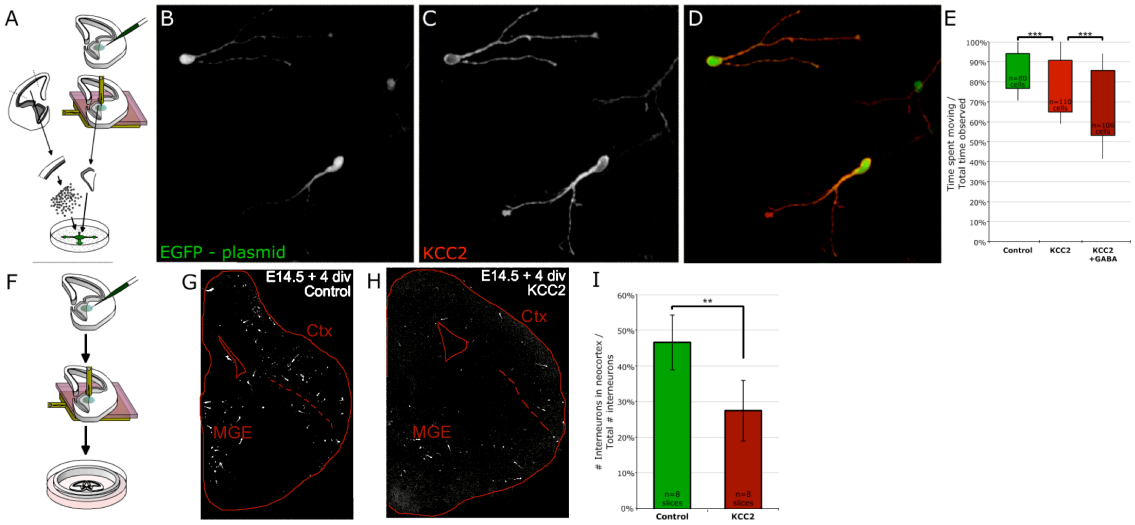

Figure 3.4 - Sufficiency of KCC2 in decreasing interneuron motility
(**A-E**) KCC2 was over-expressed in E14.5 wild-type MGE explants by electroporation of EGFP IRES KCC2 construct (A). (B-D) Expression was verified by high immunofluorescence after 2 div. (E) Over-expression of KCC2 alone significantly decreased interneuron travel time (p=0.0009). Application of 20μM GABA further significantly reduced travel time (p<0.0001), indicating sufficiency of KCC2 in depressing speed upon GABA addition.
(**F-I**) Electroporations of EGFP into the MGE of a slice (F) shows robust migration (G) of interneurons into the dorsal telencephalon. (H) Electroporation of EGFP IRES KCC2 in slices decreases migration to the cortex. (I) Quantification shows a significant decrease in the percentage of interneurons migrating into the cortex from the striatum in KCC2 over-expressing interneurons (p=0.0091).

Premature KCC2 expression is sufficient to reduce interneurons migration to cortex by increasing stalling frequency upon GABA application

Our initial results raise an important question: is KCC2 expression the prime intrinsic determinant of an interneuron's responsiveness to ambient GABA as a stop signal? In order to test this question, cortical interneurons were electroporated with EGFP-IRES-KCC2 expression plasmids at E14.5 (**Fig. 3.4A-D**) and time-lapsed as described above in order to determine the sufficiency of premature KCC2 expression to induce responsiveness to GABA

as a stop signal. These interneurons were time-lapsed for shorter periods of time (3 hours before and after drug addition) as their faster speeds made it difficult to retain them in the field of view for the full 12 hours used on 4.5 div interneurons. **Figure 3.4E** shows that the percent travel time in KCC2 over-expressing interneurons is significantly lower than control electroporated interneurons (78.6 ± 1.5% and 85.7 ± 1.4% respectively; $p = 0.0009$), presumably in the presence of limiting level of ambient GABA. The addition of GABA (20μM) further depressed the travel times of KCC2 over-expressing cells (68.6 ± 1.9%; $p<0.0001$ when compared to either control or KCC2 over expression alone) illustrating that KCC2 expression is sufficient to enable GABA to decrease the rate of migration (i.e. increased stalling frequency) in immature migrating interneurons.

To test the effect of KCC2 on interneuron migration *in situ*, the MGE of wild-type slices were electroporated with control (EGFP only) or KCC2-IRES-EGFP constructs and cultured for 4 days in organotypic slices *ex vivo* (**Fig. 3.4F**). Control electroporations show robust migration into the cortex (**Fig. 3.4G-H**), while KCC2 over-expressing interneurons appear restricted in their migration mostly to the striatum (**Fig. 3.5H**). The quantification of these slices shows nearly half (46.5 ± 7.7%, n=8 slices, 966 cells) of control interneurons successfully reaching the cortex while only 27.4 ± 8.5% (n = 8 slices, 642 cells; $p=0.0091$) of KCC2 over-expressing interneurons reach the cortex.

KCC2 is required for termination of cortical interneurons migration.

To further test the contribution of KCC2 towards terminating cortical interneuron migration, we sought to determine if KCC2 expression was required for termination of interneuron migration using a KCC2 knockdown approach. To do this, E14.5 MGE explants were electroporated with either control or control plus plasmid encoding short hairpin (sh)RNA interference constructs targeted against mouse KCC2 (shKCC2) and time-lapsed after 7 div i.e. when the vast majority of E14.5 interneurons have (1) upregulated KCC2

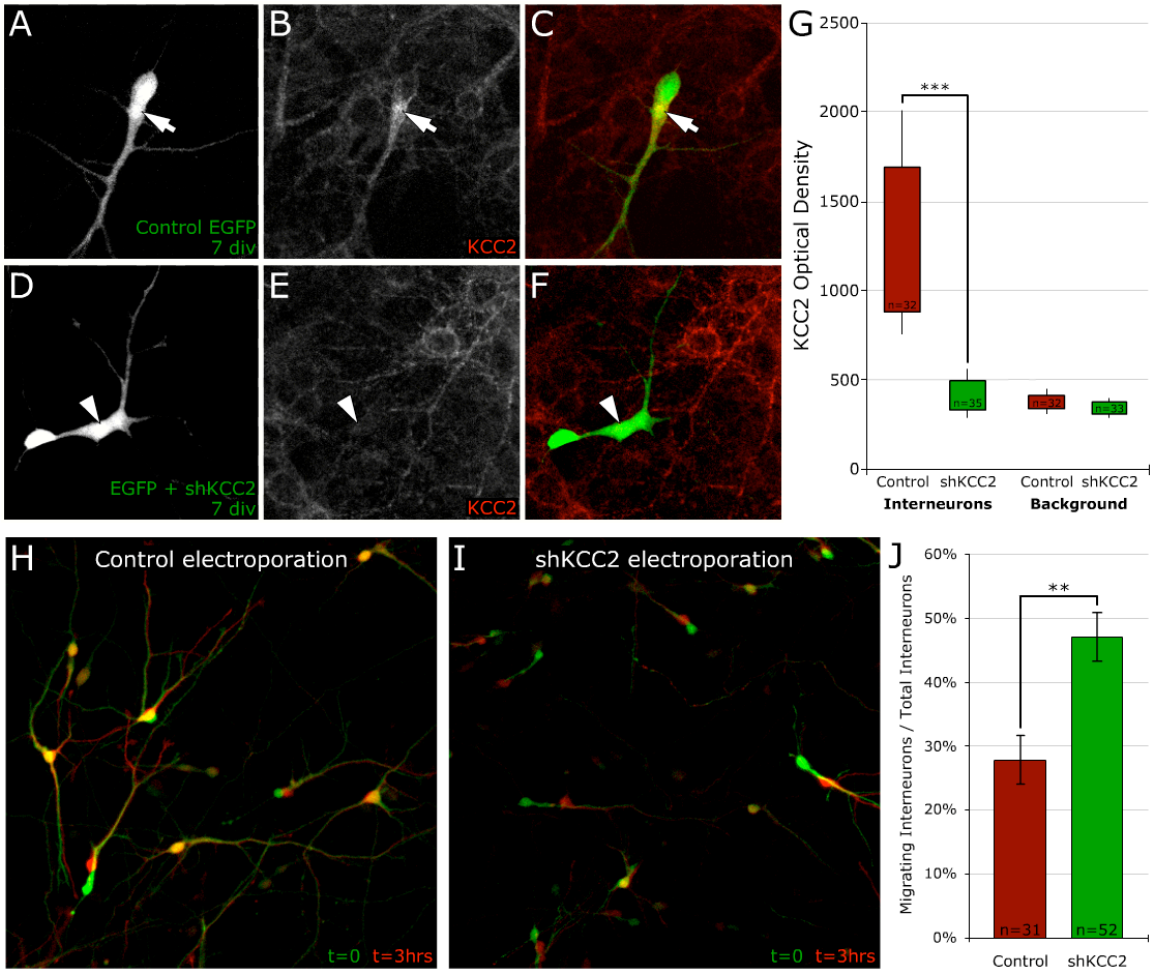

Figure 3.5 - Knocking-down KCC2 increases percentage of migrating interneurons
(A-F) Short hairpin RNAi targeted against mouse KCC2 (shKCC2) is effective in knocking-down KCC2 expression. (A-C) Interneuron electroporated with a contruct encoding EGFP at E14.5 is shown immunostained for KCC2 in red at 7 div. (D-F) Interneuron electroporated with a control EGFP and a construct encoding shKCC2 at E14.5 shows no KCC2 expression at 7 div. **(G)** Quantification shows a significant reduction in KCC2 with use of shKCC2. Measurements of background KCC2 immuno-reactivity show KCC2 is approaching undetectable levels with introduction of shKCC2. Optical density was measured in 12 bits (value range of 0-4095).
(H-J) Interneurons electroporated with either control plasmid (H) or control plus shKCC2 (**I**) are shown with initial frame (t=0) shown in green and 3 hours later shown in red. Note decrease in yellow 'co-labeled' interneurons after knocking-down KCC2 indicating more migrating interneurons. (J) Quantification shows a significant increase in the number of migrating interneurons expressing the shKCC2 (p=0.0031).

(**Fig. 3.3 and Suppl. Fig. 3.3**) and stopped migrating *in vivo* (**Fig. 3.1**) and *in vitro* (**Suppl. Fig. 3.1**). Our shRNA approach is very effective at knocking down endogenous KCC2 expression in interneurons below detectable levels using immunofluorescence (**Fig. 3.5A-G**). As shown above, only a small proportion of interneurons is still migrating by 7 div using

this electroporated explant method (27.7 ± 3.8%; n=31 cells; **Fig. 3.5H** and **3.5J**). However, knocking-down KCC2 significantly increases (almost two fold) the proportion of migrating cortical neurons to 47.1 ± 3.8% (n = 52; p = 0.0031; **Fig. 3.5I-J**). Therefore the modulation of KCC2 has a significant impact on the extension of the migratory period in cortical interneurons.

KCC2 regulates termination of migration by altering calcium influx.

Our results thus far show that KCC2 expression, coupled with activation of $GABA_A$ receptors, is tightly correlated with an increase in the stalling frequency displayed by interneurons as they migrate, however the molecular mechanisms underlying the effect of $GABA_A$ receptor activation in interneurons expressing KCC2 is unknown. The frequency of intracellular calcium dynamics has been closely linked to the migration of cerebellar granule cells (Komuro and Rakic, 1996; Kumada and Komuro, 2004), the extension of axon growth cones (Gomez et al., 1995; Gomez and Spitzer, 1999) and the stabilization of dendritic

Figure 3.6 - Calcium signals in tangentially migrating interneurons are reduced with KCC2 upregulation
(**A-B**) Migrating cortical interneurons show spontaneous calcium transients to a varying degree. (A) An mRFP-electroporated E14.5 MGE interneuron (red) was loaded with Oregon green BAPTA-AM and time-lapsed. Pseudocolored images show calcium signal at low (A') and high (A'') periods of activity. White outlines interneuron (A'''). Pseudo colored strip across bottom shows a resectioned line through the cell nucleus during the course of the time-lapse. No pharmacological treatments were required to elicit these calcium signals. (B) Traces of calcium signal in control conditions shows wide range of calcium responses.
(**C-F**) KCC2 expression ablates 0.003-0.03 Hz calcium transients. Calcium signals from Oregon green BAPTA-loaded interneurons electroporated with either mRFP and a plasmid encoding shKCC2 (C) or mRFP IRES KCC2 (KCC2; D) are shown. Interneurons with knocked down KCC2 show several calcium spikes (indicated by arrowheads) on top of a larger wave. KCC2 over-expressing interneurons do not show these types of signals. (E) A spectral analysis was done on individual cells and averaged for each group indicating a decrease in calcium signaling in the 0.003-0.03 Hz frequency range upon KCC2 over-expression. (F) The relative power spectral densities were binned into 0.003-0.03 Hz and >0.03 Hz categories. KCC2 knockdown interneurons showed significantly higher signaling activity in the range of 0.003-0.03 Hz (p=0.0084). At higher frequencies this difference disappears. KCC2 over-expressing cells show no significant difference between higher and lower frequencies indicating KCC2 expression decreases spontaneous calcium activity.
(**G-I**) Time-lapsed Lhx6-EGFP interneurons at E15 are shown with initial image (t=0) in blue, 3 hours in green, and 6 hours in red. Non-moving cells appear white. Note chelation of calcium increases the number of stationary cells (H) relative to control cells (G). (I) Quantification shows a decrease (Chi-Square Analysis p<0.0001) in the number of cells migrating after incubation with 25μM BAPTA-AM.

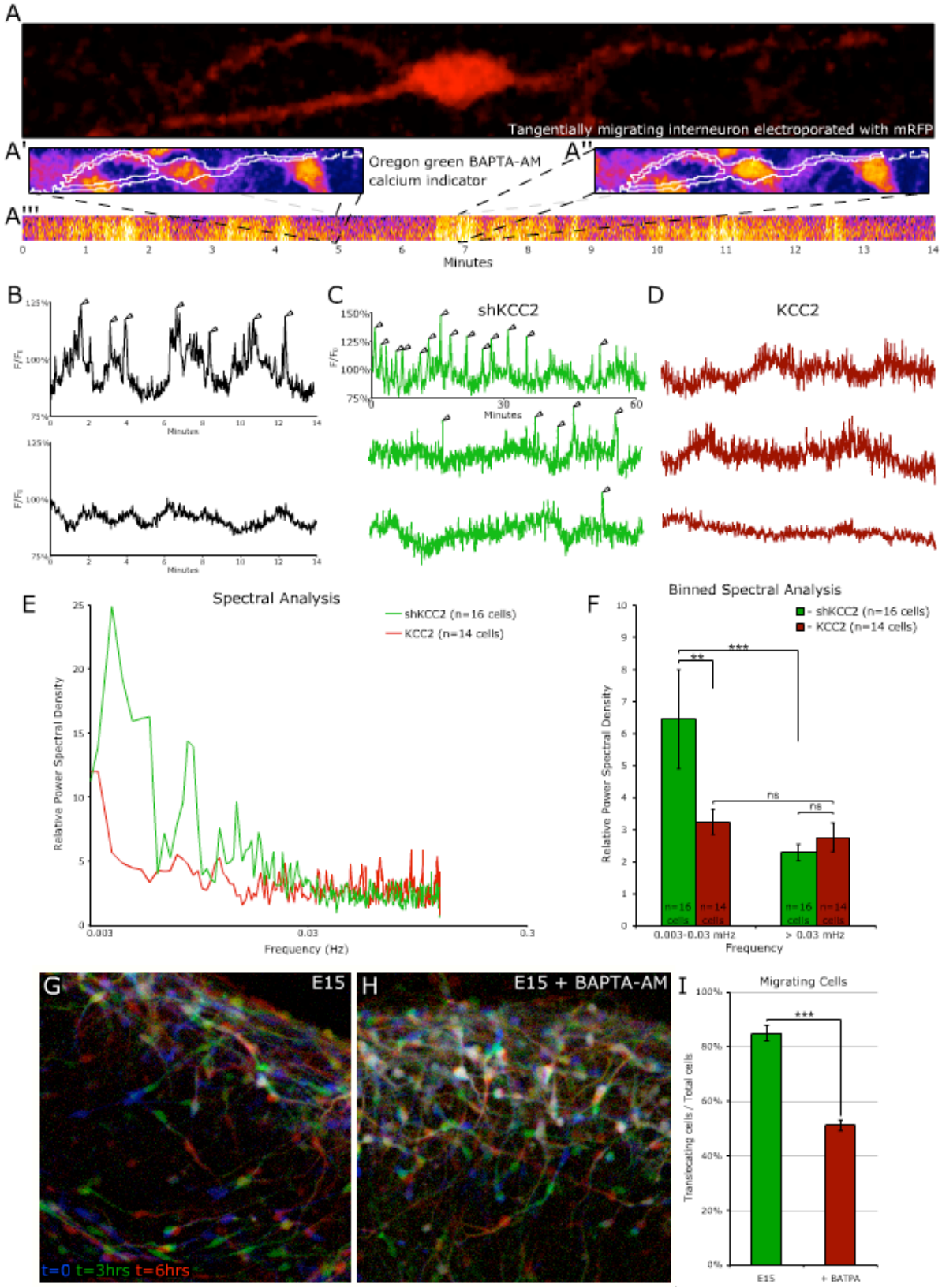
A
Tangentially migrating interneuron electroporated with mRFP
A'
A''
A'''
Oregon green BAPTA-AM
calcium indicator
Minutes
B
C
shKCC2
D
KCC2
E
Spectral Analysis
shKCC2 (n=16 cells)
KCC2 (n=14 cells)
Relative Power Spectral Density
Frequency (Hz)
F
Binned Spectral Analysis
shKCC2 (n=16 cells)
KCC2 (n=14 cells)
Relative Power Spectral Density
0.003-0.03 mHz
> 0.03 mHz
Frequency
ns
G
E15
t=0 t=3hrs t=6hrs
H
E15 + BAPTA-AM
I
Migrating Cells
Translocating cells / Total cells
E15
+ BATPA

branches in retinal ganglion cells (Lohmann et al., 2002). Interestingly, in these studies the frequency of calcium transients as been positively and negatively correlated to axon growth or cell motility. Regulating the switch of GABA from depolarizing to hyperpolarizing could alter the calcium signal frequencies within the migrating interneurons through activation of voltage sensitive calcium channels and/or release of calcium from intracellular stores. Calcium transients have been observed in migrating cortical interneurons but only upon pharmacological manipulations (Soria and Valdeolmillos, 2002) and therefore at this point, the spatial and temporal dynamics of intracellular calcium in migrating cortical interneurons have not been reported.

In order to first study intracellular calcium dynamics in migrating interneurons, we electroporated mRFP in MGE progenitors and cultured these explants on isochronic dissociated cortical neurons as a 2D substrate. These co-cultures were then loaded cells with the cell-permeant calcium-sensitive dye, Oregon Green BAPTA-AM. Calcium dynamics could clearly be monitored in some of these migrating interneurons at E14.5 + 4 div without the addition of drugs (**Fig. 3.6A-A'''**), although the occurrence was not systematic and probably dependent of the history of the cell (imaging was only performed for relatively short periods of time, 10-20 minutes, but at high temporal frequencies; **Fig. 3.6B**).

To determine if KCC2 expression can alter the frequency of these calcium transients, interneurons were electroporated with a control plasmid (red) or control plasmid plus shKCC2. At E14.5 + 4.5 div these migrating interneurons were loaded with 5μM Oregon Green BAPTA-AM and time-lapsed. **Figure 3.6C** shows calcium signals of several shKCC2 interneurons. The number of calcium transients varied from numerous as seen in the top most trace to just a few as seen in the bottom most trace.

Representative traces of KCC2 over-expressing interneurons can be seen in **Figure 3.6D** where few if any calcium transients can be observed. Again, KCC2 knockdown

interneurons often show calcium transients (indicated by arrows), while KCC2 over expressing interneurons do not. In order to quantify more systematically the frequency of these calcium transients, we performed Relative Power Spectral Density (RPSD) analysis (Uhlen, 2004) which showed a significantly higher occurrence of calcium transients at frequencies in the 0.003-0.03 Hz range in the shKCC2 interneurons compared to KCC2 over expressing interneurons (**Fig. 3.6E**). When these values were binned into 0.003-0.03 Hz versus 0.03-0.3 Hz, RPSD of shKCC2 interneurons was significantly higher than that of KCC2 over-expressing cells (**Fig. 3.6F**; $p = 0.0084$, $n = 16$ and 14 cells respectively). The shKCC2 interneurons also showed a significantly higher RPSP of 0.003-0.03 Hz frequencies over >0.03 Hz frequencies ($p < 0.0001$), while KCC2 over-expressing interneurons showed no statistical difference between high and low frequencies. This data indicates that KCC2 expression is negatively regulating the frequency of calcium transients occurring in migrating interneurons.

If there is a causal relationship between intracellular calcium transients and the termination of interneuron migration upon KCC2 up-regulation, one would expect sequestration of intracellular calcium to be sufficient to prematurely stop migration in interneurons as previously shown for cerebellar granule cells (Komuro and Rakic, 1996; Kumada and Komuro, 2004). After chelating intracellular calcium in acute slices of E14.5 + 1 div Lhx6-EGFP with 25μM BAPTA-AM for 2 hours, we performed confocal time-lapse microscopy and compared the dynamics of interneuron migration *in situ* to isochronic control slices. When comparing a control time-lapse (**Fig. 3.6G**) to a calcium-chelated slice (**Fig. 3.6H**), it is apparent that intracellular calcium chelation is sufficient to inhibit or even stop the migration in cortical interneurons. The quantification of these movies shows that most (84.9 ± 2.8%; n=8 movies and 388 cells) interneurons are migrating in control conditions while only 51.4 ± 0.3% (n=3 movies and 204 cells) of interneurons migrate when intracellular calcium is sequestered (**Fig. 3.6I**). This last result strongly suggests that intracellular calcium

transients observed in interneurons are necessary for their migration and that KCC2 upregulation is sufficient to abrogate these intracellular calcium dynamics leading to termination of interneuron migration.

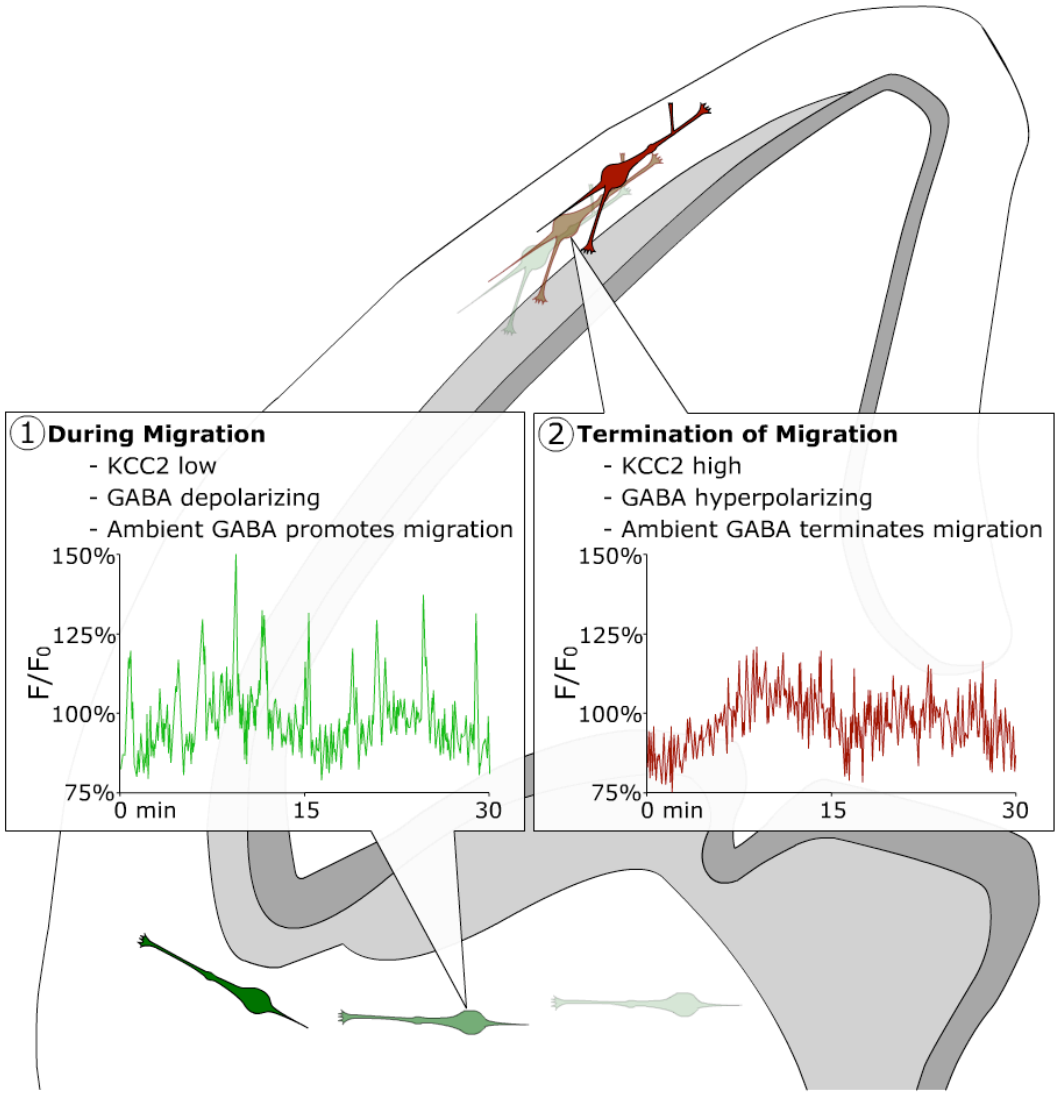

Figure 3.7 - Model explaining KCC2-dependent GABA-induced termination of tangential migration in the developing neocortex.

We propose a model whereby (**1**) interneurons initially express low KCC2 and therefore depolarize upon activation of $GABA_A$ receptors by ambient GABA, causing a calcium influx via activated VDCC's (shown in bottom tracing), which stimulates movement and (**2**) that up-regulation of KCC2 renders activation of $GABA_A$ receptors by ambient GABA hyperpolarizing, reducing calcium signaling (shown in top tracing) and terminating tangential migration.

DISCUSSION

Our results demonstrate that activation of $GABA_A$ receptor by ambient GABA present in the environment of migrating interneurons plays a critical role in the termination of interneuron migration. Interestingly, $GABA_A$ receptor activation is only triggering termination of migration in interneurons upregulating KCC2, which only occurs once migrating interneurons reach the cortical plate.

Given these results, we propose that interneuron migration begins with low expression of KCC2. At this point ambient GABA is depolarizing and facilitates migration by increasing the amount of time the interneurons spend moving i.e. by decreasing their stalling frequency. Assuming interneurons are the primary source of GABA to the cortex this mechanism may facilitate the migration of densely packed interneurons within the marginal and lower intermediate zones. After reaching the cortex KCC2 is upregulated, making GABA hyperpolarizing.

GABA has been previously proposed to modulate interneuron migration, although the direction of modulation often varies depending on experimental approach (reviewed in Owens and Kriegstein, 2002). The opening of ionotropic $GABA_A$ receptors enhances both chemotaxis and chemokinesis in cortical dissociations although $GABA_A$ receptor activation largely hinders migration of GAD+ cells in the cortical plate (Behar et al., 1996; Behar et al., 1998). In spite of GABA's possible hampering effect on migration, other studies have revealed a positive effect of $GABA_A$ receptor activation on radial (Manent et al., 2005) and tangential migration (Cuzon et al., 2006). An interesting study done by Cuzon and colleagues showed that GABA facilitated the migration of interneurons to the cortex without affecting their speed (2006). We believe our results build upon these findings by showing that, although GABA does not affect moving speed, it does affect the travel time of migrating interneurons. By studying this phenomenon with respect to individual interneuron

responsiveness to GABA application and KCC2 expression, we believe we have found a basis for variable responses to $GABA_A$ activation in interneuron migration.

Although KCC2's contribution in setting the reversal potential of GABA has been firmly established, little is known as to why this shift takes place. A recent article by Cancedda and colleagues shows that GABAergic excitation is necessary to attain control levels of dendritic arborization (Cancedda et al., 2007). Down-regulation of KCC2 accompanies long-term potentiation (Wang et al., 2006) and may be a fundamental part of this process. As the removal of the subplate decreases KCC2 expression and prevents the formation of ocular dominance columns (Kanold et al., 2003; Kanold and Shatz, 2006), the regulation of KCC2 may also play a prominent role in the development of the critical period.

The details of when and where the chloride gradient reversal renders GABA inhibitory have only recently been explored. Far from being a global homogeneous up-regulation of KCC2, large differences have been found between brain regions during development (Belenky et al., 2008; Belmonte et al., 2004; Gilbert et al., 2007). The chloride gradient has even been found to vary greatly between adjacent neurons within the same structure (Gilbert et al., 2007). Our results add further complexity to this regulation in showing a heterogeneous up-regulation within tangentially migrating cortical interneurons.

Although our results were significant, in no experiment performed did all interneurons within a category respond uniformly. There are many factors that could affect the responsiveness of a cell to KCC2 expression. KCC2 activity can be modulated by localization, oligomerization and phosphorylation (Adragna et al., 2004; Blaesse et al., 2006; Lee et al., 2007; Wake et al., 2007).

Knowing what factors regulate KCC2 expression in cortical interneurons would greatly aid in completing a model for the termination interneuron migration. Several experimental manipulations such as the induction of long-term potentiation, magnesium removal, neuronal stress, seizure kindling and sub-plate ablation, have been shown to

decrease KCC2 expression (Galanopoulou, 2007; Kanold and Shatz, 2006; Rivera et al., 2004; Wake et al., 2007; Wang et al., 2006). Many experiments have been conducted - with sometimes conflicting results - on the role of BDNF (Miletic and Miletic, 2007; Rivera et al., 2002; Rivera et al., 2004) and GABA (Ganguly et al., 2001; Kriegstein and Owens, 2001; Leitch et al., 2005; Ludwig et al., 2003; Titz et al., 2003; Toyoda et al., 2003) in regulating KCC2 expression, which may indicate a multiplicity of KCC2 regulatory pathways that vary greatly between cell types and subtle differences in experimental conditions.

Our data suggest that a possible mechanism underlying KCC2 function in stopping interneuron migration is the modulation of the frequency intracellular calcium transients. There are many ways to activate calcium signaling through voltage-dependent calcium channel activation within migrating interneurons. Migrating cortical interneurons have been shown to respond to application of AMPA, NMDA, Kainate and $GABA_A$ receptor agonists (Manent et al., 2006; Metin et al., 2000; Soriano et al., 1992). Modulators downstream of calcium may be another source of diversity in the responses observed. Differential turning response of axon growth cones to calcium elevations is dependent on a CaMKII/Calcineurin switch (Wen et al., 2004). It would be of interest to test if such a switch in the expression of Calcium effectors might underlie its effects on interneuron migration.

Calcium has often been tied to the process of cellular migration. The GABA-induced changes in neuronal chemotaxis mentioned previously were shown to be calcium-dependent (Behar et al., 1996). Extension of axonal growth cones - which closely resemble the leading processes of migrating interneurons - move at a rate inversely proportional to their calcium signal frequency. Altering the calcium signal frequency of these axons was sufficient to induce the corresponding change in axon extension rate (Gomez et al., 1995; Gomez and Spitzer, 1999; Kater and Mills, 1991). Conversely, the rate of migration of cerebellar granule cells is directly proportional to the rate of movement. In this case, a loss of calcium transients was correlated with and sufficient to induce termination of cerebellar

granule cell migration (Komuro and Kumada, 2005; Komuro and Rakic, 1996; Kumada and Komuro, 2004).

The long-term consequences of altering the window of migration for interneurons could be quite drastic for cortical circuit assembly. Improper distribution of interneurons may result in cell death in areas where local densities of interneurons are too high (Fuerst et al., 2008) and epileptic activity where too low (Cobos et al., 2005; Li et al., 2008). As the inhibitory network appears integral in the setting of the critical period (Hensch, 2005) extending or retracting the establishment of this network could either force a critical period before the surrounding architecture is ready or delay its onset. Not surprisingly, several pathologies have been associated with alterations in interneuron number such as ASD and schizophrenia. Future experiments will determine the extent to which perturbation in GABA/$GABA_A$ receptor/KCC2/Calcium signaling in migrating interneurons is affecting the assembly and the function of cortical circuitry.

Experimental Procedures

Animals

Lhx6-EGFP BAC transgenic were kindly provided by Dr Mary-Beth Hatten and Nat Heintz (Rockefeller Univ. GENSAT Consortium) were bred on a Balb/C background and maintained in a 12/12 hours light:dark cycle. Day following overnight breeding is considered as E0.5.

Tissue preparation and sectioning

To prepare avertin 40x stock solution, 1g of 2,2,2-tribromoethanol (99%) (840-2; Sigma-Aldrich, St. Louis MO) was dissolved with 1mL of Tert-amyl alcohol (99%) (246-3; Sigma-Aldrich, St. Louis MO) in a glass container and stored at 4^{o}C protected from light for no more than 6 months before use. Working solution was made adding 40x stock solution

to 37° C PBS dropwise. Intraperitioneal injections were made of 250-300uL per 10 grams of mouse body weight. After the pups failed to respond to a toe prick the mice were perfused with 4% PFA in PBS made from 16% Paraformaldehyde solution (Cat. # 15710, Electron Microscopy Sciences, Hatfield PA). Brains were then dissected and fixed overnight in PFA before rinsing 3x 30 minutes with PBS, shaking at room temp, sectioning to 80 μm with a vibratome (VT1000S; Leica; Wetzlar, Germany) and immunostained.

Immunostaining for slices and dissociations.

Made blocking solution (1 g BSA (A7906, Sigma-Aldrich, St. Louis MO)/10 mL PBS; 0.3% Triton X-100 (X-100, Sigma-Aldrich, St. Louis MO) and stored at 4°C). After rinsing in PBS 3x15 min to remove 4% PFA, incubated overnight in blocking solution at 4°C on shaker. Incubated overnight in blocking solution with 1:1000 primary (Chicken polyclonal anti-EGFP (A10262; Invitrogen - Molecular Probes, Eugene OR); Rabbit polyclonal anti-KCC2 (07-432; Upstate, Temecula CA) against residues 932-1043 of rat KCC2; Mouse monoclonal anti-Map2 (Clone HM-2; Sigma-Aldrich, St. Louis MO) at 4°C on shaker. Washed 7x15 min in PBS. Washed 1x15 minutes blocking solution with 5% goat serum. Incubated overnight in blocking solution, 5% goat serum with 1:1000 secondary antibody (488 goat polyclonal anti-chicken, A11039; 546 goat polyclonal anti-rabbit, A11035; 647 goat polyclonal anti-rabbit, A21245; 647 goat polyclonal anti-mouse, A21236; Invitrogen - Molecular Probes, Eugene OR) at 4°C on shaker. Washed 5x15min in PBS and mounted with GelMount (Biomeda Corp, Foster City CA).

Pharmacology

After control time-lapse session, 20μM GABA, made from 20mM stock in ddH2O (A-5835; Sigma-Aldrich, St. Louis MO) was added to cultures before time-lapsing for second session. 10μM Bicuculline Methoiodide (BMI) was added from 10mM stock in ddH2O (2503;

Tocris, Ellisville, MO). 25μM BAPTA-AM made from 10mM stock in DMSO (B1205; Invitrogen - Molecular Probes, Eugene OR) was added to media underneath slice insert and allowed to load for 2 hours before imaging session.

Calcium imaging/quantification

A stock solution of calcium indicator was made by adding 10uL DMSO (D2650; Sigma-Aldrich, St. Louis MO) to 50μg of Oregon Green 488 BAPTA-1, AM (OGB-1; O6807; Invitrogen - Molecular Probes, Eugene OR). After vortexing for 1 min 5x2μL aliquots were frozen at –80^{o}C. Warm 9.12μL Pluronic F-127 in 20% DMSO (P3000MP; Invitrogen - Molecular Probes, Eugene OR) was then added to one aliquot of stock solution. After vortexing for 1 min, a 5μM working solution was made by adding 5μL of pluronic - stock solution to 715μL HBSS and vortexing for another minute.

Interneurons electroporated with pCIG4-Tomato (gift from Dr. Tom Maynard, University of North Carolina - Chapel Hill) or pCIG4-Tomato-IRES-hKCC2 were loaded with working solution at 4 div by removing media from dissociation (saving it at 37^{o}C) and washing 3x in 37^{o}C HBSS. Working solution was applied to the dish and incubated for 30min at room temperature, while protected from light. Cells were then washed once with HBSS, once with 37^{o}C serum free media, and then the old conditioned media was added back to the dish.

Imaging sessions were done by sequentially scanning the red (plasmid) and green (OGB-1) channels with an open pinhole to allow faster scanning (once every 4 seconds). Data was extracted from these movies by designing a macro for ImageJ (NIH, Bethesda MD), which divides the green by the red channel to correct for changes in cell thickness as the interneuron migrates. The macro also masks out all data not corresponding to the cell bodies of interneurons as they migrate. The average intensity values of these cell bodies

were measured and used to calculate a Fluorescence/Fluorescence at t=0 (F/F_0) for every frame.

The spectral analysis was done using the protocol and SpectralAnalysis tool designed for MatLab (The Mathworks, Natick MA) by Per Uhlen (Uhlen, 2004). Using this tool, a Hanning filter was applied to the data to remove edge effects at the beginning and end of the movie. Then a Fourier transformation was done using $2x10^9$ bins to separate the F/F_0 data from its time component and view the relative power spectral density for each frequency in every cell.

Construction of multi-welled dishes

Sylgard 184 silicone elastomer, base & curing agent (Dow Corning Corporation, Midland MI) was to used to attach cut rings of 10mL Stripette (4101; Corning Incorporated, Corning NY) to FluoroDish (FD-35-100, World Precision Instruments, Inc., Sarasota FL). Two days of cure time were allowed before use of these multi-welled chambers.

Constructs

- pCIG4-tomato - gift from Dr. Tom Maynard (University of North Carolina - Chapel Hill)
- pCIG4-hKCC2-IRES-tomato
- pMES-KCC2 hKCC2-IRES-EGFP gift from David Mount (Harvard Insitute of Medicine, Harvard University) and Dr. Karl Kandler (University of Pittsburgh)
- pMES control – gift from Dr. Catherine E. Krull (University of Missouri – Columbia MO)
- shKCC2 – Short hairpin RNAi targeting vector was designed using Ambion's Insert Design Tool (http://www.ambion.com/) against sequence spanning amino acids 2874-2894 of mouse KCC2 (5'-AGCGTGTGACAATGAGGAGAA-3'). The shKCC2

was cloned into pSilencer 2.0-U6 (Applied Biosystems - Ambion, Austin TX) for expression.

Ex vivo electroporation and organotypic slice culture

Dorsal electroporations were used to label progenitors of pyramidal cells with before dissociations. Intact decapitated E14.5 wild-type heads were punctured through the skull at the junction between the 2 cortical hemispheres and the developing midbrain. Trough this hole a small glass capillary pippette (electrode puller and glass capillary) filled with pCIG4-Tomato (greater than 1μg/μL endotoxin free plasmid DNA; MEGA EF Kit; Clontech, Mountain View CA) and Fast Green FCF (0.5% at 1:20; Sigma-Aldrich, St. Louis MO), could inject into the lateral ventricals by positioning the tip between the eyes and 1 mm off midline. A Picospritzer III (General Valve) was used for the injection using several 10psi 5ms pulses to fill both ventricals. Following the injection 4x 50V 100ms pulse / 100ms pause currents were applied to each hemisphere with an ECM 830 electroporator (BCX) using Genepaddles (Model 542, BTX) with the negative electrode paddle positioned underneath the head and the positive one parallel to the ventricle. Brains were then either dissociated or sliced as normal.

Slicing for *ex vivo* organotypic cortical slice culture

Brains were removed, with pia intact, from skull into 4^{o}C HBSS complete (HBSSc; Polleux et al., 2002). Twenty-five milliliters of 3% low melting agar in HBSSc was heated by microwaving at 30% power until boiling three times while inverting several times between each boil. A 3mm layer of agar was allowed to chill on bottom of tear away dish (Cat#18646C; Polysciences; Warrington PA) until solid. The remaining agar was poured into the cast, on ice, and stirred with a digital thermometer until it read 50^{o}C. It was then removed from the ice and placed on the bench top and continually stirred while cooling. At 42^{o}C dissected brains were removed from the HBSSc with a spatula (Cat#10090-13; Fine

Science Tools; Foster City CA) and blotted with Kimwipes (Cat#34120; Kimberly-Clark Professional; Roswell GA) to remove excess media. Upon addition to the agar brains were batted around to remove any excess media. After remaining brains were added they were positioned so that the rostral caudal axis was parallel to the bottom of the dish. The cast was placed on ice until the agar was cold to the touch. Mounted brains were then cut coronally to 300 μm sections and either mounted onto inserts (Cat# 353102; Becton Dickinson Labware; Franklin Lakes NJ) for culture or confocal inserts (PICM ORG; Millipore; Cork, Ireland) for culture and time-lapse. Slice media was added under the insert as described previously (Polleux et al., 2002).

MGE slice electroporations

Before mounting, slices were electroporated directly into the MGE to label migrating interneurons. A 1mm section of agar was cut and placed over the positive electrode. A coronal section containing the MGE was then placed on the agar. One pulse of DNA (greater than 1μg/μL endotoxin free plasmid DNA; MEGA EF Kit; Clontech, Mountain View CA) and Fast Green FCF (0.5% at 1:20; Sigma-Aldrich, St. Louis MO) was picospritzed into the ventricular zone and sub-ventricular zone of the MGE. To the negative electrode media was applied with a pippette and used to connect the circuit by touching the media to the top of the slice. When only the MGE/striatum is between the paddles a 5x 60V 5ms pulse / 500 ms pause was applied (Cobos et al., 2007). Slices could then be cultured as normal.

Explanting to dissociated cortical cultures

E14.5 dissociations were conducted as described previously (Polleux et al., 2002). Explants from E14.5 EGFP or electroporated MGEs (same as slice electroporation protocol) were then cut into 6-8 pieces and explanted to the dish after the dissociation had time settle for 30 minutes and had serum free media applied. Multi-well chambers were plated at a

density equal to that of the normal dishes by diluting to 500,000 cell per mL and applying 300uL of dissociate. One to three explants were applied to each dish.

Confocal microscopy

Confocal microscopy on fixed tissue was done as described previously (Hand et al., 2005). Time-lapse microscopy was done as described previously (Hand et al., 2005) with an imaging frequency of a picture taken every 10 minutes for migration studies. These movies are played back at a rate of 7 frames per second (sped up 4200x real time). Calcium imaging movies were and every 4 seconds for calcium imaging sessions (see calcium imaging section for details).

Quantification of migration dynamics

Positions of interneuron cell bodies were recorded frame by frame using ImageJ (NIH, Bethesda MD). The movement of these cells over time was extracted using Excel custom functions and macros (Microsoft). Average speed was calculated as the total time of movie divided by the total distance traveled. Moving speed was calculated as the total time the cell was moving divided by the total distance traveled. Percent travel time was quantified as the total time spent moving divided by the total time of the movie. Even after applying stack registry (Turboreg and Stackreg; Thévenaz et al., 1998) to align the images some vibrations were still present. After visually comparing distances measures to actual movements observed, it was determined that movements less than 1.1 μm were noise. Therefore movements below the threshold of 1.1 μm were considered to be not moving for all movies.

Quantification of KCC2 optical density was measured with ImageJ (NIH). For data matched to time-lapse information, post-hoc KCC2 immunostained interneurons were sampled with a consistent sampling radius in the three most intense portions of the cell.

These were typically located, though not limited to, the base of the leading process. The average of these three values was used for binning and plotting the corresponding cell's time-lapse information. For up-regulation info, including confirmation of the short hairpin's knockdown potential, only the most intense sampling radius was used for quantifications.

Supplemental Data

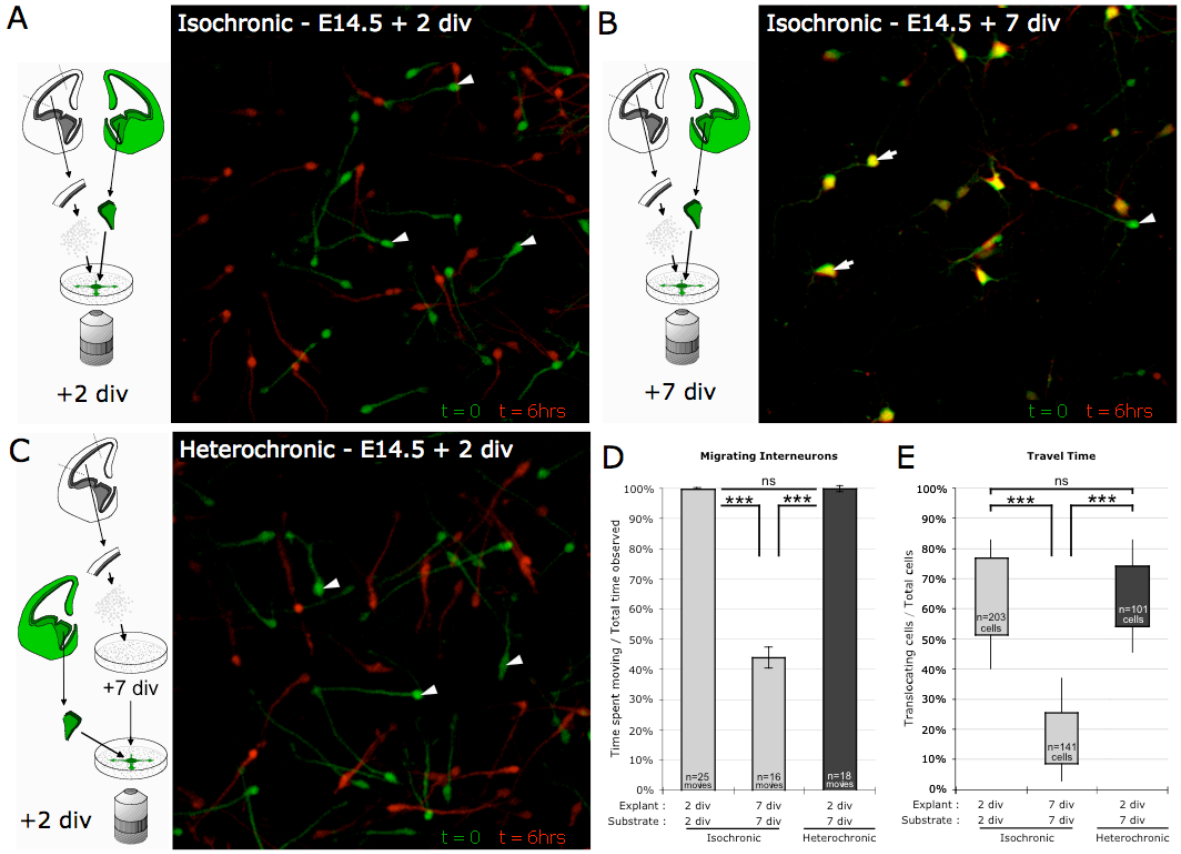

Supplemental Figure 3.1 - Termination of migration has a cell autonomous component

E14.5 wild-type cortical cells are dissociated, plated and co-cultured with EGFP-expressing MGE explants. Frame corresponding to the start of imaging (t=0) is pseudo-colored in green. Image taken six hours later is pseudo-colored in red. Yellow cell bodies correspond to interneurons that stopped migrating. Note isochronic cultures of interneurons phenocopy reduced travel time from 2div(**A**) to 7 div (**B**) as observed *in situ*. In heterochronic cultures (**C**), dissociated E14.5 wild-type substrate was aged 7-9 days before placing E14.5 EGFP-MGE explants.
Quantification shows no significant difference in percentage of migrating interneurons (**E**) or travel time (**D**) on an aged substrate indicating interneurons require a cell autonomous maturation to slow and terminate migration.

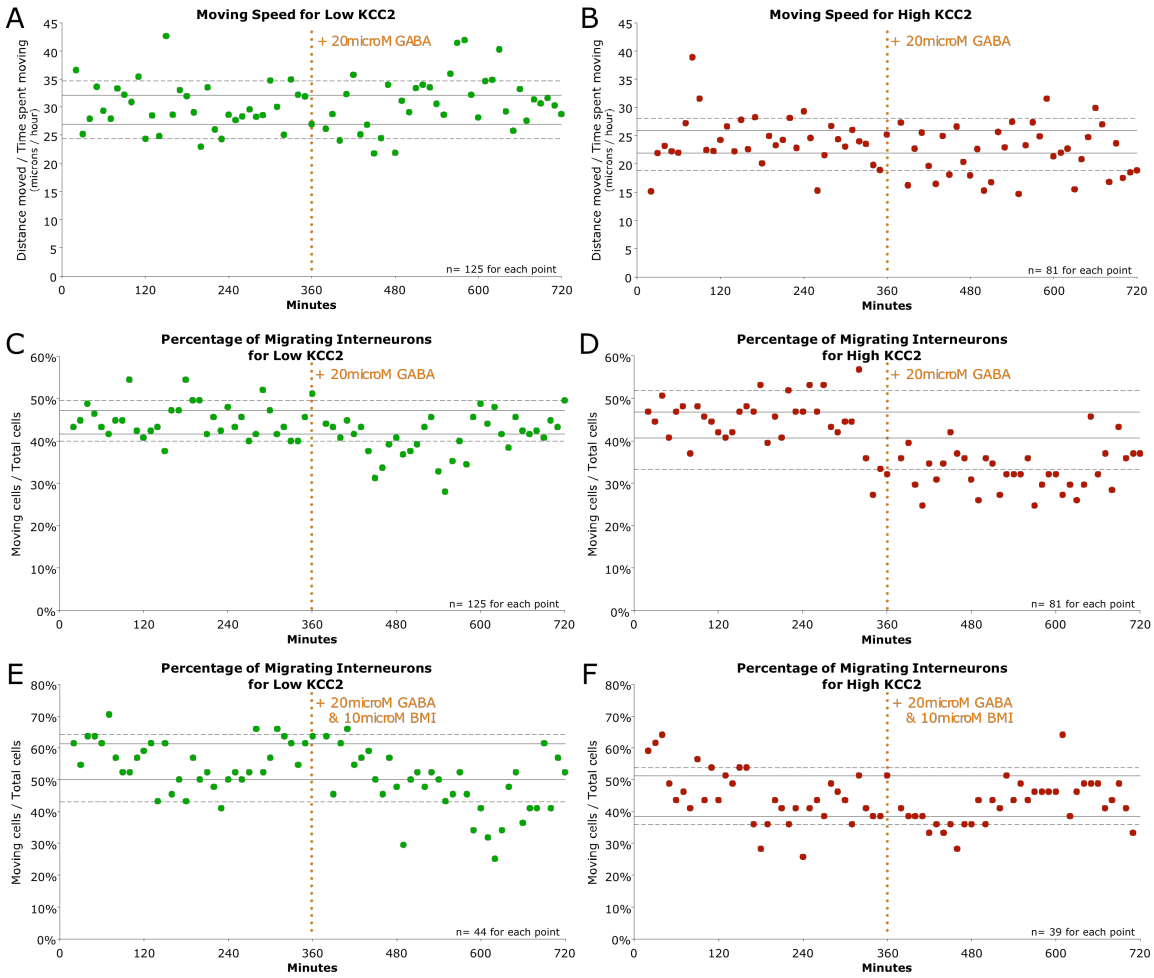

Supplemental Figure 3.2 - Frame by frame responses to GABA addition

(A-F) Data shown in Figure 2E-F is shown here as frame by frame average values of interneurons binned into low and high KCC2 populations. Dotted yellow line shows addition of 20microM GABA (**A-D**) or 20microM GABA + 10microM BMI (**E,F**). Solid black lines indicate pre-drug 25th and 75th percentiles. Dotted black lines indicate pre-drug 10th and 90th percentiles. Note drops in average speed and travel time after GABA addition for high KCC2 expressing interneurons (**B,D**) but not with co-application of GABA and $GABA_A$ antagonist BMI (**F**). Note also travel time decrease in low KCC2-expressing interneurons when GABA is co-applied with BMI.

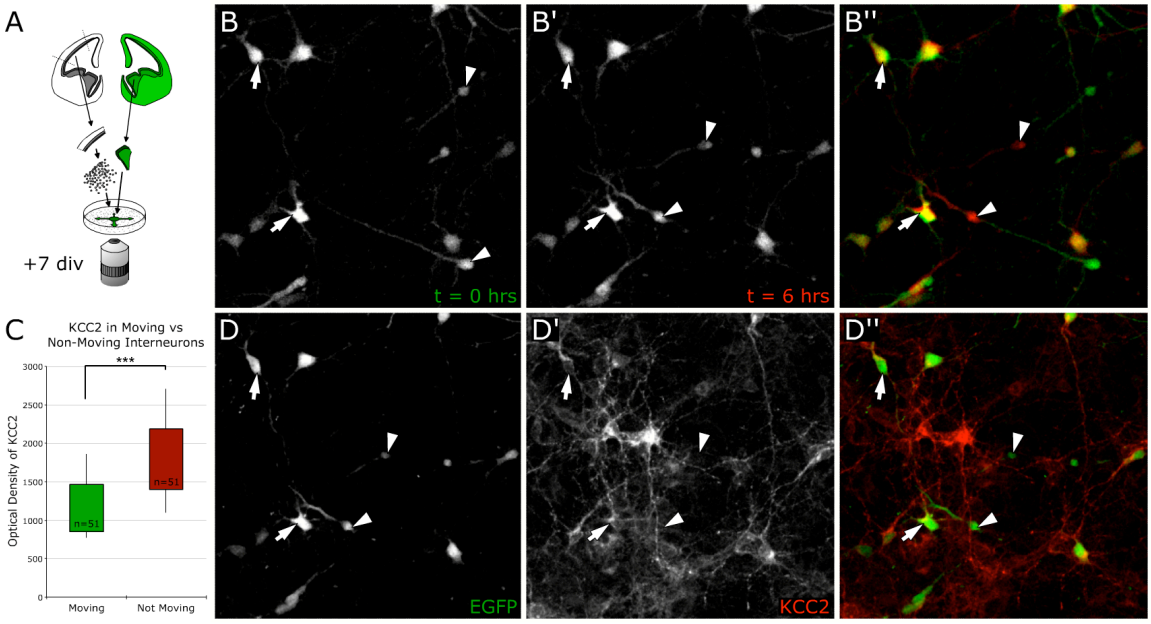

Supplemental Figure 3.3 - KCC2 correlated with termination of interneuron migration

(**A**) E14.5 EGFP-MGE explants were placed on E14.5 wild-type dissociations and cultured for 7div. These interneurons were then time-lapsed for 6 hours (**B**), fixed and immunostained for KCC2. (**C**) Binning interneurons into moving and non-moving populations reveals significantly higher KCC2 expression in the non-moving population ($p<0.0001$). Note yellow co-labeling of KCC2 with interneurons in **D** matches yellow 'co-labeling' in time-lapse representation (B''), indicating KCC2 expressing interneurons have terminated migration by 7 div.

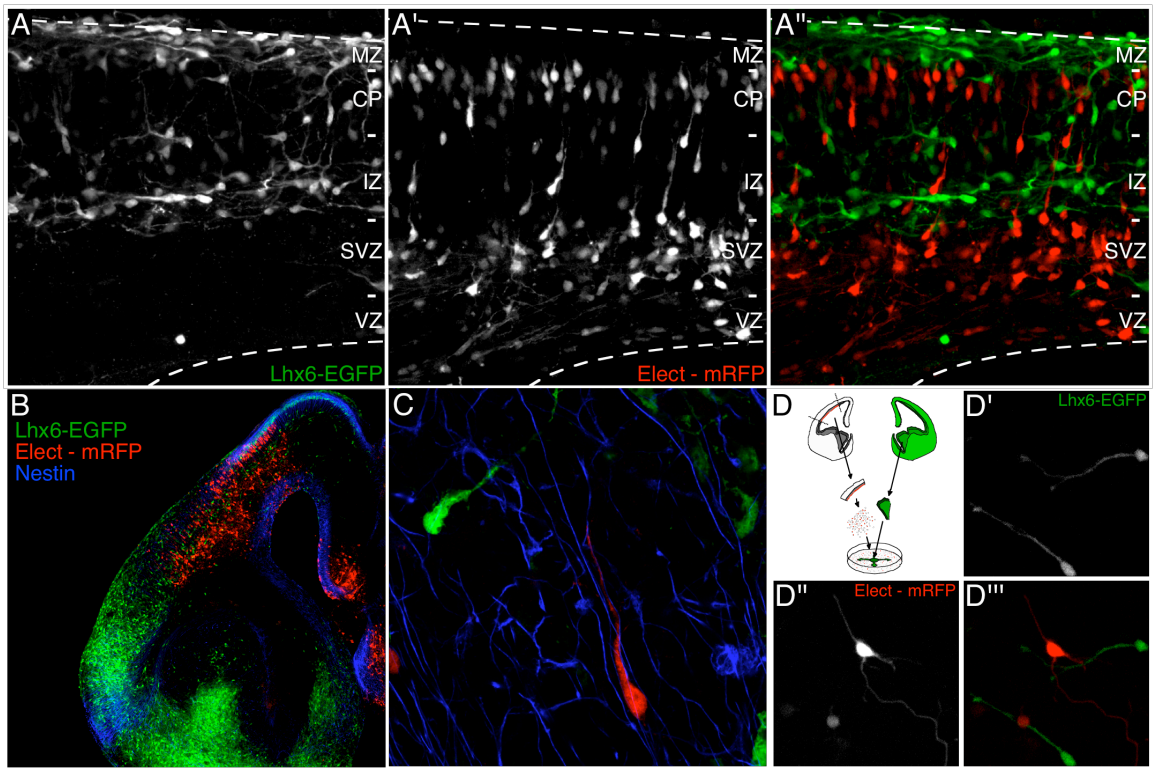

Supplemental Figure 3.4 - Dorsal electroporation specifically labels pyramidal cells

(**A-C**) Lhx6-EGFP pups were electroporated with monomeric red fluorescent protein (mRFP) and cultured 3 days showing no co-labeling indicating this is an effective method to specifically label pyramidal cells. (**D**) Dissociating electroporated wild-type pyramidal cells and applying an EGFP-MGE explant enables concurrent culturing of labeled interneurons and pyramidal cells.

CHAPTER FOUR

Discussion

The role of Ngn2 in the specification of pyramidal neuron migration and morphology

The Polleux Laboratory ran into several limitations in its attempts to understand the role of Neurogenin2 (Ngn2) in pyramidal neuron differentiation (Mattar et al., 2004; Schuurmans et al., 2004; Seibt et al., 2003). Ngn2 is a basic helix-loop-helix (bHLH) transcription factor whose expression contributes to the specification of their glutamatergic identity (Schuurmans et al., 2004). When trying to assess the effect of Ngn2 on other aspects of pyramidal neuron identity, such as migration and morphology, the results were highly subjective (FIGURE - graph user counts). This variability brought into question the consistency of our measurements and cast doubt on our objectivity in the quantification of neuronal morphology. It was therefore necessary for me to develop an automated method of assessing pyramidal cell morphology. To do this, I developed a java-based ImageJ plugin to count and measure the width of individual neurites automatically. ImageJ is an open source image analysis program designed by the National Institute of Health. The ImageJ plugin used the neurite information to calculate a pyramidal morphology index (PMI) to quantitatively reflect neuronal polarity **(Fig. 2.8O)**. A polarized pyramidal neuron will have a very high PMI while a multipolar interneuron will have a low one **(Fig. 2.8N)**. The automated measurement of PMI standardized our counting methods, ensuring the polarity measurements were not dependent upon unintentional bias, background lighting or personal

preferences. This plugin helped to quickly and consistently assess the role of Ngn2, and specifically the role of tyrosine residue 241 phosphorylation, in determining pyramidal cell polarity.

The quantification methods developed for the Ngn2 study represented a major step towards unbiased analysis of neuronal morphology and neuronal migration. Results obtained using the Pyramidal Morphology Index (PMI) were adapted to reflect subjective assessment of neuronal morphology by a trained observer. As a result, this plugin has been requested by several labs to analyze morphology in their own investigations. In improving the reliability of our own measurements, this field of investigation was also given a tool to help standardize the quantification of neural polarity, allowing better comparisons between research labs.

Similar subjectivity problems were encountered, when analyzing the role of Ngn2 in the specification of the radial migration properties of pyramidal neurons. Experiments in which I electroporated radial progenitors with a variety of Ngn2 constructs produced a striking effect in migration, but the quantification of thousands of cells in just one slice could take days. Time was not the only consideration. The same subjectivity problems noted above in counting neurite number also came into play. Lighting, user preferences and fatigue drastically influenced whether a given spot was considered a neuron. To address this problem, it was again necessary to program software for image analysis. Cell positions were extracted using ImageJ. These cell positions could then be quantified in terms of how far each neuron had migrated form the ventricular zone after the creation of a Visual Basic for Applications (VBA) program designed for that purpose. This computational analysis allowed the counting of thousands of cells in a given slice, enabling the laboratory to provide a quantitative comparative analysis of data that is often only shown as a single qualitative picture. Although imaging is extremely beneficial in understanding the nervous system, it

can also be limited by the subjectivity of the user. The use of image analysis software greatly helped in bypassing these limitations.

The neuronal migration quantification program, designed to quickly and reliably calculate cell positions, succeeded as well. The number of cells counted per condition in this investigation was approximately twenty thousand. In a field where results of this type are typically shown with cell counts in the hundreds - or often just a picture without analysis - this represents major advancement in accurately reporting results. Given the intra-slice variability within a single condition, it is difficult to believe publications that simply show a picture with no quantifications.

The limitations of interpreting static images also became apparent after close review and quantification of these electroporated slices. We realized it was difficult to make inferences about the extent of migration, an extremely dynamic process, using fixed slices. If neurons appeared trapped in the intermediate zone, it was impossible to tell if they had stopped migrating and further differentiated to a non-motile state or if aberrant migration was occurring. This was an essential question in determining whether Ngn2 was involved in migration itself or in controlling other aspects of differentiation such as polarity. While analyzing fixed images of neurons has provided informative snap-shots of cortical development, the gaps in information left room for speculation and guessing.

A look toward time-lapse confocal microscopy

Static imaging often leave gaps in our interpretation of neural development. A method used to fill in these gaps by many scientists has been the use of time-lapse analysis. This type of analysis has increased exponentially our understanding of the mechanisms underlying the development of the central nervous system. If fact, most of the migration information discussed above was either a direct result of, or stemmed from knowledge gained, through time-lapse confocal microscopy of cortical slices.

Steven Noctor, Arnold Kreigstein and colleagues have contributed much to our understanding of radial migration by extensive use of time-lapse microscopy. They labeled radial progenitors by injecting low titers of a EGFP-expressing retrovirus into the lateral ventricle of rat embryos. Individual fluorescently-labeled radial progenitors and their progeny could now be directly observed using time-lapse. After countless hours of observation, they were able to connect the transitions made during different phases of radial migration. They observed radially migrating neurons enter the multipolar phase of the SVZ. From there they watched these abventricular divisions result in either two progenitors or two post-mitotic neurons (Noctor et al., 2004). They also watched these neurons migrate back to the same clonally related radial glia fiber and proceed to the cortical plate (Noctor et al., 2001). Without directly observing the same cell undergo these dynamic transitions the gaps between these phases of radial migration might still be unknown.

The migratory patterns of other neuronal sub-populations have also been elucidated using time-lapse microscopy. Hitoshi Kommuro, Pasko Rakic and colleagues have made huge strides in determining the role of calcium transients in the termination of cerebellar granule cell migration using this method. Calcium transients were not only correlated with slowed and terminated migration, but were also necessary for continuation of migration as chelating intracellular calcium with BAPTA-AM caused a premature termination of migration (Komuro and Kumada, 2005; Komuro and Rakic, 1996; Kumada and Komuro, 2004). Tim Gomez and colleagues found the inverse relationship between axon growth cone extension and calcium transients. In this system decreased calcium frequency was correlated with increased growth cone extension. Inhibiting calcium signaling in this situation caused an increase of growth (Gomez et al., 1995; Gomez and Spitzer, 1999). The assessment of speed and movement in these other dynamic systems would not have been possible without directly observing the dynamics of these events.

The success of time-lapse in resolving so many different aspects of neural development made it an appealing method for our analysis of radial migration with respect to Ngn2. By implementing time-lapse confocal microscopy of electroporated slices, I was able to directly observe the behavior of radially migrating pyramidal cells expressing both control and mutant forms of Ngn2. Time-lapse analysis of radial migration properties of control and $Ngn2^{Y241F}$ expressing neurons provided critical information in the understanding of Ngn2 function. Where PMI analysis of dendritic neuronal morphology showed that phosphorylation of tyrosine residue 241 was involved in either repressing the outgrowth of multiple neurites or enhancing the formation of a single apical dendrite (Hand and Bortone et al. Neuron 2005), the migration assays were difficult to interpret as fixed images. The electroporation of $Ngn2^{Y241F}$ in cortical progenitors in slice culture did show a deficit in reaching the cortical plate. This could have been the result of either a premature differentiation of dendrites, or a transition to an ineffective mechanism of migration. The time-lapse results revealed the latter: (1) the processes of Ngn2 Y241F expressing neurons were highly motile leading to the absence of a polarized leading process extension and (2) the soma was incapable of translocating properly. The formation of multiple processes may have disrupted interactions between the migrating neuron and the radial glial scaffold, which would disrupt it migration (Anton et al., 1996). and prevented its migration to the cortical plate.

It would be interesting to determine if the initiation of multipolar migration is a positive or negative effect: Does phosphorylation at tyrosine residue 241 of Ngn2 promote pyramidal morphology and migration or does it repress multipolar morphology and migration? Expressing a transcriptionally inactive yet phosphorylatable Ngn2 AQ mutant in cortical interneurons could answer this question. The AQ mutation would ensure the observed effects were not due to transcriptional functions of Ngn2.

This study revealed several instances of pleiotropy. Ngn2, a transcription factor known for its transcriptional role in neural differentiation, also played a transcriptionally independent role in specifying polarity. Furthermore, the same residue that specified unipolar morphology in dendrite formation also specified unipolar morphology in migration.

The role of GABA in terminating interneuron migration

Having seen the power of combining computational analysis with time-lapse in our study of Ngn2, I applied these approaches to study the dynamics of tangential migration. As mentioned previously, there is a glaring void in the literature with respect to when tangential migration of interneurons ends during cortical development. The lack of a known substrate for interneurons makes it particularly difficult to predict when and where these cells stop migrating using conventional static imaging methods. The termination of interneuron migration was thus characterized using time-lapse analysis of Lhx6-EGFP BAC transgenic mice obtained from the GENSAT consortium. Quite unexpectedly, the characterization of this phenomenon led directly to another great question in interneuron migration: What is the effect of $GABA_A$ receptor activation on migrating interneurons?

Previous research on this topic yielded contradictory results: $GABA_A$ receptor activation has been reported to inhibit the migration of interneurons (Behar et al., 1996; Behar et al., 1998), while having a positive effect on interneuron migration to the cortex (Cuzon et al., 2006). The cause of these contradictory results were largely due to indirect observations of migration, improperly identifying cell types and ignoring interneuron heterogeneity with respect to KCC2 expression. By making a detailed analysis on the effect of GABA application on individual interneurons I was able to resolve the effect of $GABA_A$ receptor activation, KCC2 expression and the termination of interneuron migration.

Early attempts to answer this question by Behar and colleagues using Boyden micro-chemotaxis chambers, found that GABA can stimulate the migration of interneurons at

micromolar concentrations. Because the movement of these cells was not dependent on a gradient of GABA, the migration was deemed chemokinetic – stimulating movement as opposed to a chemotactic, directional response. $GABA_B$ and $GABA_C$ receptor agonists blocked this chemokinetic response, but not $GABA_A$ receptor agonists (Behar et al., 1996). This group produced another publication where the cortical plate was separated from the ventricular zones before being dissociated. They found dissociated cultures of dorsal telencephalic neurons were particularly rich in GABAergic neurons. These GABAergic neurons responded similarly to their previous investigation (Behar et al., 1996). They reported $GABA_A$ receptor activation only caused a chemotactic response in non-GABAergic cells of the VZ (Behar et al., 1996; Behar et al., 1998). This research is often cited as evidence that GABA increases the motility of cortical interneurons through the activation of $GABA_B$ and $GABA_C$ receptors.

Although these experiments represent an important step towards showing an effect of GABA during early neocortical development, there are several difficulties in their interpretation. The main concern is that they did not observe migration dynamics in vivo but rather depend on the use of a rather artificial Boyden chamber in vitro system. Another problem with not imaging migration directly is that GABA is known to increase cell size (Inglefield and Schwartz-Bloom, 1998; Marty et al., 1996). Since the wells of the microchemotaxis chambers used were 8microns in diameter, it is possible that the measured effect was not dependent upon migration, but of being able to pass through the pores. The choice of substrate further confounds the interpretation of these results. A coating of poly-D-lysine was used. In our experience, cortical interneurons are extremely sensitive to their extracellular substrate and in our hands do not migrate on poly-D-lysine only (Bortone and Polleux unpublished observations). This is why we used a dissociated ‘carpet’ of cortical neurons or extracellular matrix (ECM) protein mixture like collagen or Matrigel (Wichterle et al., 1997; Bortone and Polleux unpublished results). The result of the

Behar study did much to implicate a role for GABA in the cortex, but without the direct observation of migration using time-lapse and the positive identification of cortical interneurons, it is difficult to tell exactly what that role might be.

A more recent study performed by Virginia Cuzon and colleagues both labeled interneurons and directly observed their migration using time-lapse microscopy (2006). Interneurons were identified by using explants of MGE from a mouse constitutively expressing enhanced green fluorescent protein (EGFP). EGFP-expressing interneurons could then migrate out from this explant and be readily identifiable on the wild-type cortical background. In slices of cortex they found that inhibiting $GABA_A$ receptors hindered the migration of interneurons from the striatum into the cortex. They measured the speed of these migrating interneurons and did not notice a significant change between controls, $GABA_A$ agonist and $GABA_A$ antagonist treated populations. They suggested that somehow the entry of these interneurons into the cortex was prohibited at the corticostriatal boundary (2006).

Again, there were several limitations that may hinder the resolution of the role of $GABA_A$ receptor activation in cortical interneurons. **Chapter 3** of this dissertation research has shown that interneurons expressing high levels of KCC2 respond to $GABA_A$ receptor activation by stopping more often. This effect would not have been detected in the study by Cuzon and colleagues for several reasons: (1) In the Cuzon study (2006) time-lapse experiments were only conducted for up to 3 hours. For interneurons that migrate in a saltatory start-stop manner, this is not a very long time to get a baseline measurement of speed. We made twelve-hour observations to reduce the noise inherent to saltatory locomotion. (2) Many cells were excluded from their quantification. Only moving interneurons that were heading in a particular direction were counted. Since the effect of $GABA_A$ receptor activation on migrating interneurons is to change the proportion of cells that move, and not how fast they move, this method would not be able to detect the results found

in our study. By specifically looking at the proportion of time the interneurons travel and the percentage of interneurons moving, we could clearly detect the effect of GABA in terminating interneuron migration. (3) Interneuron data was not segregated based on KCC2 expression. Upon GABA application, heterogeneity of KCC2 expression within the interneuron population results in high KCC2 expressing interneurons pausing more often while low KCC2 expressing interneurons are unaffected. Including these groups together dilutes the effect. To resolve the effect of $GABA_A$ receptor activation on interneuron migration, we tracked the individual responses of interneurons to GABA and segregated the effect based on KCC2 expression. This detailed analysis enabled the role of GABA in the termination of interneuron migration to be observed for the first time.

GABA signaling during neuronal development

Decarboxylation of glutamate by GAD65/67 enzyme is not the only way to synthesize GABA *in vivo*. GABA-transaminase (GABA-T) can catalyze GABA from α-ketoglutarate and is present in the mammalian brain (Tillakaratne et al., 1995). GABA can also be synthesized through putrescine (Tillakaratne et al., 1995). GAD67 knockouts showed less immunostaining for GABA (Asada et al., 1997), although homeostatic mechanisms may enhance cellular responsiveness to GABA that is present, perhaps by up-regulating $GABA_A$ receptors. Additionally, GABA is not the only known agonist to $GABA_A$ receptors. Taurine can activate these receptors as well (Hussy et al., 1997). Interestingly, allopregnanolone is a positive allosteric modulator of $GABA_A$. This neurosteroid is present in large concentrations before parturition. Immediately prior to birth allopregnanolone levels drop drastically, affecting signaling through $GABA_A$ receptors (Herbison, 2001). Another birth related hormone is oxytocin. Its release transiently suppresses GABAergic inhibition by reducing intracellular chloride concentrations (Tyzio et al., 2006), prior to inducing birth.

Perhaps these hormones serve to reduce GABAergic excitation and up-regulate KCC2 to terminate the migration of some interneurons prior to birth.

Alterations in the window of tangential migration would also be expected in KCC2 knockout or knockdown mice. Without KCC2, GABA would remain depolarizing which might result in increased stimulation of voltage dependent calcium channels (VDCC) and prolong interneuron migration thereby delaying inhibitory synaptogenesis. Interestingly, a 'reduction' of parvalbumin positive interneurons was observed in the cortex of homozygous hypomorphic KCC2 mice by P10-11. Parvalbumin is not expressed in immature migrating interneurons; it is up regulated after the first postnatal week of cortical development *in vivo* (Soriano et al., 1992). The authors attributed a lack of parvalbumin positive interneurons to death induced by excessive seizure activity (Woo et al., 2002). An alternative explanation for a lack of parvalbumin positive interneurons in the KCC2 hypomorphic mice is that their terminal differentiation (including expression of Parvalbumin) might simply be delayed due to a prolonged migratory behavior. Also potentially in line with our observations, rat pups treated prenatally with nimodipine (an L-type Ca^{2+} channel antagonist) showed precocious expression of parvalbumin and S-100ß (Buwalda et al., 1994). Our results would suggest that the antagonism of intracellular calcium transients would cause cortical interneurons to terminate migration and begin expressing more mature markers of interneurons prematurely.

Finally, alterations in the termination of interneuron migration might also affect the time-course of synaptogenesis. If premature KCC2 expression causes a premature termination of interneuron migration then one might expect GABAergic synapses to form prematurely. In rat hippocampal cultures, precocious expression of KCC2 causes an enhancement in GABAergic synapses (Chudotvorova et al., 2005). Perhaps this enhancement was caused by an early termination of interneuron migration in these cultures. This could be tested in our system to see if the expression of KCC2 interneurons results in

an enhancement of GABAergic synaptogenesis. Other processes may be affected by KCC2 regulation as well.

Long-term potentiation and depression of migration

Long-term potentiation (LTP) of synapse strength has been correlated with a decrease in KCC2 expression (Wang et al., 2006). LTP is a well know phenomenon, whereby a period of high frequency presynaptic stimulation increases the size of the resulting excitatory post-synaptic potential (EPSC). Although synapses do not exist on tangentially migrating interneurons (Metin et al., 2000), the activation of $GABA_A$ receptors on low KCC2 expressing interneurons may provide a stimulatory mechanism, which results in a long-term potentiation of movement. It would be interesting to see if a brief $GABA_A$ receptor stimulation could potentiate movement of interneurons. The KCC2 variability observed in interneurons may therefore be a reflection of the interneuron excitatory history as it progressed along its migratory route. Similarly, one might expect a long-term depression (LTD) of movement in high KCC2 expressing interneurons. To find the mechanisms of LTP and LTD at work in migration - a non-synaptic context - would be an extremely interesting finding.

Role of other neurotransmitters

GABA may not be the only neurotransmitter involved in the process of interneuron migration. Interneuron migration may ultimately be affected by calcium signaling. Calcium transients have been stimulated in tangentially migrating interneurons with AMPA, NMDA and Kainate receptor agonists (Metin et al., 2000; Poluch et al., 2003; Soria and Valdeolmillos, 2002), implying glutamate may modulate interneuron migration as well. Metin and colleagues further observed vesicle containing corticofugal growth cones and neurites in close proximity with interneurons (Metin et al., 2000). This raises the possibility that

glutamate-mediated calcium transients may also affect the migration or the termination of migration in interneurons. Contrary to this suggestion, activating AMPA receptors causes a retraction of the leading process in migrating interneurons. This retraction is interpreted as a reduction in migratory capacity (Poluch et al., 2003). However, interneurons often migrate much faster with smaller neurites (Bortone and Polleux unpublished observations). Given the positive correlation between GABA-induced calcium signaling and interneuron migration observed in **Chapter 3** of this dissertation, it is possible calcium transients induced by glutamate also serve to stimulate migration and prevent the termination of migration.

Differentiation

This process of KCC2 regulation may also affect the differentiation of interneurons. The work of Spitzer and colleagues has shown a correlation between the calcium influx and neurotransmitter choice of *Xenopus* embryonic spinal neurons. Increased calcium influx resulted in more neurons expressing the inhibitory neurotransmitters, glycine and GABA. Decreased calcium influx led to more neurons expressing markers of excitatory neurotransmitters, vesicular glutamate transporter and choline acetyltransferase (Borodinsky et al., 2004; Spitzer et al., 2004). Although it is unlikely the calcium history of mammalian cortical interneurons is changing their inhibitory nature, other aspects of their differentiation may be affected. A similar phenomenon may be at work in zebrafish, where precocious expression of KCC2 results in fewer Dbx1 expressing interneurons (Reynolds et al., 2008).

Tiling

GABA may act through an autocrine signaling mechanism to modify the spacing or tiling of interneurons within the cortex. Interneurons possess both $GABA_A$ receptors and the ability to stimulate them by the release of GABA while migrating (Cuzon et al., 2006; Poluch

and Konig, 2002). In my initial studies at the Polleux Lab, I observed some interesting calcium transients when the leading processes of interneurons touched one another. This contact was followed by an immediate retraction of the processes and a turn in the opposite direction (see figure). The study of this phenomenon was discontinued because it did not happen consistently. Perhaps the consistency was relative to KCC2 expression. If KCC2 regulates the responsiveness of interneurons to one another, alterations in its expression may dramatically affect the spacing of interneurons in the cortex.

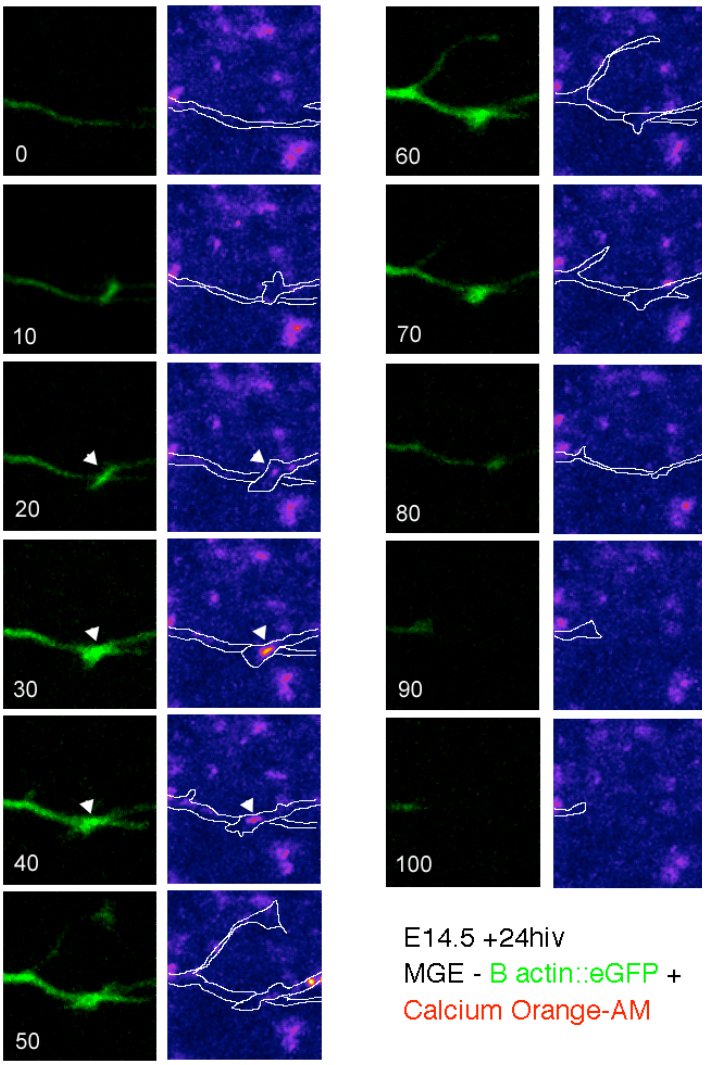

Figure 4.1 - Interneuron display contact mediated repulsion with concomitant calcium fluctuations
Time-lapse sequence of interneuron processes (green) and corresponding Calcium Orange-AM signal (pseudo colored) are shown. Time in minutes is shown on each frame. Process on left is contacted by process on right at time = 20 minutes. Note the corresponding calcium signal in the calcium channel. Both processes respond by retracting. The interneuron on the left (not shown) translocated away in the opposite direction of the contacted neurite.

Neuropathologies

There could be a number of neuropathologies affected by alterations in KCC2 expression. The function of interneurons is often suspected as a contributor to many diseases such as epilepsy and spectrum disorders like autism spectrum disorder, schizophrenia and Tourette-syndrome (Levitt et al., 2004; Polleux and Lauder, 2004),

although the hard evidence for this model is critically lacking. One of the most interesting correlations in that regard is the increased risk for epilepsy in ASD (Canitano, 2007).

Alterations of BDNF levels or its receptor, TrkB, have been found in autism, epilepsy and schizophrenia patients (Angelucci et al., 2005; Connolly et al., 2006; Hashimoto et al., 2006; Nelson et al., 2001; Tsai, 2006). Interestingly, BDNF expression is often inversely correlated with KCC2 expression. Deletion of the subplate during development causes an increase in BDNF and a decrease of KCC2 expression in the cortex (Kanold and Shatz, 2006). Application of BDNF to slices also causes a decrease in KCC2 expression (Rivera et al., 2002), which is mediated through TrkB activation of both Shc/FRS-2 and PLC-gamma pathways (Rivera et al., 2004). If the increases in BDNF expression seen in many neuropathologies result in decreased KCC2 expression during the migration of interneurons, one might expect the termination of migration to be affected. All of these conditions have noted deficits in interneuron function (Benes and Berretta, 2001; de Lanerolle et al., 1989; Levitt et al., 2004; Polleux and Lauder, 2004; Rubenstein and Merzenich, 2003). Perhaps alterations in the termination of interneuron migration can prevent interneurons from arriving at the appropriate locations. Very different pathologies can result from very similar causes. Multiple sclerosis and rheumatory arthritis arise from different manifestations of an autoimmune disorder and is genetically inherited (Toussirot et al., 2006). As mentioned previously, epilepsy and autism are also comorbid (Canitano, 2007). Perhaps these pathologies manifest from defects in terminating interneuron migration, resulting in altered density and spacing.

Even subtle delays in the timing of interneuron development could have dire consequences. GABAergic activity is essential in setting the critical period in the visual system. If this critical period is delayed deficits arise in cortical plasticity and visual acuity (Hensch, 2005). Perhaps altered critical periods, due to defects in termination of

interneuron migration, could result in a loss of the plasticity required to establish the appropriate connections and synaptic strengths.

In mouse models Rett-syndrome (MECP2 knockout) and Fragile-X (Fmr1 knockout), two syndromes including (but not limited too) autistic features, a delay in the expression of parvalbumin positive interneurons has been reported (Fukuda et al., 2005; Selby et al., 2007). It would be interesting to know if these mouse models also show alterations in the timing of terminating interneuron migration. Likewise it would be interesting to know if human individuals with these neuropathologies have a similar delay of parvalbumin expression and a delayed termination of interneuron migration. Since inhibiting calcium signaling in these interneurons was sufficient to stop interneuron migration, perhaps the use of nimodipine (an L-type calcium channel blocker already in used for the treatment of high blood pressure) could be used to stop interneuron migration as a therapeutic target in ASD mouse models. As mentioned previously, this same drug caused the early expression of parvalbumin in mice (Buwalda et al., 1994), and could rescue a defect in delayed termination of interneuron migration.

Finally, if KCC2 can aid in the termination of migration, then cells that are migrating when they should not, as in tumor metastasis, may have a defect in KCC2 expression. GABA affects some forms of cancer metastasis (Ortega, 2003). It would be interesting to see if altering KCC2 expression has an effect on the migration of neuroblastomas. Such evidence would provide a new pharmacological target in the treatment of cancer.

Final thoughts

In conclusion, there have been many theories as to why GABA undergoes this reversal from excitation to inhibitory. Ion gradients are metabolically costly to build and to maintain. This expense may be more than a young neuron can afford. Alternatively, the fine regulation of local KCC2 expression could be a way to enable both excitatory and

inhibitory inputs in a primitive one-neurotransmitter organism. Nevertheless this detail of ontogeny has provided a foothold for natural selection to regulate the termination of interneuron migration in the neocortex.

Bibliography

Aboitiz, F., and Montiel, J. (2007). Origin and evolution of the vertebrate telencephalon, with special reference to the mammalian neocortex. Adv Anat Embryol Cell Biol *193*, 1-112.

Adragna, N. C., Di Fulvio, M., and Lauf, P. K. (2004). Regulation of K-Cl cotransport: from function to genes. J Membr Biol *201*, 109-137.

Aertsen, A., and Braitenberg, V., eds. (1992). Information Processing in the Cortex (New York: Springer-Verlag).

Akerman, C. J., and Cline, H. T. (2007). Refining the roles of GABAergic signaling during neural circuit formation. Trends Neurosci *30*, 382-389.

Alvarez-Buylla, A., Herrera, D. G., and Wichterle, H. (2000). The subventricular zone: source of neuronal precursors for brain repair. Prog Brain Res *127*, 1-11.

Anderson, S. A., Eisenstat, D. D., Shi, L., and Rubenstein, J. L. (1997). Interneuron migration from basal forebrain to neocortex: dependence on Dlx genes. Science *278*, 474-476.

Angelucci, F., Brene, S., and Mathe, A. A. (2005). BDNF in schizophrenia, depression and corresponding animal models. Mol Psychiatry *10*, 345-352.

Angevine, J. B.,Jr., and Sidman, R. L. (1961). Autoradiographic Study of Cell Migration during Histogenesis of Cerebral Cortex in the Mouse. Nature *192*, 766-768.

Anton, E. S., Cameron, R. S., and Rakic, P. (1996). Role of neuron-glial junctional domain proteins in the maintenance and termination of neuronal migration across the embryonic cerebral wall. J Neurosci *16*, 2283-2293.

Arthur, W. T., and Burridge, K. (2001). RhoA inactivation by p190RhoGAP regulates cell spreading and migration by promoting membrane protrusion and polarity. Mol Biol Cell *12*, 2711-2720.

Bai, J., Ramos, R. L., Ackman, J. B., Thomas, A. M., Lee, R. V., and LoTurco, J. J. (2003). RNAi reveals doublecortin is required for radial migration in rat neocortex. Nat Neurosci *6*, 1277-1283.

Bar, I., Lambert de Rouvroit, C., and Goffinet, A. M. (2000). The evolution of cortical development. An hypothesis based on the role of the Reelin signaling pathway. Trends Neurosci *23*, 633-638.

Barnes, A. P., Lilley, B. N., Pan, Y. A., Plummer, L. J., Powell, A. W., Raines, A. N., Sanes, J. R., and Polleux, F. (2007). LKB1 and SAD kinases define a pathway required for the polarization of cortical neurons. Cell *129*, 549-563.

Behar, T. N., Li, Y. X., Tran, H. T., Ma, W., Dunlap, V., Scott, C., and Barker, J. L. (1996). GABA stimulates chemotaxis and chemokinesis of embryonic cortical neurons via calcium-dependent mechanisms. J Neurosci *16*, 1808-1818.

Behar, T. N., Schaffner, A. E., Scott, C. A., O'Connell, C., and Barker, J. L. (1998). Differential response of cortical plate and ventricular zone cells to GABA as a migration stimulus. J Neurosci *18*, 6378-6387.

Belenky, M. A., Yarom, Y., and Pickard, G. E. (2008). Heterogeneous expression of gamma-aminobutyric acid and gamma-aminobutyric acid-associated receptors and transporters in the rat suprachiasmatic nucleus. J Comp Neurol *506*, 708-732.

Belmonte, M. K., Cook, E. H., Jr., Anderson, G. M., Rubenstein, J. L., Greenough, W. T., Beckel-Mitchener, A., Courchesne, E., Boulanger, L. M., Powell, S. B., Levitt, P. R., Perry, E. K., Jiang, Y. H., DeLorey, T. M., and Tierney, E. (2004). Autism as a disorder of neural information processing: directions for research and targets for therapy. Mol Psychiatry *9*, 646-663.

Ben-Ari, Y. (2002). Excitatory actions of gaba during development: the nature of the nurture. Nat Rev Neurosci *3*, 728-739.

Ben-Ari, Y., Khalilov, I., Represa, A., and Gozlan, H. (2004). Interneurons set the tune of developing networks. Trends Neurosci *27*, 422-427.

Benes, F. M., and Berretta, S. (2001). GABAergic interneurons: implications for understanding schizophrenia and bipolar disorder. Neuropsychopharmacology *25*, 1-27.

Berry, M., and Rogers, A. W. (1965). The migration of neuroblasts in the developing cerebral cortex. J Anat *99*, 691-709.

Bertrand, N., Castro, D. S., and Guillemot, F. (2002). Proneural genes and the specification of neural cell types. Nat Rev Neurosci *3*, 517-530.

Blaesse, P., Guillemin, I., Schindler, J., Schweizer, M., Delpire, E., Khiroug, L., Friauf, E., and Nothwang, H. G. (2006). Oligomerization of KCC2 correlates with development of inhibitory neurotransmission. J Neurosci *26*, 10407-10419.

Blom, N., Gammeltoft, S., and Brunak, S. (1999). Sequence and structure-based prediction of eukaryotic protein phosphorylation sites. J Mol Biol *294*, 1351-1362.

Borodinsky, L. N., Root, C. M., Cronin, J. A., Sann, S. B., Gu, X., and Spitzer, N. C. (2004). Activity-dependent homeostatic specification of transmitter expression in embryonic neurons. Nature *429*, 523-530.

Braak, H., and Braak, E. (1986). Ratio of pyramidal cells versus non-pyramidal cells in the human frontal isocortex and changes in ratio with ageing and Alzheimer's disease. Prog Brain Res *70*, 185-212.

Brown, M., Keynes, R., and Lumsden, A. (2001). The Developing Brain (New York: Oxford University Press).

Butt, S. J., Fuccillo, M., Nery, S., Noctor, S., Kriegstein, A., Corbin, J. G., and Fishell, G. (2005). The temporal and spatial origins of cortical interneurons predict their physiological subtype. Neuron *48*, 591-604.

Buwalda, B., Naber, R., Nyakas, C., and Luiten, P. G. (1994). Nimodipine accelerates the postnatal development of parvalbumin and S-100 beta immunoreactivity in the rat brain. Brain Res Dev Brain Res *78*, 210-216.

Callaway, E. M., and Sanes, J. R. (2006). New technologies. Curr Opin Neurobiol *16*, 540-542.

Cancedda, L., Fiumelli, H., Chen, K., and Poo, M. M. (2007). Excitatory GABA action is essential for morphological maturation of cortical neurons in vivo. J Neurosci *27*, 5224-5235.

Canitano, R. (2007). Epilepsy in autism spectrum disorders. Eur Child Adolesc Psychiatry *16*, 61-66.

Chudotvorova, I., Ivanov, A., Rama, S., Hubner, C. A., Pellegrino, C., Ben-Ari, Y., and Medina, I. (2005). Early expression of KCC2 in rat hippocampal cultures augments expression of functional GABA synapses. J Physiol *566*, 671-679.

Cobos, I., Borello, U., and Rubenstein, J. L. (2007). Dlx transcription factors promote migration through repression of axon and dendrite growth. Neuron *54*, 873-888.

Cobos, I., Calcagnotto, M. E., Vilaythong, A. J., Thwin, M. T., Noebels, J. L., Baraban, S. C., and Rubenstein, J. L. (2005). Mice lacking Dlx1 show subtype-specific loss of interneurons, reduced inhibition and epilepsy. Nat Neurosci *8*, 1059-1068.

Cobos, I., Long, J. E., Thwin, M. T., and Rubenstein, J. L. (2006). Cellular patterns of transcription factor expression in developing cortical interneurons. Cereb Cortex *16 Suppl 1*, i82-8.

Connolly, A. M., Chez, M., Streif, E. M., Keeling, R. M., Golumbek, P. T., Kwon, J. M., Riviello, J. J., Robinson, R. G., Neuman, R. J., and Deuel, R. M. (2006). Brain-derived neurotrophic factor and autoantibodies to neural antigens in sera of children with autistic spectrum disorders, Landau-Kleffner syndrome, and epilepsy. Biol Psychiatry *59*, 354-363.

Conti, F., Minelli, A., and Melone, M. (2004). GABA transporters in the mammalian cerebral cortex: localization, development and pathological implications. Brain Res Brain Res Rev *45*, 196-212.

Coyle, I. P., Koh, Y. H., Lee, W. C., Slind, J., Fergestad, T., Littleton, J. T., and Ganetzky, B. (2004). Nervous wreck, an SH3 adaptor protein that interacts with Wsp, regulates synaptic growth in Drosophila. Neuron *41*, 521-534.

Cuzon, V. C., Yeh, P. W., Cheng, Q., and Yeh, H. H. (2006). Ambient GABA promotes cortical entry of tangentially migrating cells derived from the medial ganglionic eminence. Cereb Cortex *16*, 1377-1388.

de Lanerolle, N. C., Kim, J. H., Robbins, R. J., and Spencer, D. D. (1989). Hippocampal interneuron loss and plasticity in human temporal lobe epilepsy. Brain Res *495*, 387-395.

DeDiego, I., Smith-Fernandez, A., and Fairen, A. (1994). Cortical cells that migrate beyond area boundaries: characterization of an early neuronal population in the lower intermediate zone of prenatal rats. Eur J Neurosci *6*, 983-997.

DeFelipe, J., Alonso-Nanclares, L., and Arellano, J. I. (2002). Microstructure of the neocortex: comparative aspects. J Neurocytol *31*, 299-316.

Del Rio, J. A., Martinez, A., Auladell, C., and Soriano, E. (2000). Developmental history of the subplate and developing white matter in the murine neocortex. Neuronal organization and relationship with the main afferent systems at embryonic and perinatal stages. Cereb Cortex *10*, 784-801.

Denaxa, M., Chan, C. H., Schachner, M., Parnavelas, J. G., and Karagogeos, D. (2001). The adhesion molecule TAG-1 mediates the migration of cortical interneurons from the ganglionic eminence along the corticofugal fiber system. Development *128*, 4635-4644.

des Portes, V., Pinard, J. M., Billuart, P., Vinet, M. C., Koulakoff, A., Carrie, A., Gelot, A., Dupuis, E., Motte, J., Berwald-Netter, Y., Catala, M., Kahn, A., Beldjord, C., and Chelly, J. (1998). A novel CNS gene required for neuronal migration and involved in X-linked subcortical laminar heterotopia and lissencephaly syndrome. Cell *92*, 51-61.

Douglas, R. J., and Martin, K. A. (2007). Mapping the matrix: the ways of neocortex. Neuron *56*, 226-238.

Dulabon, L., Olson, E. C., Taglienti, M. G., Eisenhuth, S., McGrath, B., Walsh, C. A., Kreidberg, J. A., and Anton, E. S. (2000). Reelin binds alpha3beta1 integrin and inhibits neuronal migration. Neuron *27*, 33-44.

Flames, N., Long, J. E., Garratt, A. N., Fischer, T. M., Gassmann, M., Birchmeier, C., Lai, C., Rubenstein, J. L., and Marin, O. (2004). Short- and long-range attraction of cortical GABAergic interneurons by neuregulin-1. Neuron *44*, 251-261.

Flames, N., and Marin, O. (2005). Developmental mechanisms underlying the generation of cortical interneuron diversity. Neuron *46*, 377-381.

Fode, C., Gradwohl, G., Morin, X., Dierich, A., LeMeur, M., Goridis, C., and Guillemot, F. (1998). The bHLH protein NEUROGENIN 2 is a determination factor for epibranchial placode-derived sensory neurons. Neuron *20*, 483-494.

Fode, C., Ma, Q., Casarosa, S., Ang, S. L., Anderson, D. J., and Guillemot, F. (2000). A role for neural determination genes in specifying the dorsoventral identity of telencephalic neurons. Genes Dev *14*, 67-80.

Freund, T. F. (2003). Interneuron Diversity series: Rhythm and mood in perisomatic inhibition. Trends Neurosci *26*, 489-495.

Fritschy, J. M., and Brunig, I. (2003). Formation and plasticity of GABAergic synapses: physiological mechanisms and pathophysiological implications. Pharmacol Ther *98*, 299-323.

Fuerst, P. G., Koizumi, A., Masland, R. H., and Burgess, R. W. (2008). Neurite arborization and mosaic spacing in the mouse retina require DSCAM. Nature *451*, 470-474.

Fukuda, T., Itoh, M., Ichikawa, T., Washiyama, K., and Goto, Y. (2005). Delayed maturation of neuronal architecture and synaptogenesis in cerebral cortex of Mecp2-deficient mice. J Neuropathol Exp Neurol *64*, 537-544.

Galanopoulou, A. S. (2007). Developmental patterns in the regulation of chloride homeostasis and GABA(A) receptor signaling by seizures. Epilepsia *48 Suppl 5*, 14-18.

Ganguly, K., Schinder, A. F., Wong, S. T., and Poo, M. (2001). GABA itself promotes the developmental switch of neuronal GABAergic responses from excitation to inhibition. Cell *105*, 521-532.

Gaudilliere, B., Konishi, Y., de la Iglesia, N., Yao, G., and Bonni, A. (2004). A CaMKII-NeuroD Signaling Pathway Specifies Dendritic Morphogenesis. Neuron *41*, 229-241.

Gilbert, D., Franjic-Wurtz, C., Funk, K., Gensch, T., Frings, S., and Mohrlen, F. (2007). Differential maturation of chloride homeostasis in primary afferent neurons of the somatosensory system. Int J Dev Neurosci *25*, 479-489.

Gleeson, J. G., Allen, K. M., Fox, J. W., Lamperti, E. D., Berkovic, S., Scheffer, I., Cooper, E. C., Dobyns, W. B., Minnerath, S. R., Ross, M. E., and Walsh, C. A. (1998). Doublecortin, a brain-specific gene mutated in human X-linked lissencephaly and double cortex syndrome, encodes a putative signaling protein. Cell *92*, 63-72.

Goffinet, A. M. (1984). Events governing organization of postmigratory neurons: studies on brain development in normal and reeler mice. Brain Res *319*, 261-296.

Gomez, T. M., Snow, D. M., and Letourneau, P. C. (1995). Characterization of spontaneous calcium transients in nerve growth cones and their effect on growth cone migration. Neuron *14*, 1233-1246.

Gomez, T. M., and Spitzer, N. C. (1999). In vivo regulation of axon extension and pathfinding by growth-cone calcium transients. Nature *397*, 350-355.

Gong, S., Zheng, C., Doughty, M. L., Losos, K., Didkovsky, N., Schambra, U. B., Nowak, N. J., Joyner, A., Leblanc, G., Hatten, M. E., and Heintz, N. (2003). A gene expression atlas of the central nervous system based on bacterial artificial chromosomes. Nature *425*, 917-925.

Gupta, A., Tsai, L. H., and Wynshaw-Boris, A. (2002). Life is a journey: a genetic look at neocortical development. Nat Rev Genet *3*, 342-355.

Hand, R., Bortone, D., Mattar, P., Nguyen, L., Heng, J. I., Guerrier, S., Boutt, E., Peters, E., Barnes, A. P., Parras, C., Schuurmans, C., Guillemot, F., and Polleux, F. (2005). Phosphorylation of Neurogenin2 specifies the migration properties and the dendritic morphology of pyramidal neurons in the neocortex. Neuron *48*, 45-62.

Hasegawa, H., Ashigaki, S., Takamatsu, M., Suzuki-Migishima, R., Ohbayashi, N., Itoh, N., Takada, S., and Tanabe, Y. (2004). Laminar patterning in the developing neocortex by temporally coordinated fibroblast growth factor signaling. J Neurosci *24*, 8711-8719.

Hashimoto, K., Iwata, Y., Nakamura, K., Tsujii, M., Tsuchiya, K. J., Sekine, Y., Suzuki, K., Minabe, Y., Takei, N., Iyo, M., and Mori, N. (2006). Reduced serum levels of brain-derived neurotrophic factor in adult male patients with autism. Prog Neuropsychopharmacol Biol Psychiatry *30*, 1529-1531.

Hassan, B. A., Bermingham, N. A., He, Y., Sun, Y., Jan, Y. N., Zoghbi, H. Y., and Bellen, H. J. (2000). atonal regulates neurite arborization but does not act as a proneural gene in the Drosophila brain. Neuron *25*, 549-561.

Hatanaka, Y., and Murakami, F. (2002). In vitro analysis of the origin, migratory behavior, and maturation of cortical pyramidal cells. J Comp Neurol *454*, 1-14.

Hausser, M., Spruston, N., and Stuart, G. J. (2000). Diversity and dynamics of dendritic signaling. Science *290*, 739-744.

Hayashi, K., Ohshima, T., and Mikoshiba, K. (2002). Pak1 is involved in dendrite initiation as a downstream effector of Rac1 in cortical neurons. Mol Cell Neurosci *20*, 579-594.

Heintz, N. (2004). Gene expression nervous system atlas (GENSAT). Nat Neurosci *7*, 483.

Hensch, T. K. (2005). Critical period plasticity in local cortical circuits. Nat Rev Neurosci *6*, 877-888.

Herbison, A. E. (2001). Physiological roles for the neurosteroid allopregnanolone in the modulation of brain function during pregnancy and parturition. Prog Brain Res *133*, 39-47.

Huang, H. P., Liu, M., El-Hodiri, H. M., Chu, K., Jamrich, M., and Tsai, M. J. (2000a). Regulation of the pancreatic islet-specific gene BETA2 (neuroD) by neurogenin 3. Mol Cell Biol *20*, 3292-3307.

Huang, M. L., Hsu, C. H., and Chien, C. T. (2000b). The proneural gene amos promotes multiple dendritic neuron formation in the Drosophila peripheral nervous system. Neuron *25*, 57-67.

Huber, A. B., Kolodkin, A. L., Ginty, D. D., and Cloutier, J. F. (2003). Signaling at the growth cone: ligand-receptor complexes and the control of axon growth and guidance. Annu Rev Neurosci *26*, 509-563.

Hussy, N., Deleuze, C., Pantaloni, A., Desarmenien, M. G., and Moos, F. (1997). Agonist action of taurine on glycine receptors in rat supraoptic magnocellular neurones: possible role in osmoregulation. J Physiol *502*, 609-621.

Inglefield, J. R., and Schwartz-Bloom, R. D. (1998). Activation of excitatory amino acid receptors in the rat hippocampal slice increases intracellular Cl- and cell volume. J Neurochem *71*, 1396-1404.

Jan, Y. N., and Jan, L. Y. (2003). The control of dendrite development. Neuron *40*, 229-242.

Jarman, A. P., Grau, Y., Jan, L. Y., and Jan, Y. N. (1993). atonal is a proneural gene that directs chordotonal organ formation in the Drosophila peripheral nervous system. Cell *73*, 1307-1321.

Kanold, P. O., Kara, P., Reid, R. C., and Shatz, C. J. (2003). Role of subplate neurons in functional maturation of visual cortical columns. Science *301*, 521-525.

Kanold, P. O., and Shatz, C. J. (2006). Subplate neurons regulate maturation of cortical inhibition and outcome of ocular dominance plasticity. Neuron *51*, 627-638.

Kasthuri, N., and Lichtman, J. W. (2007). The rise of the 'projectome'. Nat Methods *4*, 307-308.

Kater, S. B., and Mills, L. R. (1991). Regulation of growth cone behavior by calcium. J Neurosci *11*, 891-899.

Katoh, M. (2004). Identification and characterization of human FCHSD1 and FCHSD2 genes in silico. Int J Mol Med *13*, 749-754.

Kawaguchi, Y., and Kondo, S. (2002). Parvalbumin, somatostatin and cholecystokinin as chemical markers for specific GABAergic interneuron types in the rat frontal cortex. J Neurocytol *31*, 277-287.

Kawauchi, T., Chihama, K., Nabeshima, Y., and Hoshino, M. (2003). The in vivo roles of STEF/Tiam1, Rac1 and JNK in cortical neuronal migration. Embo J *22*, 4190-4201.

Komuro, H., and Kumada, T. (2005). Ca2+ transients control CNS neuronal migration. Cell Calcium *37*, 387-393.

Komuro, H., and Rakic, P. (1996). Intracellular Ca2+ fluctuations modulate the rate of neuronal migration. Neuron *17*, 275-285.

Kriegstein, A. R., and Noctor, S. C. (2004). Patterns of neuronal migration in the embryonic cortex. Trends Neurosci *27*, 392-399.

Kriegstein, A. R., and Owens, D. F. (2001). GABA may act as a self-limiting trophic factor at developing synapses. Sci STKE *2001*, PE1.

Kumada, T., and Komuro, H. (2004). Completion of neuronal migration regulated by loss of Ca(2+) transients. Proc Natl Acad Sci U S A *101*, 8479-8484.

Lavdas, A. A., Grigoriou, M., Pachnis, V., and Parnavelas, J. G. (1999). The medial ganglionic eminence gives rise to a population of early neurons in the developing cerebral cortex. J Neurosci *19*, 7881-7888.

Lee, H. H., Walker, J. A., Williams, J. R., Goodier, R. J., Payne, J. A., and Moss, S. J. (2007). Direct protein kinase C-dependent phosphorylation regulates the cell surface stability and activity of the potassium chloride cotransporter KCC2. J Biol Chem *282*, 29777-29784.

Lee, S. K., and Pfaff, S. L. (2003). Synchronization of neurogenesis and motor neuron specification by direct coupling of bHLH and homeodomain transcription factors. Neuron *38*, 731-745.

Leitch, E., Coaker, J., Young, C., Mehta, V., and Sernagor, E. (2005). GABA type-A activity controls its own developmental polarity switch in the maturing retina. J Neurosci *25*, 4801-4805.

Levitt, P., Eagleson, K. L., and Powell, E. M. (2004). Regulation of neocortical interneuron development and the implications for neurodevelopmental disorders. Trends Neurosci *27*, 400-406.

Li, G., Adesnik, H., Li, J., Long, J., Nicoll, R. A., Rubenstein, J. L., and Pleasure, S. J. (2008). Regional distribution of cortical interneurons and development of inhibitory tone are regulated by Cxcl12/Cxcr4 signaling. J Neurosci *28*, 1085-1098.

Lichtman, J. W. (2007). Connectomics in Brainbow Mice.

Lohmann, C., Myhr, K. L., and Wong, R. O. (2002). Transmitter-evoked local calcium release stabilizes developing dendrites. Nature *418*, 177-181.

Lopez-Bendito, G., Lujan, R., Shigemoto, R., Ganter, P., Paulsen, O., and Molnar, Z. (2003). Blockade of GABA(B) receptors alters the tangential migration of cortical neurons. Cereb Cortex *13*, 932-942.

Lopez-Bendito, G., Sanchez-Alcaniz, J. A., Pla, R., Borrell, V., Pico, E., Valdeolmillos, M., and Marin, O. (2008). Chemokine signaling controls intracortical migration and final distribution of GABAergic interneurons. J Neurosci *28*, 1613-1624.

Lu, J., Karadsheh, M., and Delpire, E. (1999). Developmental regulation of the neuronal-specific isoform of K-Cl cotransporter KCC2 in postnatal rat brains. J Neurobiol *39*, 558-568.

Ludwig, A., Li, H., Saarma, M., Kaila, K., and Rivera, C. (2003). Developmental up-regulation of KCC2 in the absence of GABAergic and glutamatergic transmission. Eur J Neurosci *18*, 3199-3206.

Lujan, R., Shigemoto, R., and Lopez-Bendito, G. (2005). Glutamate and GABA receptor signalling in the developing brain. Neuroscience *130*, 567-580.

Ma, Q., Fode, C., Guillemot, F., and Anderson, D. J. (1999). Neurogenin1 and neurogenin2 control two distinct waves of neurogenesis in developing dorsal root ganglia. Genes Dev *13*, 1717-1728.

Manent, J. B., Demarque, M., Jorquera, I., Pellegrino, C., Ben-Ari, Y., Aniksztejn, L., and Represa, A. (2005). A noncanonical release of GABA and glutamate modulates neuronal migration. J Neurosci *25*, 4755-4765.

Manent, J. B., Jorquera, I., Ben-Ari, Y., Aniksztejn, L., and Represa, A. (2006). Glutamate acting on AMPA but not NMDA receptors modulates the migration of hippocampal interneurons. J Neurosci *26*, 5901-5909.

Marin, O., and Rubenstein, J. L. (2003). Cell migration in the forebrain. Annu Rev Neurosci *26*, 441-483.

Marin, O., Yaron, A., Bagri, A., Tessier-Lavigne, M., and Rubenstein, J. L. (2001). Sorting of striatal and cortical interneurons regulated by semaphorin-neuropilin interactions. Science *293*, 872-875.

Markram, H., Toledo-Rodriguez, M., Wang, Y., Gupta, A., Silberberg, G., and Wu, C. (2004). Interneurons of the neocortical inhibitory system. Nat Rev Neurosci *5*, 793-807.

Martin, K. A. (2002). Microcircuits in visual cortex. Curr Opin Neurobiol *12*, 418-425.

Marty, S., Berninger, B., Carroll, P., and Thoenen, H. (1996). GABAergic stimulation regulates the phenotype of hippocampal interneurons through the regulation of brain-derived neurotrophic factor. Neuron *16*, 565-570.

Mattar, P., Britz, O., Johannes, C., Nieto, M., Ma, L., Rebeyka, A., Klenin, N., Polleux, F., Guillemot, F., and Schuurmans, C. (2004). A screen for downstream effectors of Neurogenin2 in the embryonic neocortex. Dev Biol *273*, 373-389.

McConnell, S. K. (1988). Fates of visual cortical neurons in the ferret after isochronic and heterochronic transplantation. J Neurosci *8*, 945-974.

McConnell, S. K., and Kaznowski, C. E. (1991). Cell cycle dependence of laminar determination in developing neocortex. Science *254*, 282-285.

McManus, M. F., Nasrallah, I. M., Gopal, P. P., Baek, W. S., and Golden, J. A. (2004). Axon mediated interneuron migration. J Neuropathol Exp Neurol *63*, 932-941.

Megason, S. G., and McMahon, A. P. (2002). A mitogen gradient of dorsal midline Wnts organizes growth in the CNS. Development *129*, 2087-2098.

Metin, C., Denizot, J. P., and Ropert, N. (2000). Intermediate zone cells express calcium-permeable AMPA receptors and establish close contact with growing axons. J Neurosci *20*, 696-708.

Miletic, G., and Miletic, V. (2007). Loose ligation of the sciatic nerve is associated with TrkB receptor-dependent decreases in KCC2 protein levels in the ipsilateral spinal dorsal horn. Pain

Miller, M. (1981). Maturation of rat visual cortex. I. A quantitative study of Golgi-impregnated pyramidal neurons. J Neurocytol *10*, 859-878.

Miller, M. W. (1986). Maturation of rat visual cortex. III. Postnatal morphogenesis and synaptogenesis of local circuit neurons. Brain Res *390*, 271-285.

Miyata, T., Kawaguchi, A., Saito, K., Kawano, M., Muto, T., and Ogawa, M. (2004). Asymmetric production of surface-dividing and non-surface-dividing cortical progenitor cells. Development *131*, 3133-3145.

Mizuguchi, R., Sugimori, M., Takebayashi, H., Kosako, H., Nagao, M., Yoshida, S., Nabeshima, Y., Shimamura, K., and Nakafuku, M. (2001). Combinatorial roles of olig2 and neurogenin2 in the coordinated induction of pan-neuronal and subtype-specific properties of motoneurons. Neuron *31*, 757-771.

Molla, R., Garcia-Verdugo, J. M., Lopez-Garcia, C., and Martin-Perez, V. (1986). Neuronal development of the chick cerebral cortex. A Golgi study. J Hirnforsch *27*, 625-637.

Molyneaux, B. J., Arlotta, P., Menezes, J. R., and Macklis, J. D. (2007). Neuronal subtype specification in the cerebral cortex. Nat Rev Neurosci *8*, 427-437.

Moore, K. B., Schneider, M. L., and Vetter, M. L. (2002). Posttranslational mechanisms control the timing of bHLH function and regulate retinal cell fate. Neuron *34*, 183-195.

Mountcastle, V. B. (1997). The columnar organization of the neocortex. Brain *120*, 701-722.

Murciano, A., Zamora, J., Lopez-Sanchez, J., and Frade, J. M. (2002). Interkinetic nuclear movement may provide spatial clues to the regulation of neurogenesis. Mol Cell Neurosci *21*, 285-300.

Nadarajah, B., and Parnavelas, J. G. (2002). Modes of neuronal migration in the developing cerebral cortex. Nat Rev Neurosci *3*, 423-432.

Nakada, Y., Hunsaker, T. L., Henke, R. M., and Johnson, J. E. (2004). Distinct domains within Mash1 and Math1 are required for function in neuronal differentiation versus neuronal cell-type specification. Development *131*, 1319-1330.

Nelson, K. B., Grether, J. K., Croen, L. A., Dambrosia, J. M., Dickens, B. F., Jelliffe, L. L., Hansen, R. L., and Phillips, T. M. (2001). Neuropeptides and neurotrophins in neonatal blood of children with autism or mental retardation. Ann Neurol *49*, 597-606.

Nery, S., Fishell, G., and Corbin, J. G. (2002). The caudal ganglionic eminence is a source of distinct cortical and subcortical cell populations. Nat Neurosci *5*, 1279-1287.

Nieto, M., Schuurmans, C., Britz, O., and Guillemot, F. (2001). Neural bHLH genes control the neuronal versus glial fate decision in cortical progenitors. Neuron *29*, 401-413.

Nieuwenhuys, R. (1994). The neocortex. An overview of its evolutionary development, structural organization and synaptology. Anat Embryol (Berl) *190*, 307-337.

Noctor, S. C., Flint, A. C., Weissman, T. A., Dammerman, R. S., and Kriegstein, A. R. (2001). Neurons derived from radial glial cells establish radial units in neocortex. Nature *409*, 714-720.

Noctor, S. C., Martinez-Cerdeno, V., Ivic, L., and Kriegstein, A. R. (2004). Cortical neurons arise in symmetric and asymmetric division zones and migrate through specific phases. Nat Neurosci *7*, 136-144.

O'Rourke, N. A., Sullivan, D. P., Kaznowski, C. E., Jacobs, A. A., and McConnell, S. K. (1995). Tangential migration of neurons in the developing cerebral cortex. Development *121*, 2165-2176.

Olenik, C., Aktories, K., and Meyer, D. K. (1999). Differential expression of the small GTP-binding proteins RhoA, RhoB, Cdc42u and Cdc42b in developing rat neocortex. Brain Res Mol Brain Res *70*, 9-17.

Olson, E. C., Schinder, A. F., Dantzker, J. L., Marcus, E. A., Spitzer, N. C., and Harris, W. A. (1998). Properties of ectopic neurons induced by Xenopus neurogenin1 misexpression. Mol Cell Neurosci *12*, 281-299.

Olson, M. F., Ashworth, A., and Hall, A. (1995). An essential role for Rho, Rac, and Cdc42 GTPases in cell cycle progression through G1. Science *269*, 1270-1272.

Ortega, A. (2003). A new role for GABA: inhibition of tumor cell migration. Trends Pharmacol Sci *24*, 151-154.

Owens, D. F., and Kriegstein, A. R. (2002). Is there more to GABA than synaptic inhibition? Nat Rev Neurosci *3*, 715-727.

Parras, C. M., Schuurmans, C., Scardigli, R., Kim, J., Anderson, D. J., and Guillemot, F. (2002). Divergent functions of the proneural genes Mash1 and Ngn2 in the specification of neuronal subtype identity. Genes Dev *16*, 324-338.

Payne, J. A., Stevenson, T. J., and Donaldson, L. F. (1996). Molecular characterization of a putative K-Cl cotransporter in rat brain. A neuronal-specific isoform. J Biol Chem *271*, 16245-16252.

Peters, A., and Edward, G.J., eds. (1984). Cerebral Cortex (New York: Plenum Press).

Peters, A., and Kara, D. A. (1985a). The neuronal composition of area 17 of rat visual cortex. I. The pyramidal cells. J Comp Neurol *234*, 218-241.

Peters, A., and Kara, D. A. (1985b). The neuronal composition of area 17 of rat visual cortex. II. The nonpyramidal cells. J Comp Neurol *234*, 242-263.

Peters, A., Kara, D. A., and Harriman, K. M. (1985). The neuronal composition of area 17 of rat visual cortex. III. Numerical considerations. J Comp Neurol *238*, 263-274.

Pierri, J. N., Chaudry, A. S., Woo, T. U., and Lewis, D. A. (1999). Alterations in chandelier neuron axon terminals in the prefrontal cortex of schizophrenic subjects. Am J Psychiatry *156*, 1709-1719.

Pinto Lord, M. C., and Caviness, V. S., Jr. (1979). Determinants of cell shape and orientation: a comparative Golgi analysis of cell-axon interrelationships in the developing neocortex of normal and reeler mice. J Comp Neurol *187*, 49-69.

Pinto-Lord, M. C., Evrard, P., and Caviness, V. S., Jr. (1982). Obstructed neuronal migration along radial glial fibers in the neocortex of the reeler mouse: a Golgi-EM analysis. Brain Res *256*, 379-393.

Polleux, F., Dehay, C., and Kennedy, H. (1997). The timetable of laminar neurogenesis contributes to the specification of cortical areas in mouse isocortex. J Comp Neurol *385*, 95-116.

Polleux, F., and Ghosh, A. (2002). The slice overlay assay: a versatile tool to study the influence of extracellular signals on neuronal development. Sci STKE *2002*, PL9.

Polleux, F., and Lauder, J. M. (2004). Toward a developmental neurobiology of autism. Ment Retard Dev Disabil Res Rev *10*, 303-317.

Polleux, F., Morrow, T., and Ghosh, A. (2000). Semaphorin 3A is a chemoattractant for cortical apical dendrites. Nature *404*, 567-573.

Polleux, F., Whitford, K. L., Dijkhuizen, P. A., Vitalis, T., and Ghosh, A. (2002). Control of cortical interneuron migration by neurotrophins and PI3-kinase signaling. Development *129*, 3147-3160.

Poluch, S., and Konig, N. (2002). AMPA receptor activation induces GABA release from neurons migrating tangentially in the intermediate zone of embryonic rat neocortex. Eur J Neurosci *16*, 350-354.

Poluch, S., Rossel, M., and Konig, N. (2003). AMPA-evoked ion influx is strongest in tangential neurons of the rat neocortical intermediate zone close to the front of the migratory stream. Dev Dyn *227*, 416-421.

Pozas, E., and Ibanez, C. F. (2005). GDNF and GFRalpha1 promote differentiation and tangential migration of cortical GABAergic neurons. Neuron *45*, 701-713.

Puri, P. L., and Sartorelli, V. (2000). Regulation of muscle regulatory factors by DNA-binding, interacting proteins, and post-transcriptional modifications. J Cell Physiol *185*, 155-173.

Purves, D., Augustine, G. J., Fitzpatrick, D., Hall, W. C., LaMantia, A. S., McNamara, J. O., and Williams, S. M. (2004). Neuroscience (Sunderland, MA: Sinauer Associates, Inc.).

Quan, X. J., Denayer, T., Yan, J., Jafar-Nejad, H., Philippi, A., Lichtarge, O., Vleminckx, K., and Hassan, B. A. (2004). Evolution of neural precursor selection: functional divergence of proneural proteins. Development *131*, 1679-1689.

Rakic, P. (1972). Mode of cell migration to the superficial layers of fetal monkey neocortex. J Comp Neurol *145*, 61-83.

Reynolds, A., Brustein, E., Liao, M., Mercado, A., Babilonia, E., Mount, D. B., and Drapeau, P. (2008). Neurogenic role of the depolarizing chloride gradient revealed by global overexpression of KCC2 from the onset of development. J Neurosci *28*, 1588-1597.

Ridley, A. J., Schwartz, M. A., Burridge, K., Firtel, R. A., Ginsberg, M. H., Borisy, G., Parsons, J. T., and Horwitz, A. R. (2003). Cell migration: integrating signals from front to back. Science *302*, 1704-1709.

Rivera, C., Li, H., Thomas-Crusells, J., Lahtinen, H., Viitanen, T., Nanobashvili, A., Kokaia, Z., Airaksinen, M. S., Voipio, J., Kaila, K., and Saarma, M. (2002). BDNF-induced TrkB activation down-regulates the K+-Cl- cotransporter KCC2 and impairs neuronal Cl- extrusion. J Cell Biol *159*, 747-752.

Rivera, C., Voipio, J., Payne, J. A., Ruusuvuori, E., Lahtinen, H., Lamsa, K., Pirvola, U., Saarma, M., and Kaila, K. (1999). The K+/Cl- co-transporter KCC2 renders GABA hyperpolarizing during neuronal maturation. Nature *397*, 251-255.

Rivera, C., Voipio, J., Thomas-Crusells, J., Li, H., Emri, Z., Sipila, S., Payne, J. A., Minichiello, L., Saarma, M., and Kaila, K. (2004). Mechanism of activity-dependent downregulation of the neuron-specific K-Cl cotransporter KCC2. J Neurosci *24*, 4683-4691.

Ross, S. E., Greenberg, M. E., and Stiles, C. D. (2003). Basic helix-loop-helix factors in cortical development. Neuron *39*, 13-25.

Rubenstein, J. L., and Merzenich, M. M. (2003). Model of autism: increased ratio of excitation/inhibition in key neural systems. Genes Brain Behav *2*, 255-267.

Sauer, F. C. (1935). Mitosis in the Neural Tube. The Journal of Comparative Neurology *62*, 377-405.

Scardigli, R., Schuurmans, C., Gradwohl, G., and Guillemot, F. (2001). Crossregulation between Neurogenin2 and pathways specifying neuronal identity in the spinal cord. Neuron *31*, 203-217.

Schmechel, D. E., and Rakic, P. (1979). A Golgi study of radial glial cells in developing monkey telencephalon: morphogenesis and transformation into astrocytes. Anat Embryol (Berl) *156*, 115-152.

Schuurmans, C., Armant, O., Nieto, M., Stenman, J. M., Britz, O., Klenin, N., Brown, C., Langevin, L. M., Seibt, J., Tang, H., Cunningham, J. M., Dyck, R., Walsh, C., Campbell, K., Polleux, F., and Guillemot, F. (2004). Sequential phases of cortical specification involve Neurogenin-dependent and -independent pathways. EMBO J *23*, 2892-2902.

Schuurmans, C., and Guillemot, F. (2002). Molecular mechanisms underlying cell fate specification in the developing telencephalon. Curr Opin Neurobiol *12*, 26-34.

Scott, E. K., and Luo, L. (2001). How do dendrites take their shape? Nat Neurosci *4*, 359-365.

Seibt, J., Schuurmans, C., Gradwhol, G., Dehay, C., Vanderhaeghen, P., Guillemot, F., and Polleux, F. (2003). Neurogenin2 specifies the connectivity of thalamic neurons by controlling axon responsiveness to intermediate target cues. Neuron *39*, 439-452.

Selby, L., Zhang, C., and Sun, Q. Q. (2007). Major defects in neocortical GABAergic inhibitory circuits in mice lacking the fragile X mental retardation protein. Neurosci Lett *412*, 227-232.

Sharma, A., Moore, M., Marcora, E., Lee, J. E., Qiu, Y., Samaras, S., and Stein, R. (1999). The NeuroD1/BETA2 sequences essential for insulin gene transcription colocalize with those necessary for neurogenesis and p300/CREB binding protein binding. Mol Cell Biol *19*, 704-713.

Shephard, G. M. (1994). Neurobiology (New York: Oxford University Press).

Shu, T., Ayala, R., Nguyen, M. D., Xie, Z., Gleeson, J. G., and Tsai, L. H. (2004). Ndel1 operates in a common pathway with LIS1 and cytoplasmic dynein to regulate cortical neuronal positioning. Neuron *44*, 263-277.

Sidman, R. L., and Rakic, P. (1973). Neuronal migration, with special reference to developing human brain: a review. Brain Res *62*, 1-35.

Skowronska-Krawczyk, D., Ballivet, M., Dynlacht, B. D., and Matter, J. M. (2004). Highly specific interactions between bHLH transcription factors and chromatin during retina development. Development *131*, 4447-4454.

Sloper, J. J. (1973). An electron microscopic study of the neurons of the primate motor and somatic sensory cortices. J Neurocytol *2*, 351-359.

Sloper, J. J., Hiorns, R. W., and Powell, T. P. (1979). A qualitative and quantitative electron microscopic study of the neurons in the primate motor and somatic sensory cortices. Philos Trans R Soc Lond B Biol Sci *285*, 141-171.

Smith, C. I., Islam, T. C., Mattsson, P. T., Mohamed, A. J., Nore, B. F., and Vihinen, M. (2001). The Tec family of cytoplasmic tyrosine kinases: mammalian Btk, Bmx, Itk, Tec, Txk and homologs in other species. Bioessays *23*, 436-446.

Soria, J. M., and Valdeolmillos, M. (2002). Receptor-activated calcium signals in tangentially migrating cortical cells. Cereb Cortex *12*, 831-839.

Soriano, E., Del Rio, J. A., Ferrer, I., Auladell, C., De Lecea, L., and Alcantara, S. (1992). Late appearance of parvalbumin-immunoreactive neurons in the rodent cerebral cortex does not follow an 'inside-out' sequence. Neurosci Lett *142*, 147-150.

Spitzer, N. C., Root, C. M., and Borodinsky, L. N. (2004). Orchestrating neuronal differentiation: patterns of Ca2+ spikes specify transmitter choice. Trends Neurosci *27*, 415-421.

Sporns, O., Tononi, G., and Kotter, R. (2005). The human connectome: A structural description of the human brain. PLoS Comput Biol *1*, e42.

Sulston, J. E., Schierenberg, E., White, J. G., and Thomson, J. N. (1983). The embryonic cell lineage of the nematode Caenorhabditis elegans. Dev Biol *100*, 64-119.

Sun, Y., Nadal-Vicens, M., Misono, S., Lin, M. Z., Zubiaga, A., Hua, X., Fan, G., and Greenberg, M. E. (2001). Neurogenin promotes neurogenesis and inhibits glial differentiation by independent mechanisms. Cell *104*, 365-376.

Super, H., Soriano, E., and Uylings, H. B. (1998). The functions of the preplate in development and evolution of the neocortex and hippocampus. Brain Res Brain Res Rev *27*, 40-64.

Sussel, L., Marin, O., Kimura, S., and Rubenstein, J. L. (1999). Loss of Nkx2.1 homeobox gene function results in a ventral to dorsal molecular respecification within the basal telencephalon: evidence for a transformation of the pallidum into the striatum. Development *126*, 3359-3370.

Sutor, B., and Luhmann, H. J. (1995). Development of excitatory and inhibitory postsynaptic potentials in the rat neocortex. Perspect Dev Neurobiol *2*, 409-419.

Tabata, H., and Nakajima, K. (2001). Efficient in utero gene transfer system to the developing mouse brain using electroporation: visualization of neuronal migration in the developing cortex. Neuroscience *103*, 865-872.

Tabata, H., and Nakajima, K. (2003). Multipolar migration: the third mode of radial neuronal migration in the developing cerebral cortex. J Neurosci *23*, 9996-10001.

Talikka, M., Perez, S. E., and Zimmerman, K. (2002). Distinct patterns of downstream target activation are specified by the helix-loop-helix domain of proneural basic helix-loop-helix transcription factors. Dev Biol *247*, 137-148.

Tamamaki, N., Fujimori, K., Nojyo, Y., Kaneko, T., and Takauji, R. (2003). Evidence that Sema3A and Sema3F regulate the migration of GABAergic neurons in the developing neocortex. J Comp Neurol *455*, 238-248.

Tamamaki, N., Fujimori, K. E., and Takauji, R. (1997). Origin and route of tangentially migrating neurons in the developing neocortical intermediate zone. J Neurosci *17*, 8313-8323.

Tanaka, D. H., Maekawa, K., Yanagawa, Y., Obata, K., and Murakami, F. (2006). Multidirectional and multizonal tangential migration of GABAergic interneurons in the developing cerebral cortex. Development *133*, 2167-2176.

Tessier-Lavigne, M., and Goodman, C. S. (1996). The molecular biology of axon guidance. Science *274*, 1123-1133.

Thevenaz, P., Ruttimann, U. E., and Unser, M. (1998). A pyramid approach to subpixel registration based on intensity. IEEE Trans Image Process *7*, 27-41.

Threadgill, R., Bobb, K., and Ghosh, A. (1997). Regulation of dendritic growth and remodeling by Rho, Rac, and Cdc42. Neuron *19*, 625-634.

Tillakaratne, N. J., Medina-Kauwe, L., and Gibson, K. M. (1995). gamma-Aminobutyric acid (GABA) metabolism in mammalian neural and nonneural tissues. Comp Biochem Physiol A Physiol *112*, 247-263.

Titz, S., Hans, M., Kelsch, W., Lewen, A., Swandulla, D., and Misgeld, U. (2003). Hyperpolarizing inhibition develops without trophic support by GABA in cultured rat midbrain neurons. J Physiol *550*, 719-730.

Tombol, T. (1974). An electron microscopic study of the neurons of the visual cortex. J Neurocytol *3*, 525-531.

Toussirot, E., Pertuiset, E., Martin, A., Melac-Ducamp, S., Alcalay, M., Grardel, B., Seror, P., Perdriger, A., Wendling, D., Mulleman, D., Beraneck, L., and Mariette, X. (2006). Association of rheumatoid arthritis with multiple sclerosis: report of 14 cases and discussion of its significance. J Rheumatol *33*, 1027-1028.

Toyoda, H., Ohno, K., Yamada, J., Ikeda, M., Okabe, A., Sato, K., Hashimoto, K., and Fukuda, A. (2003). Induction of NMDA and GABAA receptor-mediated Ca2+ oscillations with KCC2 mRNA downregulation in injured facial motoneurons. J Neurophysiol *89*, 1353-1362.

Tsai, H. M., Garber, B. B., and Larramendi, L. M. (1981a). 3H-thymidine autoradiographic analysis of telencephalic histogenesis in the chick embryo: I. Neuronal birthdates of telencephalic compartments in situ. J Comp Neurol *198*, 275-292.

Tsai, H. M., Garber, B. B., and Larramendi, L. M. (1981b). 3H-thymidine autoradiographic analysis of telencephalic histogenesis in the chick embryo: II. Dynamics of neuronal migration, displacement, and aggregation. J Comp Neurol *198*, 293-306.

Tsai, S. J. (2006). TrkB partial agonists: potential treatment strategy for epilepsy, mania, and autism. Med Hypotheses *66*, 173-175.

Tyzio, R., Cossart, R., Khalilov, I., Minlebaev, M., Hubner, C. A., Represa, A., Ben-Ari, Y., and Khazipov, R. (2006). Maternal oxytocin triggers a transient inhibitory switch in GABA signaling in the fetal brain during delivery. Science *314*, 1788-1792.

Uhlen, P. (2004). Spectral analysis of calcium oscillations. Sci STKE *2004*, pl15.

Valcanis, H., and Tan, S. S. (2003). Layer specification of transplanted interneurons in developing mouse neocortex. J Neurosci *23*, 5113-5122.

Van Aelst, L., and Cline, H. T. (2004). Rho GTPases and activity-dependent dendrite development. Curr Opin Neurobiol *14*, 297-304.

Vojtek, A. B., Taylor, J., DeRuiter, S. L., Yu, J. Y., Figueroa, C., Kwok, R. P., and Turner, D. L. (2003). Akt regulates basic helix-loop-helix transcription factor-coactivator complex formation and activity during neuronal differentiation. Mol Cell Biol *23*, 4417-4427.

Wake, H., Watanabe, M., Moorhouse, A. J., Kanematsu, T., Horibe, S., Matsukawa, N., Asai, K., Ojika, K., Hirata, M., and Nabekura, J. (2007). Early changes in KCC2 phosphorylation in response to neuronal stress result in functional downregulation. J Neurosci *27*, 1642-1650.

Wang, W., Gong, N., and Xu, T. L. (2006). Downregulation of KCC2 following LTP contributes to EPSP-spike potentiation in rat hippocampus. Biochem Biophys Res Commun *343*, 1209-1215.

Wen, Z., Guirland, C., Ming, G. L., and Zheng, J. Q. (2004). A CaMKII/calcineurin switch controls the direction of Ca(2+)-dependent growth cone guidance. Neuron *43*, 835-846.

White, J. G., Southgate, E., Thomson, J. N., and Brenner, S. (1976). The structure of the ventral nerve cord of Caenorhabditis elegans. Philos Trans R Soc Lond B Biol Sci *275*, 327-348.

Whitford, K. L., Dijkhuizen, P., Polleux, F., and Ghosh, A. (2002). Molecular control of cortical dendrite development. Annu Rev Neurosci *25*, 127-149.

Wichterle, H., Garcia-Verdugo, J. M., and Alvarez-Buylla, A. (1997). Direct evidence for homotypic, glia-independent neuronal migration. Neuron *18*, 779-791.

Wichterle, H., Turnbull, D. H., Nery, S., Fishell, G., and Alvarez-Buylla, A. (2001). In utero fate mapping reveals distinct migratory pathways and fates of neurons born in the mammalian basal forebrain. Development *128*, 3759-3771.

Wiesel, T. N., Hubel, D. H., and Lam, D. M. (1974). Autoradiographic demonstration of ocular-dominance columns in the monkey striate cortex by means of transneuronal transport. Brain Res *79*, 273-279.

Winfield, D. A., Gatter, K. C., and Powell, T. P. (1980). An electron microscopic study of the types and proportions of neurons in the cortex of the motor and visual areas of the cat and rat. Brain *103*, 245-258.

Wonders, C. P., and Anderson, S. A. (2006). The origin and specification of cortical interneurons. Nat Rev Neurosci *7*, 687-696.

Wong, K., Ren, X. R., Huang, Y. Z., Xie, Y., Liu, G., Saito, H., Tang, H., Wen, L., Brady-Kalnay, S. M., Mei, L., Wu, J. Y., Xiong, W. C., and Rao, Y. (2001). Signal transduction in neuronal migration: roles of GTPase activating proteins and the small GTPase Cdc42 in the Slit-Robo pathway. Cell *107*, 209-221.

Wong, R. O., and Ghosh, A. (2002). Activity-dependent regulation of dendritic growth and patterning. Nat Rev Neurosci *3*, 803-812.

Woo, N. S., Lu, J., England, R., McClellan, R., Dufour, S., Mount, D. B., Deutch, A. Y., Lovinger, D. M., and Delpire, E. (2002). Hyperexcitability and epilepsy associated with disruption of the mouse neuronal-specific K-Cl cotransporter gene. Hippocampus *12*, 258-268.

Yokota, Y., Gashghaei, H. T., Han, C., Watson, H., Campbell, K. J., and Anton, E. S. (2007). Radial glial dependent and independent dynamics of interneuronal migration in the developing cerebral cortex. PLoS ONE *2*, e794.

Yu, T. W., and Bargmann, C. I. (2001). Dynamic regulation of axon guidance. Nat Neurosci *4 Suppl*, 1169-1176.

Zhu, Y., Li, H., Zhou, L., Wu, J. Y., and Rao, Y. (1999). Cellular and molecular guidance of GABAergic neuronal migration from an extracortical origin to the neocortex. Neuron *23*, 473-485.